Active layer and permafrost thermal regimes in the ice-free areas of Antarctica

Filip Hrbáček [a,*], Marc Oliva [b], Christel Hansen [c], Megan Balks [d], Tanya Ann O'Neill [d], Miguel Angel de Pablo [e], Stefano Ponti [f], Miguel Ramos [g], Gonçalo Vieira [h], Andrey Abramov [i], Lucia Kaplan Pastíriková [a], Mauro Guglielmin [f], Gabriel Goyanes [h], Marcio Rocha Francelino [j], Carlos Schaefer [j], Denis Lacelle [k]

[a] *Department of Geography, Faculty of Science, Masaryk University, Kotlářská 2, 611 37, Brno, Czech Republic*
[b] *Department of Geography, Universitat de Barcelona, C/Montalegre 6-8, 3r, 08001 Barcelona, Spain*
[c] *Department of Geography, Geoinformatics and Meteorology, University of Pretoria, Private Bag X20, Hatfield 0028, South Africa*
[d] *School of Sciences - Te Aka Mātuatua, The University of Waikato, Gate 1, Knighton Road, Hamilton 3240, New Zealand*
[e] *Unidad de Geología, Departamento de Geología, Geografía y Medio Ambiente, Universidad de Alcalá, Ctra. A-II Km 33, 6. 28805, Alcalá de Henares, Spain*
[f] *University Insubria, Department of Theoretical and Applied Sciences, Via J.H. Dunant, 21100, Varese, Italy*
[g] *Physics and Mathematics department, Universidad de Alcalá, Calle el Escorial, 19-21, 28805 Alcalá de Henares, Madrid, Španělsko*
[h] *Centro de Estudos Geográficos, IGOT - Universidade de Lisboa, Rua Branca Edmée Marques, 1600-276 Lisboa, Portugal*
[i] *Soil cryology department, Institute of Physicochemical and biological problems in soil science, Russian Academy of Science, Pushchino, Russia*
[j] *Department of Soils of the Federal University of Viçosa, 36570, Viçosa, Brazil*
[k] *Department of Geography, Environment and Geomatics, University of Ottawa, Ontario, ON, K1N 6N5, Canada*

ARTICLE INFO

Keywords:
Ground thermal regime
Active layer thickness
Climate change
Antarctic ice-free environment
Cryosols
Gelisols
Permafrost

ABSTRACT

Ice-free areas occupy <0.5% of Antarctica and are unevenly distributed across the continent. Terrestrial ecosystem dynamics in ice free areas are strongly influenced by permafrost and the associated active layer. These features are the least studied component of the cryosphere in Antarctica, with sparse data from permanent study sites mainly providing information related to the ground thermal regime and active layer thickness (ALT). One of the most important results of the International Polar Year (IPY, 2007/08) was an increase in ground thermal regime monitoring sites, and consequently our knowledge of Antarctic permafrost dynamics. Now, 15 years after the IPY, we provide the first comprehensive summary of the state of permafrost across Antarctica, including the sub-Antarctic Islands, with analyses of spatial and temporal patterns of the dominant external factors (climate, lithology, biota, and hydric regime) on the ground thermal regime and active layer thickness. The mean annual ground temperatures of the active layer and uppermost part of the permafrost in Antarctica remain just below 0 °C in the warmest parts of the Antarctic Peninsula, and were below −20 °C in mountainous regions of the continent. The ALT varies between a few cm in the coldest, mountainous, parts of the Transantarctic Mountains up to >5 m in bedrock sites in the Antarctic Peninsula. The deepest and most variable ALTs (ca. 40 to >500 cm) were found in the Antarctic Peninsula, whereas the maximum ALT generally did not exceed 90 cm in Victoria Land and East Antarctica. Notably, found that the mean annual near-surface temperature follows the latitudinal gradient of −0.9 °C/deg. (R^2 = 0.9) and the active layer thickness 3.7 cm/deg. (R^2 = 0.64). The continuous permafrost occurs in the vast majority of the ice-free areas in Antarctica. The modelling of temperature on the top of the permafrost indicates also the permafrost presence in South Orkneys and South Georgia. The only areas where deep boreholes and geophysical surveys indicates discontinuous or sporadic permafrost are South Shetlands and Western Antarctic Peninsula.

* Corresponding author.
E-mail address: hrbacekfilip@gmail.com (F. Hrbáček).

1. Introduction

The Antarctic ice-free environments constitute one of the rarest terrestrial ecosystems on Earth. The total ice-free surface in Antarctica is estimated to extend from ca. 45,000 to 70,000 km^2 (Vieira et al., 2010; Terauds and Lee, 2016; Lee et al., 2017; Brooks et al., 2019; Gerrish et al., 2020), which represents less than 0.5% of the surface of the Antarctic continent. The ice-free areas consist of a mosaic of surfaces varying from very small rocky outcrops (< 0.1 km^2) and nunataks, up to large oases (> 100 km^2) distributed along the coastlines and isolated areas in the interior of the continent. The relief of the ice-free areas has been formed over time scales ranging from millions of years, to the accelerated glacial retreat detected in some areas over the last few decades. As a result, the ice-free environments have been shaped by a combination of glacial, periglacial, paraglacial, and other geomorphic processes, producing a variety of landforms (e.g. Ruiz-Fernández et al., 2019; Oliva and Ruiz-Fernández, 2020).

Permafrost and seasonally thawed active layer are key elements of the cryosphere in Antarctic ice-free environments (Ugolini and Bockheim, 2008). The presence or absence of permafrost is of importance for geomorphological, soil, hydrological, and edaphic processes, and terrestrial ecosystem dynamics in Antarctica (e.g. Guglielmin et al., 2014a). Therefore, the thickness of the active layer, or permafrost presence, are key descriptors of Antarctic terrestrial environments. As active layer thickness (ALT) and the distribution of permafrost are sensitive to climate variability, warming, as recorded for the Antarctic Peninsula over the second half of the 20th century (Turner et al., 2020), may lead to a deepening of the active layer and permafrost degradation that, in turn, triggers changes in soil thermal and hydrological regimes. Furthermore, shifts in temperature and moisture regimes affect the abundance of biota (e.g. Convey and Peck, 2019). Permafrost underlies most of the Antarctic continent. The vast majority comprises subglacial permafrost, in both non-cryotic and cryotic forms, below cold- and warm-based glaciers (e.g. Dawson et al., 2022). However, it is unclear whether permafrost is present below subglacial lakes (Dawson et al., 2022), and the extent of submarine permafrost, which has been reported in some areas in Antarctica (e.g.; Guglielmin et al., 2014b) is also poorly understood. In ice-free terrain, permafrost is mostly continuous and absent only in coastal fringes of the western Antarctic Peninsula (Bockheim et al., 2013).

Major progress in Antarctic active layer and permafrost research began during the International Polar Year in 2007/08, when more than 50 new boreholes shallower than 2 m were drilled across the Antarctic continent (Vieira et al., 2010). Since then, the main research topics have aimed at characterizing the ground thermal regime and active layer thickness under the effect of different factors including; atmospheric temperature (e.g. Adlam et al., 2010; Lacelle et al., 2016), snow cover (e.g., Guglielmin et al., 2014b; de Pablo et al., 2017; Ramos et al., 2020; Farzamian et al., 2020; Hrbáček et al., 2021a), lithological conditions (Hrbáček et al., 2017a, 2017b), topography (Carshalton et al., 2022; Chaves et al., 2017; Ferreira et al., 2017;; Francelino et al., 2011; Goyanes et al., 2014; Oliva et al., 2017a; Vieira and Ramos, 2003) or vegetation (Michel et al., 2012; Vieira et al., 2014; Hrbáček et al., 2020a; Cannone et al., 2021). Insights into spatial variability of the active layer mostly come from the monitoring sites of the Circumpolar Active Layer Monitoring – South (CALM-S) programme (Brown et al., 2000; Guglielmin, 2006). Only a few CALM-S sites have been installed in Antarctica due to the hard ground surface conditions (i.e. mostly bedrock, frost-shattering deposits or stony tills) that prevent mechanical probing or other means of spatial measurement of ALT (Guglielmin, 2006; Vieira et al., 2010; de Pablo et al., 2013, 2014, 2018; Guglielmin et al., 2014a; Ramos et al., 2017; Hrbáček et al., 2017a, 2021a, 2021b). Less attention has been given to the thermal state of the deeper permafrost layers. Due to logistical and technical constraints, only a few boreholes have been drilled to reach the depth of zero annual amplitude, typically 10–20 m (Biskaborn et al., 2019).

The harsh climate, environmental conditions, and remoteness of Antarctica, and the technical and logistical difficulties, limit active layer and permafrost research. Thus publications are often fragmented covering short-time, or limited spatial scales. Therefore, we provide a synthesis of the literature on topics related to the active layer thermal regime, active layer thickness, and the permafrost thermal regime, over the last decade, across Antarctica. Particularly, we set three major objectives, which allow us to comprehensively describe the spatial-temporal patterns of the active layer and permafrost in Antarctica:

1) Provide a synthesis of the main results describing active layer and permafrost thermal dynamics in Antarctica.
2) Assess the spatial variability of the Antarctic active layer and permafrost thermal regime.
3) Determine the role of the major parameters driving the thermal state of the active layer and permafrost.

2. Methods

2.1. Geographical analysis

The area of interest of this review includes the Antarctic continent and the surrounding sub-Antarctic Islands. We defined four main regions and twelve sub-regions based on the geographical and climatic conditions (Table 1). A description of each area is provided in the Results section. To determine the total area of each ice-free region, we followed Brooks et al. (2019) and used the combination of most recent data of automatically derived rock outcrops for Antarctica from Landsat-8 in high resolution and vector polygons of rock outcrops derived in the period 1960s to 2019 in high resolution (Antarctic Digital Database; Gerrish et al., 2020). The total extension of polygons of Antarctic ice-free area including South Orkneys is 52,720 km^2. Note, that the selected resolution significantly affects the total extension. For example, the ice-free areas on medium resolution cover more than 70,000 km^2 and was used for example by Terauds and Lee et al. (2016) or Lee et al. (2017).

The lack of widespread monitoring sites across the continent determined slightly different regionalization to that used in other studies such as widely used Antarctic Conservation Biogeographic Regions (ACBRs) by Terauds and Lee (2016). Some of ACBRs were not included in this study due absence of data, except those modelled at continental scale by Obu et al. (2020). The reference MAAT for each region was derived from the READER database.

2.2. Literature synthesis

For each region (Table 1), we provided a synthesis of the scientific literature focusing on the active layer and permafrost thermal regime and/or thickness published since 2011 (Fig. 1). This year was selected as it follows the first synthesis by Vieira et al. (2010) who summarized the progress of active layer and permafrost research during the International Polar Year (2007–2008), including data from previous years. The particular datasets are then analysed for the period from 2006 which serves as a starting point for multiple measurements or experiments including most of the CALM-S sites (Hrbáček et al., 2021b) and, therefore, represents an important milestone for active layer and permafrost research in Antarctica.

Our aim was to extract the following parameters provided in the literature:

- Study period, number of monitoring sites, and depth of installations
- Mean annual air temperature (MAAT)
- Mean annual near-surface ground temperature (MAGT; depths varied between 2 and 10 cm)
- Mean annual temperature on the top of the permafrost table (MAPT). Particular depths are variable for every locality.

Table 1
Overview of study areas.

Region	Sub-region	Ice-free area (km^2)	ACBR[1]	MAAT[2] (°C)	Reference station
Antarctic Peninsula	South Shetlands	572	3	−2.1	Bellingshausen
	Western AP	9000	3,4,15	−2.7	Faraday
	Eastern AP		1	−8.0	Marambio
West Antarctica	Ellsworth Mountains	2140	11	n/a	n/a
	Other regions	776	12	−12.4*	Russkaya
East Antarctica	Queen Maud Land	4485	6	−10.1	Novolazarevskaya
	other regions	9100	5, 7	−11.1	Mawson
Victoria Land and Transantarctic Mountains	McMurdo Dry Valleys		9	−15.8	McMurdo
	North Victoria Land Transantarctic Mountains	26,480	8		
Sub-Antarctic Islands	South Orkneys	167	2	−3.1	Orcadas
	Other Islands	n/a	n/a	0–9	Marion Island

[1] Antarctic Conservation Biogeographic Regions defined by Terauds and Lee (2016).
[2] Mean Annual Air Temperature *1980–1990.

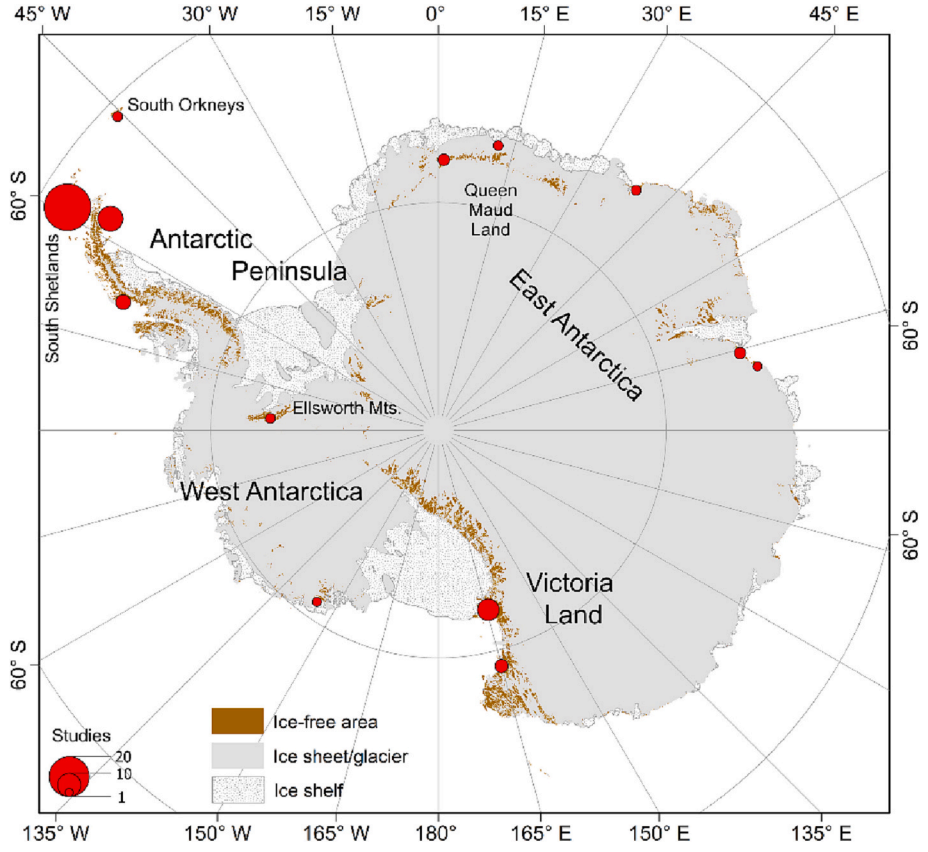

Fig. 1. The spatial distribution, and the number, of studies focused on active layer, or permafrost, thermal regime conducted in Antarctica since 2011.

- Active layer thickness (ALT) defined as a maximum annual depth of the interpolated 0 °C isotherm
- Mean value of mechanically measured active layer thickness on CALM-S sites
- The annual sum of near-surface freezing (FDD) and thawing (TDD) degree day indices
- Freezing and thawing n-factors calculated as a ratio between air and near-surface degree days

These parameters are widely used in permafrost research in Arctic, Antarctic and Alpine environments and are described in detail in the Glossary of Permafrost and Related Ground-Ice Terms (Harris et al., 1988).

We summarized the results in Tables 1 to 8, and datasets providing MAGT, MAPT and ALT for at least 3 consecutive years were displayed as plots. Data variability within each Antarctic region was also evaluated. Finally, using available datasets, we estimated the trend of MAGT for the South Shetlands, Eastern Antarctic Peninsula, East Antarctica and Victoria Land. As the data miss the full temporal overlap, we set year 2011 when the highest data overlay was available as the baseline year for calculation of temperature anomalies. It allows a regional comparison of annual temperature change from sites with heterogeneous climate conditions. The temporal variability of ALT datasets long at least 7 years were then analysed individually for each of the study sites. The resulting trends were investigated using Mann-Kendal statistics with Sen's slope to estimate the trends in the MAKESENS application (Salmi et al., 2002).

Table 2
Selected characteristics of the sites in the South Shetland Island region.

Area	Study site	Study period	Profiles	Profile Depth (cm)	MAAT[1] (°C)	MASGT[2] (°C)	MAPT[3] (°C)	ALT (cm)	TDD (°C·day)	FDD (°C·day)	thawing n-factor	freezing n-factor	Reference
King George Island	Fildes Peninsula (Brazilian sites)	2008–2012	1	85	−2	−1.2 (−0.3 to −1.7)	−1.1	89 to 102.5	ca 200 to 250	−527 to −819			Michel et al., 2012, 2014
	Fildes Peninsula (Bellingshausen)	2008–2016	1	500	−2.3	−0.6	−0.7	60* / 300					Obu et al., 2020; Osokin et al., 2020, Hrbáček et al., 2021a, 2021b
	Lion Rumps	4/2009–1/2011	2	80	−3	−0.9 to −1.9	−0.9 to −1.8	120 to 147				ca 0.4 to 1	Almeida et al., 2014
	Low Head	3/2011–12/2015	1	100	−3.1	−1.5	−1.5	98 to 106	282 to 438	−715 to −1061			Almeida et al., 2017
	Potter Peninsula	2/2008–1/2009	1	90		−0.9	−0.9	92	281	−532			Michel et al., 2012
	Keller Peninsula	2011–2014	2	80	−2.9 to −4.8	−1.7 to −2.8							Chaves et al., 2017
	Keller Peninsula	12/10–1/11	5	30				45 to 70					Lee et al., 2016
Livingston Island	Limnopolar Lake	2009–2018	1	130	−1.7 to −3.2	−0.3 to −1.4		50*/150	36 to 290	−261 to −664			de Pablo et al., 2013, 2014, 2016, 2018
	Domo, Escondido and Cerro Negro Lakes	2/2014–1/2015	3	80	−2.6 to −2.7	−0.7 to −1.3		85 to 115	76 to 134	−311 to −577	–	0.11 to 0.64	Hrbáček et al., 2016a, Oliva et al., 2017a, 2017b
	Rotsch Glacier Transect	2/2017–2/2019	10	40	−2.1	0 to −1.3		102	183 to 321	−241 to −682	1.5 to 2.63	0.27 to 0.76	Hrbáček et al., 2020b
		1/2015	1 (5)	40				90 to 150					Correia et al., 2017
	Mount Reina Sofia (PG1, PG2)	2008–2015	2	110; 25 m	−2.9 to −6.5			20 to 500					Correia et al., 2012; Ramos et al., 2020
	Hurd Peninsula (PAP, CALM, SH, CR, MET, INC, NI)	2007; 2009	7	400 to 800		−0.8 to −1.8		100 to >600	145 to 318	−294 to −1042	0.76 to 10.95	0.43 to 0.80	Ferreira et al., 2017
Deception Island	Port Foster	2011	2	80	−2.6	0 to −1							Goyanes et al., 2014
	Crater Lake CALM-S	2006–2014	1	100 to 450	−3	−1.7		23–36 [1]					Ramos et al., 2017
Other areas	Coppermine Peninsula (Robert Island)	2014–2016	2			ca −1.5 to −2			ca 10 to 70	ca −500 to −700			Thomazini et al., 2020

[1] Mean annual air temperature.
[2] Mean annual near-surface ground temperature.
[3] Mean annual temperature of the permafrost table.
* Probing measurement.

Table 3
Selected characteristics of sites in the Western Antarctic Peninsula region.

Area	Study site	Study period	Profiles	Profile Depth (cm)	MAAT[1] (°C)	MASGT[2] (°C)	MAPT[3] (°C)	ALT (cm)	TDD (°C·day)	FDD (°C·day)	thawing n-factor	freezing n-factor	Reference
Western AP	Amesler Island		8	160 to 1400			−0.7 to −1.9	ca 1 to 17*	186 to 307				Wilhelm et al., 2015; Wilhelm and Bockheim, 2016, 2017; Uxa, 2016
	Rothera	2/2009–2/2012	3	30 m	−3	−2.7 to −4.6	−1.5 to −4.8	65 to 140 cm	186 to 618	−1143 to −1731			Guglielmin et al., 2014b
	Cierva Cove		1	160									Wilhelm and Bockheim, 2017

[1] Mean annual air temperature.
[2] Mean annual near-surface ground temperature.
[3] Mean annual temperature of the permafrost table.

3. Results

3.1. Antarctic Peninsula region

The Antarctic Peninsula region (AP) forms the northernmost tip of the Antarctica continent. The region, including the neighbouring sub-Antarctic islands (SAI), is located south of South America, between latitude 60°S and 75 and longitude 44°W to 75°W. The AP region, including the SAI, exceeds 540,000 km^2, of which only ca. 9500 km^2 constitute ice-free terrain (Table 1). Considering the geographical diversity of the AP, we set three major sub-regions – South Shetland Islands (SSI) Western Antarctic Peninsula (Western AP), and Eastern Antarctic Peninsula (Eastern AP).

3.1.1. South Shetland Islands

The SSI constitute an archipelago extending over 3687 km^2 in the NW sector of the Antarctic Peninsula. Located at latitudes 61–63°S and longitudes 54–62°W, the SSI run SSW-NNE, parallel to the Antarctic Peninsula, at a distance of 100–120 km. The SSI archipelago is located in a tectonically active zone with several active volcanoes (e.g. Penguin and Deception islands).

During the last glacial cycle, a large ice cap extended from the Antarctic Peninsula and covered the SSI. Post-Last Glacial Maximum warming favoured the shrinking of the ice sheet, and from ~15 to 10 ka a single ice cap, disconnected from the continent, covered the SSI archipelago (Ó Cofaigh et al., 2014). Subsequently, as temperatures increased, at the onset of the Holocene, glacial masses were limited to the respective islands. Holocene glacial shrinking has exposed the land surface on the margins of some of the islands (Oliva et al., 2019), which are still heavily glaciated (between 85 and 100% of the total island surface covered by ice).

The SSI record the highest mean annual air temperatures of Antarctica, with values of ~ − 2 °C at sea level (e.g. Turner et al., 2020) and an annual precipitation between 500 and 800 mm (Bañón et al., 2013). Snow cover generally persists on the ground for 8–9 months per year. The archipelago is composed of Late Palaeozoic to Quaternary sedimentary, metamorphic, plutonic and volcanic rocks (López-Martínez et al., 2016). The scarce ice-free areas in the SSI archipelago are affected by active periglacial dynamics, with intense frost weathering (Simas et al., 2008; López-Martínez et al., 2012). Vegetation cover is scarce and mostly composed of mosses and grasses along the Holocene marine terraces with abundant lichens on relatively flat areas near lakes and ponds (Ruiz-Fernández et al., 2017).

3.1.1.1. King George Island. King George Island is the largest island in the SSI archipelago with an area of 1124 km^2. The ice-free surfaces occupy ca. 190 km^2 of the island, mainly concentrated in several peninsulas, including; Fildes (30 km^2), Keller (10 km^2) and Barton peninsulas (10 km^2). The deglaciation of Maxwell Bay (south of Fildes Peninsula) began between 17 and 14 ka cal BP and was fastest between 7 and 6 ka (Yoon et al., 1997; Simms et al., 2011; Oliva et al., 2023). The deglaciation of the smaller peninsulas began around 8 ka cal BP- (Barton Peninsula; Oliva et al., 2019). The topography of the ice-free areas is dominated by volcanic outcrops reaching ca. 120 to 150 m a.s.l. surrounded by a relatively flat area. The current MAAT on King George Islands is around −2.1 °C (Tables 1, 2), with a recent warming rate of 0.13 °C/decade over the period 1968–2015 (Oliva et al., 2017b). The annual precipitation is around 500–1000 mm, with prevailing winter snowfall and rainfall during the summer season (van Wessem et al., 2016). The vegetation forms relatively large patches of mosses or lichens in poorly drained areas. Two vascular plant species also occur in lower altitude areas (e.g. Cannone et al., 2016).

Although King George Island includes the greatest number of human infrastructures in Antarctica, research on active layer and permafrost dynamics is incipient and has mainly focused on soil biogeochemical conditions (e.g. Bockheim, 2015; Boy et al., 2016; Prater et al., 2021). The only known long-term monitoring study of active layer and permafrost temperatures, including the only CALM-S grid, has operated near Bellingshausen station since 2006 (Vieira et al., 2010; Osokin et al., 2020; Hrbáček et al., 2021b). Data from other parts of the King George Islands are fragmented with several studies describing the short-term variability of the active layer thermal regime and ALT on several peninsulas in the southern part of the island.

The MAGT near Bellingshausen Station, which has the longest record on Fildes Peninsula (2006–2015), was −0.6 °C (Hrbáček et al., 2021b). The thaw depth varied between 75 and 115 cm (Osokin et al., 2020), and the ALT commonly exceeded 300 cm in bedrock conditions (Hrbáček et al., 2021b). Michel et al. (2012, 2014) reported that ALT, on soils covered by vegetation, ranged between 89 and 102 cm (Fig. 2) and the TDD were between 200 and 400 °C·day, whereas FDD ranged from −527 to −819 °C·day (Table 2). The MAPT is around −1.5 °C.

Data from the Barton and Potter peninsulas are restricted to a short-term monitoring of active layer thermal regime and ALT. The ALT in the vicinity of King Sejong station, near to sea level on Barton Peninsula, varied between 41 and 70 cm in the summer of 2011 (Lee et al., 2016). One year of monitoring on Potter Peninsula showed MAGT of −0.7 °C and an ALT of 92 cm in summer 2008 (Michel et al., 2012).

Chaves et al. (2017) reported that the thermal regime of patterned-ground soils on the Keller Peninsula varied across the patterned ground features. The stony garlands along the edge of the striations had more rock fragments and were more susceptible to energy variations at the surface, resulting in faster thawing/freezing, with a thicker active layer, than the moss-covered polygon centre. Yet, the mean daily soil temperature was −2.1 °C, both at the border and between the polygon centre. The ALT of the patterned-ground soil was 75 cm at the polygon border, and 64 cm at the center, where temperatures remained below

Table 4
Selected characteristics of sites in the Eastern Antarctic Peninsula region.

Area	Study site	Study period	Profiles	Profile Depth (cm)	MAAT[1] (°C)	MASGT[2] (°C)	MAPT[3] (°C)	ALT (cm)	TDD (°C·day)	FDD (°C·day)	thawing n-factor	freezing n-factor	Reference
James Ross Island	J.G.Mendel	2011–2021	1	200	−6.7 (−3.9 to −8.8)	−5.4 (−3.4 to −6.8)	−5.6 (−4.4 to −6.3)	60 (50 to 67)	471 (379 to 603)	−2450* (−1783 to 2812)			Hrbáček et al., 2016b, 2017a, 2019, Hrbáček et al., 2021a, 2021b, Kaplan Pastíriková et al., 2023
	CALM-S JGM	2014–2018	1	200	same as above	−4.9 to −5.6	−5.2 to −5.8	82 to 90	416 to 502	−2230 to −2510	3.57 to 4.86	0.85 to 0.9	Hrbáček et al., 2017b, 2021a, 2021b
	Berry Hill slopes	2011–2015	1	90	−6.6 to −7.6	−5.7 to −7.0	−5.6 to −6.6	85 to 89	300 to 382	−2444 to −2810	2.4 to 4.4	0.91 to 0.97	Hrbáček et al., 2017b, 2019
	Abernethy Flats	2006–2015; 2017	1	75	−7.3 (−5.1 to −8.1)	−6.1 (−3.8 to −8.2)	−6.3 to −7.4	38 to 68	370 (386 to 432)	−2586 (−1745 to −3116)	2.35 (1.59 to 3.21)	0.93 (0.71 to 1.03)	Hrbáček et al., 2016a, 2017b, 2019, Hrbáček and Uxa, 2020, Kňažková et al., 2020
	Monolith Lake	2017	16	20	–	−5.4 to −6.7	–	–	152 to 509	−2259 to −2768	–	–	Kňažková et al., 2020
	Cape Lachman - bare ground	3/2015–2/2017	1	50	−4.3 to −7.2	−3.5 to −5.5	–	61 to 64	396 to 409	−1718 to −2425	1.64 to 1.91	0.85 to 0.94	Hrbáček et al., 2020a
	Cape Lachman - moss	3/2015–2/2017	1	50		−4.4 to −6.7	–	50	172 to 195	−1807 to 2641	0.69 to 0.95	0.93 to 0.99	
Trinity Peninsula	Hope Bay	2/2009–2/2011	2	80		−4.1 to −5.6	−4.1 to −5.3	73 to 128					Schaefer et al., 2017a, 2017b
Seymour Island	Seymour Island	3/2011–2/2012	1	100	−10.3	−8.7	−8.3	100 cm		−2985			Gjorup et al., 2020

[1] Mean annual air temperature.
[2] Mean annual near-surface ground temperature.
[3] Mean annual temperature of the permafrost table.

Table 5
Selected characteristics of the sites in West Antarctica region.

Area	Study site	Study period	Profiles	Profile Depth (cm)	MAAT[1] (°C)	MASGT[2] (°C)	MAPT[3] (°C)	ALT (cm)	TDD (°C·day)	FDD (°C·day)	thawing n-factor	freezing n-factor	Reference
Ellsworth Mountains		2012–2013	2	30	−19.8	−18.2 to −18.4	−18.3	47–48 cm	ca 40 to 150	ca −6500 to −7000		0.93–0.94	Schaefer et al., 2017a, 2017b
Ellsworth Mountains		12/2016–11/2017	1	49	−20.3		−19.3	10 to 45 cm					McKay et al., 2019
Marie Byrd Land	Russkaya	2008/2013	1				−10.4	10 to 20 cm					Bockheim, 2015; Obu et al., 2020

[1] Mean annual air temperature.
[2] Mean annual near-surface ground temperature.
[3] Mean annual temperature of the permafrost table.

Table 6
Selected characteristics of the sites in East Antarctica region.

Area	Study site	Study period	Profiles	Profile Depth (cm)	MAAT[1] (°C)	MASGT[2] (°C)	MAPT[3] (°C)	ALT (cm)	TDD (°C·day)	FDD (°C·day)	thawing n-factor	freezing n-factor	Reference
Queen Maud Land	Vesleskarvet nunatak	2009–2012	1 (20 sample points)		*-2.2 to −27.8 (= −15)? (Setting)								Hansen et al., 2013
	Vesleskarvet nunatak	2009–2013	1	60 cm	−15.9 to −18.5	−16.1		14 to 20 cm		−5448 to −5933 (near-surface); −6404 to −7214	1.00–1.02		Kotzé and Meiklejohn, 2017, Hrbáček et al., 2021a, 2021b
	Flarjuven	2008–2015	1	60 cm	−17.9	−17.5		23 (13 to 26)					Hrbáček et al., 2021a, 2021b
	Troll	2007–2015	1	200 cm	−17.4	−17.4		13 (10 to 15)					Hrbáček et al., 2021a, 2021b
	Novolazarevskaya		1		−10.3	−10.1		100 cm					Hrbáček et al., 2021a, 2021b
Prydz Bay	Vestfold Hills and Larsemann Hills oases	1/2010	4		*-9.8 to −10.2 (Objects)	−8.4		83 ± 14 cm (max 110)					Mergelov, 2014
Enderby Land	Molodyozhnaya	2008–2015	1	100 cm	−11			65 to >100 cm					Hrbáček et al., 2021a, 2021b

[1] Mean annual air temperature.
[2] Mean annual near-surface ground temperature.
[3] Mean annual temperature of the permafrost table.

0 °C at 80 cm depth (Fig. 2).

The Krakow Peninsula contains several small ice-free areas. Short-term active layer monitoring results were reported from Lions Rump (Almeida et al., 2014), whereas five-year results are available from a nearby site at Low Head (Almeida et al., 2017). Both areas are located in the eastern part of the Krakow Peninsula. At Lions Rump there was no gradient of MAGT between the surface and the top of the permafrost table. Depending on the site conditions, observed mean annual temperatures varied between −0.9 °C (moss-covered site) and − 2.0 °C (lichen-covered site) in 2009/2010, with a relatively thick active layer of about 120–150 cm (Almeida et al., 2014). A similar thermal regime pattern was observed in Low Head. The MAGT did not show any depth gradient and was −1.5 °C at both 1 and 100 cm depths (Fig. 2). The annual sum of TDD ranged between 280 and 440 °C·day, whereas the FDD were − 700 to −1100 °C·day at a depth of 1 cm. The ALT was between 98 and 106 cm (Table 2).

Overall, the ground thermal regime on King George Island over recent years correlates well with the evolution of air temperatures on the island (e.g. Michel et al., 2014; Almeida et al., 2017). The role of the factors such as vegetation, snow cover, or lithological variability has not yet been studied in detail. Although the area is considered to be in bordering conditions for continuous permafrost conditions (Bockheim et al., 2013), there are currently no reports suggesting the absence of permafrost at specific sites on King George Island. Indeed, modelled temperatures at the top of the permafrost, using Cryogrid 1 model, of less than 0 °C suggest continuous permafrost conditions on the entire island (Obu et al., 2020).

3.1.1.2. Livingston Island. Livingston is an elongated island running west-east for approximately 72 km along the 62°35′ S parallel. Livingston Island has an irregular coastline, with several peninsulas and with the relief passing from the low-lying platform of Byers Peninsula, in the west, to the very rugged Friesland mountains that rise up to 1700 m in the eastern limit of the island. Byers is the largest ice-free area of the SSI, while Hurd Peninsula, closer to the Friesland range also has several ice-free areas. Elsewhere, ice-free terrains occur in small peninsulas around the island (e.g. Elephant Point, Hannah Point, Cape Shirreff and Barnard Point), or in small nunataks. Livingston Island is glaciated in over 90% (Recondo et al., 2022) of its area and dominated in the west by the Rotch Dome, and in the east by the glaciated peaks of the Friesland, with small steep valley glaciers flowing directly into the sea.

3.1.1.3. Byers Peninsula. Byers Peninsula is 9 to 18 km long (84.7 km^2) and formed after the last deglaciation in the Holocene (e.g., Oliva et al., 2016), starting about 5000–4000 years BP (Björck et al., 1996). Byers Peninsula is of high geomorphological, periglacial, and ecological interest and has been specially protected by the Antarctic Treaty since 1966 (Quesada et al., 2009), allowing a wide variety of research activities (Benayas et al., 2013), including active layer permafrost research. The climate of Byres Peninsula is classified as wet oceanic with MAAT around −2.8 °C. Temperatures range between −25 °C in winter and + 10 °C in summer (e.g; Bañón et al., 2013), and annual precipitation, mainly as snow, is about 500–800 mm, with snow persisting on the ground surface between 8 and 9 months per year (Bañón et al., 2013; Navarro et al., 2013).

The central spine of the Byers Peninsula is characterized by a smooth, slightly wavy, platform, of about 70–100 m in elevation, with shallow basins, where lakes and ponds are located, and low mounds (Thomson and López-Martínez, 1996). A few small hills (up to 140 m a.s.l.) of eroded volcanic edifices protrude from the platform, which is characterized by Jurassic and Early Cretaceous sediments and volcanic and volcanoclastic materials (e.g., Smellie et al., 1980, 1984; López-Martínez et al., 2012; Hathway and Lomas, 1998). The coast is marked by wide present-day beaches, with 7 levels of terraces that formed during Holocene deglaciation (Oliva et al., 2016). The soils of Byers Peninsula

Table 7
Selected characteristics of the sites in Victoria Land region.

Area	Study site	Study period	Profiles	Profile Depth (cm)	MAAT[1] (°C)	MASGT[2] (°C)	MAPT[3] (°C)	ALT (cm)	TDD (°C·day)	FDD (°C·day)	thawing n-factor	freezing n-factor	Reference
Dry Valleys	Granite Harbour	2003–2018	1	90	−16 (−14.8 to −17.8)	−14 (−13.1 to −16.3)	−14 (−12.9 to −14.5)	89 cm (82 to >90 cm)					Adlam et al., 2010; Seybold et al., 2010; Hrbáček et al., 2021a, 2021b; Carshalton et al., 2022
	Marble Point	1999–2018	1	120	−18 (−16.0 to −18.7)	−17		49 cm					Adlam et al., 2010; Seybold et al., 2010; Guglielmin et al., 2011; Hrbáček et al., 2021a, 2021b; Carshalton et al., 2022
	Minna Bluff	2003–2018	1	107	−16	−17		23 cm					Adlam et al., 2010; Seybold et al., 2010; Hrbáček et al., 2021a, 2021b; Carshalton et al., 2022
	Mt Fleming	2002–2018	1	60	−23	−24		7 cm					Adlam et al., 2010; Seybold et al., 2010; Hrbáček et al., 2021a, 2021b; Carshalton et al., 2022
	Bull Pass East (Wright Valley – North)	2012–2018	1	120	–	–							Adlam et al., 2010; Seybold et al., 2010; Hrbáček et al., 2021a, 2021b; Carshalton et al., 2022
	Wright Valley – South wall	2011–2018	1	120	−17	−17							Adlam et al., 2010; Seybold et al., 2010; Hrbáček et al., 2021a, 2021b; Carshalton et al., 2022
	Wright Valley (floor)	1999–2018	1	120	−19	−19		49 cm					Adlam et al., 2010; Seybold et al., 2010; Guglielmin et al., 2011; Hrbáček et al., 2021a, 2021b; Carshalton et al., 2022
	Scott Base	1999–2018	1	120	−17	−16							Adlam et al., 2010; Seybold et al., 2010; Hrbáček et al., 2021a, 2021b; Carshalton et al., 2022
	Victoria Valley	1999–2018	1	120	−23	−23							Adlam et al., 2010; Seybold et al., 2010; Hrbáček et al., 2021a, 2021b; Carshalton et al., 2022
	Beacon Valley	2001–2012	1		−21.6 + − 0.7	−21.4 + − 0.8							Lacelle et al., 2016; Liu et al., 2018
	University Valley	2015–2016	1			ca. -23 °C							Lacelle et al., 2016
	Wormherder Creek wetland	2010–2012	1		−23.4 ± 8.3 °C	−26 ± 10.6 °C (2010)							Fisher et al., 2016
	Taylor Valley		1		−18 (Doran et al. 2002)			~10–60 cm (Bockheim et al., 2007)					Levy et al., 2011
Northern Victoria Land	Boulder Clay	1997–2012	1		−13.8 (−12.7 to −15.3)	−16.1 (−14.6 to −18.4)		24.5 (6 to 30 cm)					Guglielmin et al., 2012; Cannone et al., 2021
	Prior Island, Boulder Clay MZS, Edmonson Point, Apostrophe Island	2000 (2002) - 2013	4		−12.5 to −15.3	−0.3 to 7.8		2 to 18 cm (max 23 to 92 cm)	39 to 370.1				Guglielmin et al., 2014a, 2014b
	Edmonson Point	2015–2016	1 (3)		−16.4 to −16.6	−13.5 to −15.8		23 to 40 cm	110.8 to 702.6 (GT)	−5164.5 to −5940.2 (GT)	10.83 to 52.23	0.92 to 0.99	Hrbáček et al., 2020a

[1] Mean annual air temperature.
[2] Mean annual near-surface ground temperature.
[3] Mean annual temperature of the permafrost table.

Table 8
Selected characteristics of the sites in Sub-Antarctic Islands region.

Area	Study site	Study period	Profiles	Profile Depth (cm)	MAAT[1] (°C)	MASGT[2] (°C)	MAPT[3] (°C)	ALT (cm)	TDD (°C·day)	FDD (°C·day)	thawing n-factor	freezing n-factor	Reference
Signy Island	BG1	2006–2009, 3/2015–2/2017	1	250	−3.4 to −4.2	−1.9 to −2.9		124 to 185	231 to 538	−1074 to −1453	2.16 to 2.29	0.77 to 0.78	Guglielmin et al., 2012; Hrbáček et al., 2020a
	BG2	2006–2009	1	90		−2.0 to −2.5		83 to 163	125 to 385	−877 to −1190			Guglielmin et al., 2012
	Andreaea	2006–2009	1	90		−1.6 to −2.5		95 to 108	215 to 449	−900 to −1333			Guglielmin et al., 2012
	Sanionia	2006–2009, 3/2015–2/2017	1	60		−1.7 to −3.0		55 to 123	29 to 413	−770 to −1162	0.29 to 0.55	0.54 to 0.69	Guglielmin et al., 2012; Hrbáček et al., 2020a
Marion Island (PEIs)		2015	2	–	0.5–5.5	0.6–4.6		none	392 to 499	−95 to −195			Nel et al., 2021, Hansen, 2018 for MASGT, TDD, FDD
Campbell Islands		2015; 2017		–	3.8 to 6			none					Forte et al., 2016
Crozet Islands		2007		–	3 to 8			none					Quilty, 2007
Kerguelen Island		2006		–	2 to 9			none					Leihy et al., 2018

[1] Mean annual air temperature.
[2] Mean annual near-surface ground temperature.
[3] Mean annual temperature of the permafrost table.

are coarse-grained with a sandy silty matrix (Navas et al., 2008; Moura et al., 2012). The vegetation, classified as open tundra, is scarce and consists of patches of mosses and lichens, as well as the only two autochthonous vascular plants in Antarctica, *Deschampsia antarctica* and *Colobanthus quitensis* (e.g.; Serrano, 2003; Vera, 2011).

Prior to the IPY (2007/08) research on permafrost and frozen ground in Byers Peninsula consisted of geomorphological mapping revealing a wide variety of periglacial landforms associated with the presence of continuous permafrost, an active layer, and freeze-thaw processes (Serrano et al., 1996; López-Martínez et al., 1996, López-Martínez et al., 2012). Permafrost was also detected in the coastal Holocene terraces (Serrano et al., 1996, 2003), confirming its major role in groundwater dynamics (Cuchi et al., 2004).

In 2009, during the IPY, a TSP (Thermal State of Permafrost) and a CALM site (Limnopolar Lake CALM site A-25) were established at the Limnopolar Lake watershed for continuous temperature monitoring of the active layer and ALT measurement by mechanical probing within 100 × 100 grid (de Pablo et al., 2013, 2014, 2016, 2017, 2018, 2020). The TSP station consists of two shallow boreholes (80 and 130 cm deep) and includes devices to measure air and ground surface temperatures, as well as a snow pole to derive snow cover (de Pablo et al., 2016). Other sites for ground temperature measurements in Byers Peninsula do not provide continuous data as they were installed for the purpose of short-term monitoring. Three shallow boreholes (80 cm) are located near to lakes Domo, Escondido and Cerro Negro (Hrbáček et al., 2016a; Oliva et al., 2017a), and 9 shallow measurement pits (10 cm) were installed in a transect from Rotch Dome towards the sea (Hrbáček et al., 2020b).

Existing shallow TSP boreholes in Limnopolar Lake do not reach the permafrost table but only the active layer. Permafrost was calculated to exist at less than 1.5 m deep based on the ground temperatures at the boreholes (de Pablo et al., 2013, 2014). The temperature, estimated for 10 shallow boreholes along a transect from Roch Dome Glacier, at the top of the permafrost ranged between −0.7 °C and − 1.2 °C (Hrbáček et al., 2020b). The measured surface offset was 1.7 °C, revealing the presence of a surficial isolator. In the absence of vegetation, snow/ice is the unique possible insulation source. The presence of a zero curtain period, in the thermal signal measured at the ground surface, suggests that an ice layer formed at the base of the snow cover, during the melt period. The zero-curtain period had high interannual variability; from 30 to 90 days (de Pablo et al., 2014). Based on the ground temperatures, the annual ground thermal regime could be divided into thaw and freeze seasons (de Pablo et al., 2014). Thawing seasons ranged from 60 to 90 days while freezing periods extended from 270 to 300 days (de Pablo et al., 2014). Mean GST varied by about −1 °C with thermal amplitudes of about 15 °C (de Pablo et al., 2014).

The thaw depth measured at the CALM site decreased between 2009 and 2015, increasing again in 2016 (de Pablo et al., 2018), related to an increase in snow depth in that period (de Pablo et al., 2016, 2018, 2020). The thaw depths represent the mean value from the CALM-S site measured, usually, in early February. Therefore, the mean thaw depth was lower than the maximum ALTs, which reached about 150 cm (Fig. 2, Table 2). The difference is due to the measuring date in early February, established by logistic constraints, which is earlier than the timing of maximum thaw that usually occurs during March in this region (de Pablo et al., 2014). The ALTs at the other sites on Byers Peninsula were estimated to be ca. 85 to 115 cm (Oliva et al., 2017a; Hrbáček et al., 2020a).

Reported reduction in the freezing n-factor is likely to be due to increasing insulation of the ground surface from atmospheric conditions (de Pablo et al., 2017) due to snow cover. However, a reported reduction in snow-free days (2009 and 2015 period), limited the period in which the ground could have /thawed during the summer, or freeze during the early freeze season (de Pablo et al., 2017), reducing ground surface FDD from −670 °C day in 2011 to −230 °C day in 2013 (Table 2). Meanwhile air FDD where quite stable at about −1000 °C day (de Pablo et al., 2017, 2018). Although snow cover seems to play an important role due to

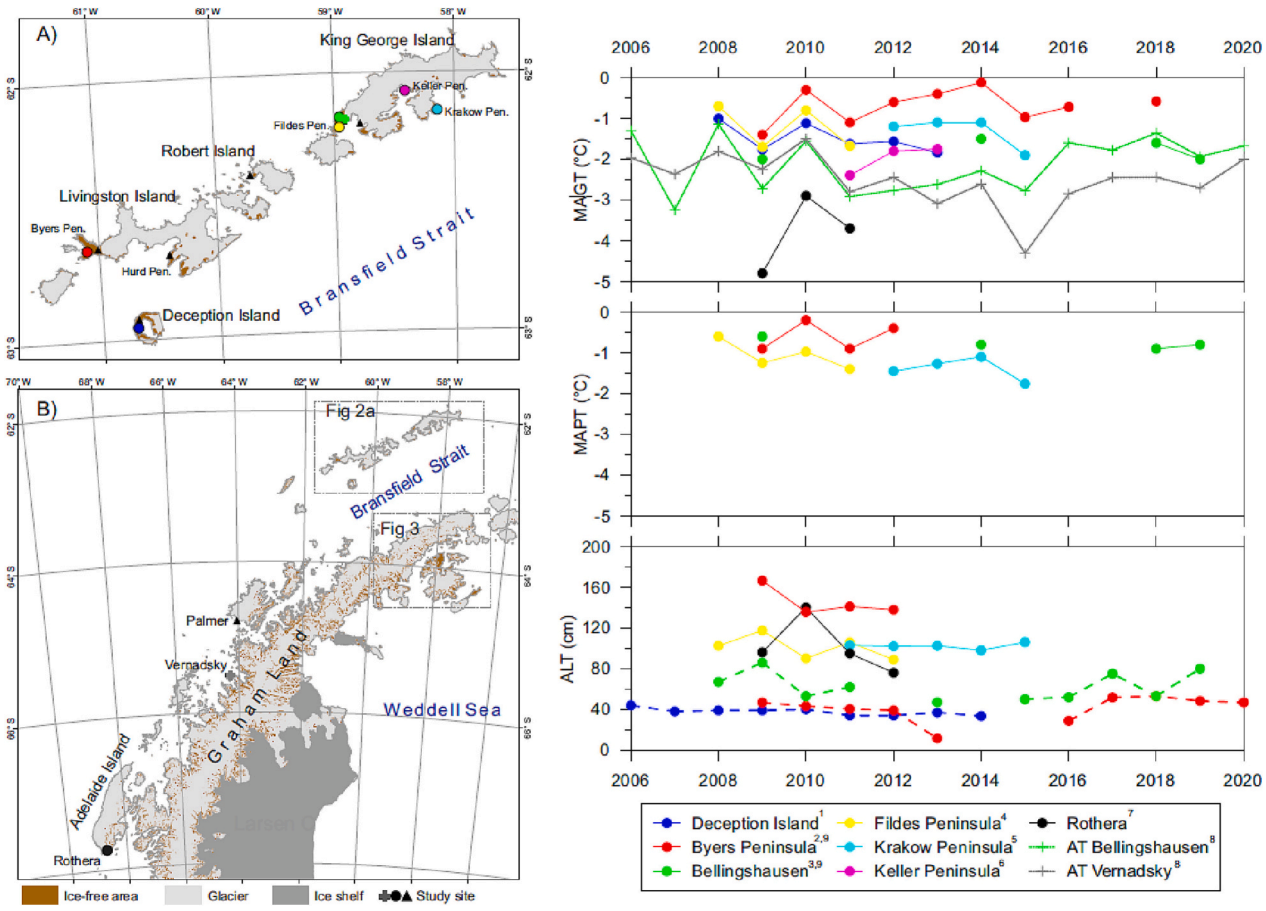

Fig. 2. The variability of mean annual near-surface ground temperature (MAGT), mean annual temperature, the permafrost table (MAPT), and active layer thickness (ALT) in selected sites of the South Shetland Islands and Western Antarctic Peninsula. Dashed line in the lowest figure indicate ALTs measured by mechanical probing. The data were extracted from studies by [1]Ramos et al., 2017; [2]de Pablo et al., 2014, 2018; [3]Hrbáček et al., 2021b; [4]Michel et al., 2014; [5]Almeida et al., 2017; [6]Chaves et al., 2017; [7]Guglielmin et al., 2014a, 2014b; [8]READER database, [9]CALM database. Black triangles indicate the position of other study sites in the region.

differential snow accumulation on the wavy relief of the peninsula central plateau (de Pablo et al., 2017), other factors such as the groundwater flow (Cuchi et al., 2004; de Pablo et al., 2013, 2014, 2018), and lithological conditions (e.g., Serrano et al., 1996; López-Martínez et al., 1996 have not yet been studied in this ice-free area, the largest of the SSI.

3.1.1.4. Hurd Peninsula. Hurd Peninsula is a small, rugged, elongated area, ca. 8 km long and 1 to 4 km wide that divides South Bay from False Bay on the southern coast of Livingston Island. Most of the peninsula is glaciated, with the Hurd Peninsula ice cap that drains through several small lobes, and with several small ice-free areas that run from sea-level to 407 m a.s.l. at Moores Peak. The bedrock is mainly composed of the Myers Bluff Formation, a turbidite sequence with alternating layers of low-grade metamorphism, claystone, and fine sandstone, with a diorite batholite in the northern sector (Pimpirev et al., 2006). Mean annual air temperatures in Hurd Peninsula are about −1.2 °C at sea level (Bañon and Vasallo, 2015), and − 4.2 °C at 275 m in Reina Sofia Peak (Ferreira et al., 2017).

Active layer and permafrost monitoring commenced in Hurd Peninsula in the 1990's near the Spanish Station Juan Carlos I. In 2000 two shallow (70 cm) boreholes were installed with continuous temperature monitoring. During the IPY 2007–08, two deep boreholes (15 and 25 m) were drilled in the Reina Sofia Peak area (Ramos and Vieira, 2009) and three new boreholes, ranging from 4 to 8 m deep, were installed across an altitudinal gradient near the Bulgarian Station St Kliment Ohridski (Vieira et al., 2010; Ferreira et al., 2017).

Permafrost in Hurd Peninsula is absent at low elevations, except in ice-cored moraines or rock-glaciers (Hauck et al., 2007). However, boreholes drilled in bedrock had a thick active layer (> 5 m), and suggest that the boundary of the continuous permafrost zone may be located above ca. 150 m a.s.l. (Ferreira et al., 2017). The shallow boreholes drilled in diamicton, below 150 m a.s.l., did not have permafrost, which suggests that there is a narrow belt of discontinuous permafrost between sea-level and ca. 150 m a.s.l.

The permafrost temperature at 25 m depth in the Permamodel-Gulbenkian 1 borehole varied between −2.0 and − 1.7 °C from 2009 to 2015, with no clear trend (Biskaborn et al., 2019). The active layer at Reina Sofia Peak, in a diamicton, was ca. 76 cm in 2009 and only 26 cm in 2015. At Reina Sofia, in 2008 and 2009 FDD ranged from −1042 to −811 °C·day and the TDD ranged from 49 and 145 °C.days (Ferreira et al., 2017). The N-Factor ranged from 0.53 to 0.57 in those same years. Papagal, located at 152 m a.s.l., had 214 TDD °C·day and − 783 FDD °C·day in 2009, with a higher freezing n-factor than Reina Sofia (0.7) (Ferreira et al., 2017, Table 2). The snow cover, mainly controlled by topography, rather than elevation, was considered the main controlling factor on the ground thermal regime (Ferreira et al., 2017). Recently, Ramos et al. (2020) have shown that the increase in snow cover thickness between 2009 and 2015 at the borehole Permamodel-Gulbenkian-2, led to the full disappearance of the active layer and to the aggradation of permafrost. However, wind-exposed boreholes in bedrock at Hurd Peninsula at Papagal and CALM Ohridski had an ALT exceeding 5 m, (Ferreira et al., 2017). Like other boreholes in the Antarctic Peninsula region, there was a general decrease in active layer thickness from 2009 to 2015 that was associated with a longer occurrence of snow

persistence in the summer season after 2009 (Oliva et al., 2017a, de Pablo et al., 2020, Ramos et al., 2020).

3.1.1.5. Deception Island. Deception Island is a composite volcano with a well-defined main cone ca. 14 km in diameter in its subaerial part and a collapse caldera of ca. 8.5 × 10 km, which is open to the sea in a 500 m breach in the SE coast. The main crater rim rises to 539 m a.s.l.at Mount Pond, with most of the rim more than 250 m a.s.l. Several glaciers are present along the rim, with the ones on the eastern side of the island flowing down to the sea-level, either to the caldera or to the outer coast. The glacier-free area is dominated by lava flows, interbedded with ash and pyroclastic deposits, both from the pre and post-caldera stages (López-Martínez and Serrano, 2002). The inner part of the rim has been affected by several volcanic eruptions, including recent ones in 1967, 1969, and 1970 (Ortiz et al., 1997). The eruptions generated large volumes of lapilli and ash that cover large areas of the island, some burying glaciers and snow patches. The island's substrate is poorly consolidated and, under the effects of the Maritime Antarctic climate, with high snow accumulation and summer temperatures favouring snowmelt and rain events, is prone to water erosion. Vegetation cover only occurs in small, localized, patches, and the lack thereof exposes the islands' soils to severe wind erosion, generating lag surfaces mainly on ridges and convex surfaces (Vieira et al., 2008). Several localities of Deception Island have high geothermal anomalies, with ground temperatures of up to about 90 °C (e.g. Cierro Caliente) and fumaroles or geothermally heated caldera waters occur at several sites. Goyanes et al. (2014) have shown that geothermal anomalies may have a local effect, for example; in the alluvial fan close to the Argentinean station, over about 100 m laterally, ground temperatures pass from a stable +10 °C all year-round, to permafrost.

Most of Deception Island shows the presence of permafrost, except at the beaches, where the influence of sea-water plays a role in warming the terrain. Permafrost and active layer monitoring was initiated in the 1990's with the installation of active layer sensors at various sites, with research focussing on the energy exchange between the soil and the atmosphere (Ramos and Aguirre-Puente, 1994). The initial activities did not include continuous monitoring, as observations were focussed on characterizing the freezing and/or thawing seasons. However, monitoring was conducted at Cerro JB in the vicinity of the Spanish Station Gabriel de Castilla and in Cerro Caliente (Ramos et al., 2007).

In 2006 a CALM-S site was installed on a small plateau in the western rim of Crater Lake (Hauck et al., 2007; Ramos et al., 2010). Continuous monitoring includes a CALM-S grid, 3 permafrost boreholes, a snow-meteorological station (de Pablo et al., 2016), several shallow boreholes, and an automatic electrical resistivity tomography monitoring system (Farzamian et al., 2020). In 2009 the Irizar CALM-S site was established at the crater rim close to Vapour Col in order to obtain data from a wind-exposed site, since Crater Lake is sheltered from the west-winds. Crater Lake comprises a soil characterized by a thick lapilli cover, which generates high insulation, and thus a shallow active layer. Irizar has a lag-surface with a more permeable soil, which results in a thicker active layer. Both CALM-S grids have continuous monitoring of active layer and permafrost temperature, and are probed once per year, generally in early February, for active layer thickness in 100 × 100 m grids. Shallow boreholes located outside the two CALM-S grids were installed at the Chilean Refuge in 2010, close to the Argentinean Station in 2011, and at Fumarole Bay in 2012.

The mean annual air temperature at Crater Lake from January 2009 to January 2014 was −3.0 °C. At the Crater Lake CALM-S site, permafrost occurs beneath a shallow active layer of 25 to 40 cm (Fig. 2) and is from 2.5 to 5 m thick, with temperatures from −0.3 to −0.9 °C (Vieira et al., 2008; Ramos et al., 2017; de Pablo et al., 2020). Crater Lake had a decreasing thaw depth from 2006 to 2014 following several years of longer lasting snow cover (Ramos et al., 2017), with de Pablo et al. (2020) reporting that the decline continued until 2016. The studies indicate that snow cover plays a major role in the shallowing of the active layer and that it may even decouple ground cooling from the slight atmospheric warming (de Pablo et al., 2020).

The Irizar CALM-S site is located in a wind-exposed setting and recorded a MAAT from −2.0 to −3.9 °C with an active layer, varying from 40 to ca. 100 cm. The thicker active layer atIrizar may be a result of the lack of the lapilli cover that insulates the ground at Crater Lake.

3.1.1.6. Other areas. Beyond the monitoring on King George Island, Livingston Island, and Deception Island, little information on active layer or permafrost is available in the region. Bockheim et al. (2013) mention the ALT on Half Moon Island (10–50 cm) and Elephant Island (15–110 cm). Thomazini et al. (2020) provided 2-years of MAGT data from Copermine Peninsula (Robert Island) revealing annual temperatures around −1.5 and − 2.0 °C (Table 2), but did not report data on ALT dynamics.

3.1.2. Western Antarctic Peninsula

The Western Antarctic Peninsula (Western AP) is located between latitude 63°S and 73°S, and longitude 57°W and 68°W. The area faces the Bellingshausen sea and is punctuated by islands, promontories, and small peninsulas, which include a complex network of straits, bays, and passages between the islands and the continental mainland. The climate of the Western AP is influenced by wet polar-maritime climates, with MAAT between −2 °C (65°S) and − 9 °C (70°S) (Cook and Vaughan, 2010). Annual precipitation is estimated at 500 to 2000 mm in the Western AP and the northern AP (van Wessem et al., 2016). Warming has been occurring with an overall MAAT increase of 0.8–3.0 °C between 1950 and 2015 (Oliva et al., 2017b; Turner et al., 2020). The Antarctic Peninsula Ice Sheet retreated from the western continental shelf break relatively rapidly after 18 ka BP, firstly in the north and subsequently the lift-off of grounded ice progressed southwards (Ó Cofaigh et al., 2014). The vegetation of the Western AP includes both the Antarctic herb tundra formation and the Antarctic non-vascular cryptogam tundra formation (Colesie et al., 2023).

Permafrost distribution in the Western AP is mostly discontinuous, with maximum estimated thicknesses around 150 m (Bockheim et al., 2013; Guglielmin et al., 2014a, 2014b). The ALT is highly variable, ranging between 30 and 500 cm (Vieira et al., 2010; Bockheim et al., 2013). Even though several research stations are located in the Western AP, few works focused on the active layer, or permafrost, have been published until recently.

3.1.2.1. Rothera Point. Rothera Point is a rocky promontory with an ice-free area of ca. 1000 × 250 m. (67.57 S, 68.12 W, 10–110 m a.s.l.) located in Adelaide Island in Marguerite Bay, south-Western AP. Marguerite Bay has a cold dry maritime climate with a MAAT of −4.2 °C and mean annual precipitation of about 500 mm (Turner et al., 2020). The bedrock is homogeneous, composed of diorite and granodiorite of mid-Cretaceous to early Tertiary age (Dewar, 1970). The deglaciation age of the Rothera Point area is still not well known, although Emslie (2001) estimated that deglaciation occurred about 6 ka BP. Permafrost is continuous here and ranges between 112 and 157 m in depth with an active layer ranging between 76 and 140 cm (Guglielmin et al., 2014b). Rock surfaces are generally covered by sporadic mosses, as well as diversity of epilithic lichens, that can strongly influence weathering processes (e.g.; Guglielmin et al., 2012).

The borehole site is located on a bedrock knob close to the "Memorial", on one of the highest summits of Rothera Point, about 100 m a.s.l. Guglielmin et al. (2014b) reported that the MAAT of Rothera Point varied between −2.7 (2010) and − 4.6 °C (2009), which was similar to the MAGT (−2.9 °C in 2010 and − 4.8 °C in 2009, Fig. 2, Table 3). According to Biskaborn et al. (2019), the permafrost temperature at the depth of zero annual amplitude decreased slightly from 2014 to 2016 representing, at least for that period, the only site in Antarctica with a

decreasing pattern of permafrost temperature. The near-surface TDD varied between 363 (2011) and 186 °C·day (2009), while FDD were lowest in 2009 (−1731 °C·day) and greatest in 2010 (−1371 °C·day). The recorded n-factor for thawing was between 2.34 (2010) and 2.69 (2011). The active layer thickness and thermal conditions are under a strong influence of winter snow cover. At Rothera, the thick cover of winter snow (> 1 m) leads to ground temperature cooling.

3.1.2.2. Palmer archipelago and Danco Coast. This sub-region consists of several islands of the Palmer Archipelago and the coastal area of the Antarctic Peninsula called Danco Coast between 64° and 66°S and 60° to 65°W . This sub-region represents the most rapidly warming area of the Antarctic Peninsula with a warming rate around +0.5 °C/decade during the last several decades (Turner et al., 2020). Currently, the MAAT is around −1.5 to −2.5 °C. Active layer and permafrost research in this area has been undertaken in the vicinity of Palmer station (Anvers and Amsler Islands) and Primavera station (Cierva Cove).

The area is expected to be in the discontinuous to sporadic permafrost zone (Bockheim et al., 2013), however, Obu et al. (2020), using Cryogrid-1, modelled negative permafrost table temperatures in the entire sub-region. The near-surface temperature on Amsler Island correlates well with both air temperature and solar radiation (Wilhelm and Bockheim, 2017). Modelling of ALT by Wilhelm et al. (2015) suggested maximum depths exceeding 15 m (Table 3), however these results were contradicted by Uxa (2016) who proposed that modelled active several meters should be several meter thinner if the volumetric latent heat of phase change is considered correctly. Ground thermal data showed the active layer is thicker than 180 cm in all areas including Cierva Cove (Wilhelm and Bockheim, 2016).

3.1.3. Eastern Antarctic Peninsula

The Eastern AP, located between latitude 63°S and 75°S, and longitude 55°W and 65°W s bordered by the mountain ridges of the Antarctic Peninsula, with maximum elevations exceeding 3000 m a.s.l. on its western fringe, and the Weddell Sea on the eastern side.

Most of the Eastern AP (> 99%) is currently covered by the Antarctic Peninsula ice sheet and smaller local glaciers. Glacial shrinking in the Eastern AP began at 18.5 ka BP, and the ice-free exposure of the lowlands occurred between 13 and 11 ka BP (e.g. Oliva and Ruiz-Fernández, 2020). Since the Early Holocene, prevailing climate conditions have driven minor glacial advances and retreats. In response to the recent warming trends, several ice-shelves broke up and glacier extension diminished (Cook and Vaughan, 2010). Currently, the Eastern AP includes a few relatively large ice-free areas in the northern sector, such as James Ross Island (ca. 500 km^2 of total ice-free surface extent), Seymour Island (ca. 80 km^2), or Vega Island (ca. 70 km^2). The ice-free areas south of 65°S are comparatively smaller (< 5 km^2) and mostly correspond to nunataks. The subglacial volcanic activity during the Late Cenozoic favoured the formation of volcanic mesas, which are widespread landform features (e.g. Davies et al., 2013; Ruiz-Fernández et al., 2019).

The climate of the Eastern AP is defined as semi-arid polar continental, with the highest MAAT of ca. −5.0 °C at sea level in the northern part of the Trinity Peninsula and decreasing towards southern parts of the region following latitudinal gradients of ca. 0.9 °C/deg. until values of ca. −17.0 °C at sea level at 75°S (e.g.; Cook and Vaughan, 2010). The Eastern AP's climate is strongly affected by the orographic barrier, formed by the mountain range along the Antarctic Peninsula, resulting in relatively low precipitation, mostly snow, estimated as 100 to 700 mm. Higher precipitation is modelled in the northern Eastern AP and in the mountainous parts of the Eastern AP (van Wessem et al., 2016). Strong warming of ca. 1.5–2.0 °C has occurred over the last 40 years in the region (Oliva et al., 2017b; Turner et al., 2020).

Terrestrial ecosystems in the northern Eastern AP are, together with the Western AP, some of the most dynamically changing parts of Antarctica in response to the MAAT increase. The entire area of the Eastern AP is underlain by continuous permafrost (Bockheim et al., 2013; Obu et al., 2020) with the modelled temperatures on the top of the permafrost between −3.0 °C in the northern tip of Trinity Peninsula and ca. −20 °C in the mountainous areas around latitude 75°S. Geomorphological dynamics of the ice-free terrain is driven by periglacial processes and paraglacial dynamics in the recently exposed areas (Davies et al., 2013; Ruiz-Fernández et al., 2019). Unlike Western AP, the vegetation of the Eastern AP has lower diversity with no vascular plants though patches of mosses, lichens, and biotic crusts occur (Peat et al., 2009).

3.1.3.1. James Ross Island, Ulu Peninsula. Permafrost research in the northern Eastern AP has largely been constrained by logistic complexity. To date, the main area for permafrost research has been the ice-free area of Ulu Peninsula (312 km^2), northern James Ross Island, with only a few studies in other areas. Intense geological and paleontological surveying has been undertaken in Eastern AP (e.g. Nelson, 1975; Olivero et al., 1986), whereas research focused on permafrost and active layer dynamics are recent and scarce.

The first pre-IPY permafrost research was limited to geophysical surveying, and geothermal gradient studies that estimated permafrost thicknesses varying between 6 and 67 m on the marine terraces of the Ulu Peninsula (Fukuda et al., 1992; Borzotta and Trombotto, 2004). Mori et al. (2006) also monitored ALT on Rink Point mesa on the SW section of Ulu Peninsula showing an annual ALT of between 60 and 80 cm. Since the IPY, research into the active layer and permafrost have been carried out more systematically in the northern part of Ulu Peninsula (e.g. Hrbáček et al., 2019; Hrbáček and Uxa, 2020). Here, ground temperatures are monitored in a network of >15 sites with shallow profiles providing continuous records with depths varying from 5 cm to 75–200 cm. Additionally, 3 CALM-S sites of sizes 50 to 50 up to 70 to 80 m have been operating since 2014, with annual probing of thaw depth.

The MAAT near Johan Gregor Mendel station (10 m a.s.l.) on the northern coast of Ulu Peninsula was −6.6 °C (2004–2020), varying from −4.0 to −9.0 °C (Kaplan Pastíriková et al., 2023). The modelled annual precipitation ranges between 300 and 700 mm (van Wessem et al., 2016) mostly in the form of snowfall in winter. MAGT in the low-lying areas below 60 m a.s.l. is around −6.0 °C, ranging from −4 to −8 °C, whereas MAGT in the topmost part of the permafrost is around −6.5 °C with a relatively low annual variability (between −5.5 and − 7.5 °C). Mean ALT values vary between 55 and 85 cm. Depending on summer climate conditions, ALT can range from 35 to 125 cm (Table 4, Fig. 3). There are noboreholes in the region providing data from depths >2 m.

The thawing season usually extends 100–120 days between late-November and early-March, associated with prevailing positive mean daily near-surface temperatures (Hrbáček et al., 2019). The total sum of TDD has a long-term mean of 300 to 400 °C·day ranging from 150 to 600 °C·day. By contrast, freezing seasons are much longer than thawing seasons with a mean duration of 240–270 days depending on annual climate conditions. The ground remains completely frozen during the winter months and does not even thaw during events with positive air temperatures (e.g. Hrbáček et al., 2019). The seasonal sum of FDD shows a mean of ca. −2600 °C·day, although it is highly variable between −1700 and − 3500 °C (Table 4).

The ground thermal regime on Ulu Peninsula correlates well (r > 0.75) with the air temperature (Hrbáček et al., 2016b, 2017b; Hrbáček et al., 2020a; Hrbáček and Uxa, 2020) and incoming radiation (Hrbáček et al., 2020a, 2020b). The ALT distribution is strongly related to local lithology and vegetation. In contrast, the effect on the ground thermal regime and ALT of snow cover is considered to be less important than lithology and vegetation (e.g. Hrbáček et al., 2019).

Lithological conditions are considered the most important factor driving differences in ALT on Ulu Peninsula. The major part of the area is formed by coarser volcanic materials and finer Cretaceous sediments.

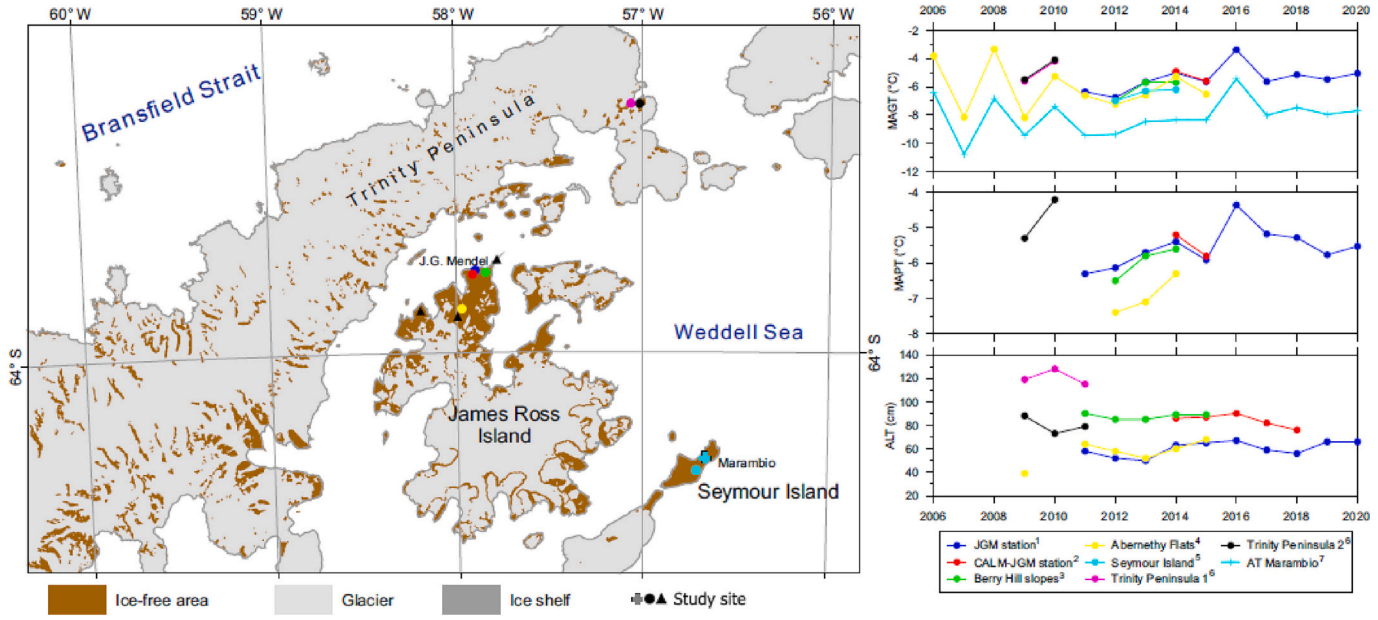

Fig. 3. The variability of mean annual near-surface ground temperature (MAGT), mean annual temperature, the permafrost table (MAPT), and active layer thickness (ALT) in selected sites of Eastern Antarctic Peninsula. The data were extracted from studies by[1]Pastirikova et al., in review;[2]Hrbáček et al., 2017a, 2021a; [3]Hrbáček et al., 2017b, 2019; [4]Hrbáček and Uxa, 2020; [5]Gjorup et al., 2020; [6]Schaefer et al., 2017a, 2017b; [7]READER database. The black triangles indicate the position of other study sites in the region.

The differences in geological composition and ground texture result in highly variable ground thermal properties (i.e. conductivity, capacity and diffusivity). An example of the lithological effects on the spatial distribution of ALT and ground thermal regime was observed on CALM-S JGM, where thermal conductivity was almost three times higher in Cretaceous sediments than in Holocene marine terrace sediments. As a result, the active layer was ca. 50 cm thicker in the Cretaceous terrain (Hrbáček et al., 2017b; Hrbáček et al., 2021b).

Vegetation exerts a weak influence on the ground thermal regime and ALT, at small-scales, as dense patches of mosses or lichens occur only in small (<100 m^2) niches. Vegetation is an efficient insulator causing 1.1–1.4 °C lower MAGT and a 10–15 cm thinner ALT in moss-covered areas than in bare ground sites (Hrbáček et al., 2020a, 2020b).

The limited effect of snow cover on the ground thermal regime is caused by its irregular accumulations during the winter. The maximum snow depth on flat surfaces can reach 30 to 50 cm in short-term events (<2 days), but it is rapidly redistributed by the strong winds which results in thin snowpacks (< 20 cm) that persist only for a few weeks (Hrbáček et al., 2016a, 2016b; Kňažková et al., 2020). Such snow packs were found to be insufficient to be an effective insulation layer, which was confirmed by the freezing n-factor values of 0.9–1.0 suggesting strong interface between atmosphere and ground surface (Table 4). In specific cases where micro relief favours snow accumulations, snow depths >70 cm may persist most of the winter season and create an efficient insulation layer.

3.1.3.2. Other parts of Eastern AP. Previous work on the active layer and permafrost in other sectors of the Eastern AP are limited to soil research studies conducted at Hope Bay (Trinity Peninsula) and on Seymour Island (Bockheim, 2015). Short records from Hope Bay (2009–2011) revealed MAGT between −3.5 °C and − 6.0 °C and ALT between 73 and 128 cm (Fig. 3, Table 4). The inter-site differences in ground thermal parameters in Hope Bay were caused by a different stage of ornithogenic activity and the presence of vegetation patches having an insulation effect on the ground thermal regime, causing active layer thinning (Schaefer et al., 2017a). An even shorter dataset from one site in Seymour Island (3/2011–1/2012) revealed very cold conditions during winter with FDD dropping to −3300 °C·day, and an ALT estimated at 100 cm (Gjorup et al., 2020).

3.2. West Antarctica

The West Antarctica region comprises Ellsworth Land, Marie Byrd Land and Edward VII Land. The ice-free areas are limited mostly to mountainous ridges. The most prominent are in the Ellsworth Mountains where the highest point in Antarctica, Vinson Massif (4892 m a.s.l.) is located. Active layer and permafrost research in the West Antarctica region is mostly limited to the Ellsworth Mountains (Schaefer et al., 2017a, 2017b; McKay et al., 2019). The only brief results from the coastal part of Marie Byrd Land report a mean annual permafrost temperature of −10.3 °C (2008–2013) in the vicinity of Ruskaya station (Bockheim, 2015; Obu et al., 2020).

3.3. Ellsworth Mountains

The Ellsworth mountains are located around 77° to 88.5°S and 78° to 87°W. The mountain ridge, ca. 350 km long and 48 km wide is formed over two major areas, Sentinel range and Heritage range, which are bisected by the Minnesota Glacier. The prevailing geology consists of marble (late Precambrian), sedimentary rocks (late Cambrian), quartzite (upper Cambrian to Devonian) and marine and terrestrial layers (Permian) (Webers et al., 1992). The ice-free areas are underlain by ice-cemented or dry permafrost and vegetation is scarce (Bockheim, 2015). The climate of Ellsworth Mountains is cold and dry with MAAT ranging from −15 °C in the coastal zone down to −35 °C on the high-elevation polar plateau. The annual precipitation is estimated to about 150–175 mm (Bromwich et al., 2004).

The only two studies in the region are from the Mount Dolence area in the Heritage Range. Schaefer et al. (2017a, 2017b) reported a mean annual ground temperature of between −18.1 °C and − 18.3 °C in the period 2012/2013 in two sites at 850 and 886 m elevation. The active layer was thawed only in December and January and the TDD was 50 to 150 °C·day. The ALT was estimated to be 47 and 48 cm (Table 5). However, the results should be considered with caution as the mean daily ground temperature at the depth of 30 cm did not exceed 0 °C. The ALT in the region is affected by the depth at where the ice table in dry

permafrost is present. McKay et al. (2019) observed the depth of the ice table to be between 10 and 45 cm in four sites elevated between 690 and 835 m.

3.4. East Antarctica

East Antarctica (EA) represents a large area in the coastal zone between 20°W and 170°E longitudinally and 65–75°S latitudinally. The ice-free areas in EA comprise ca. 10,900 km^2, and are fragmented into separate nunataks of alpine character forming small ridges penetrating the inland ice sheet. The largest ice-free areas are mountain ridges in Queen Maud Land (ca. 3500 km^2) and MacRobertson Land (ca. 5000 km^2). In spite of the presence of several research stations in the area, studies of the active layer and permafrost are scarce.

3.4.1. Queen Maud Land

Queen Maud Land lies between 20°W and 45°E. The coastline extends to 75°S at the western side, but the main part is generally about 70°S. Deglaciation of coastal oases started about 50–35 ka BP according to exposure ages and lacustrine deposits (Altmaier et al., 2011; Abramov et al., 2011). The bedrock geology of Queen Maud Land is dominated by Precambrian gneiss, formed 1 to 1.2 Ga ago, before the creation of the supercontinent Gondwana (Barrett, 1971). The climate follows both altitudinal and latitudinal gradients. The highest MAAT is in the coastal zone at 70°S (ca. −10 °C at Novolazarevskaya station in Schirmacher Hills), whereas the MAAT <15 °C are typical for the areas around 75°S (Halley research station) and mountainous areas around 1000 m a.s.l. (Kotzé and Meiklejohn, 2017). Precipitation is in the range 200–400 mm per year (Bromwich et al., 2004). No significant changes in the MAAT in the region were observed during the observational period (Turner et al., 2020).

There are two major ice-free areas with available permafrost data in Queen Maund Land – the system of nunataks near SANAE VI and Troll stations (Basen, Flårjuven, Grunehogna, Robertskollen, Schumacherfjellet, Slettfjell, Troll, Valterkulten and Vesleskarvetwith and Schirmacher Hills). The longest monitoring records are from the Basen (since 2004) and Troll (since 2007) nunataks. Overall, Queen Maud Land has a total of 10 profiles on 8 nunataks (Troll, Flårjuven, Valterkulten, Slettfjell, Schumacherfjellet, Grunehogna, Robertskollen and Vesleskarvet). Boreholes were installed on the Fossilryggen and Svea nunataks, however, these are inactive (Vieira et al., 2010). According to recent measurements, the MAATs ranged from −14 to −18 °C and ALTs range from 16 to 58 cm (Kotzé and Meiklejohn, 2017, Fig. 4, Table 6).

The Schirmacher Hills is located in the coastal area of Queen Maud Land. The oasis is 18 km long and from 0.6 to 3.5 km wide, with an elevation ranging from 10 to 226 m a.s.l. The Schirmacher Hills stretch along the slope of the continental ice shelf. In the north the oasis borders the Lazarev Ice Shelf, which separates it from the sea. Sediments in large lake depressions have been radiocarbon dated at 18–30 ka. However, soil development suggests that geomorphic surfaces are only several thousand years old. Moraine deposits dated back at 145–80 ka show evidence of past phases with larger glacial systems. Minor warming and cooling events during the current interglacial period, from 13 ka to 3 ka, have been revealed by dating sediments from dry lake beds and shallow lakes in Schirmacher Oasis. The recession of ice began in the Early Holocene and had three phases, with the main phase recorded at 6.7–2.2 ka BP (Dharwadkar et al., 2018).

The first permafrost investigations were undertaken in the vicinity of Novolazarevskaya station (Shirmacher Oasis) in 1979 finding the active layer depth in the range of 8 cm for icy algae-rich deposits and 70 cm for fine-grained dry sediments. The first site for active layer monitoring (CALM-S) was established in 2008, and boreholes for ground temperature monitoring were installed in 2009 (Abramov et al., 2011). According to recent measurements, the MAGTs in the Schirmacher Oasis are around −9 °C and ALTs are 30–120 cm (Table 6). Modelling estimated the MAGT on the top of the permafrost within the range of −8 to −10 °C (Obu et al., 2020).

3.4.2. Other parts of EA

The remaining parts of EA where some active layer and permafrost monitoring is available are Enderby Land, Princess Elizabeth Land and Wilkes Land. Deglaciation began around 30 ka in the Bunger Hills in Wilkes Land (Gore et al., 2001; Mackintosh et al., 2014), and commenced around 6 to 9 ka BP in Enderby Land (White and Fink, 2014). The geology of the majority of the area is defined by Precambrian schists, quartzites and meta-sedimentary rocks, comprising mainly granulite facies orthogenesis (Tucker et al., 2020). The MAAT of the coastal area is stable between −9 and − 11 °C without any trend detected over the last 60 years (Turner et al., 2020). Precipitation oscillated between 200 and 800 mm yr^{-1} (Bromwich et al., 2011).

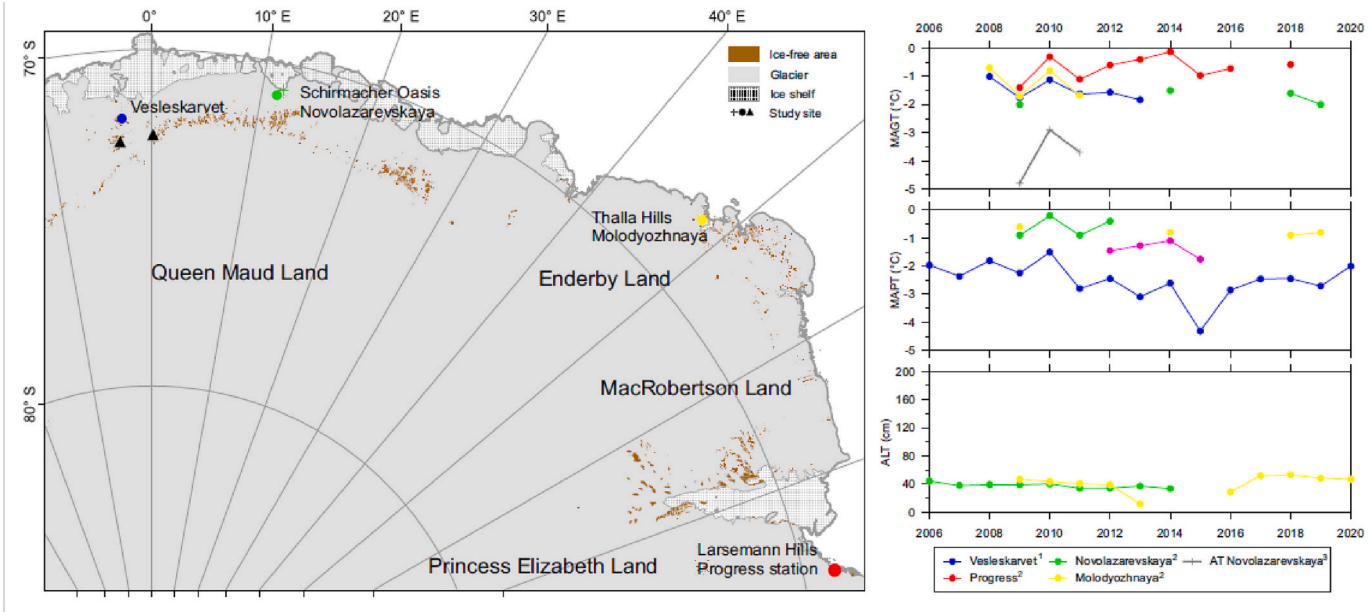

Fig. 4. The variability of mean annual near-surface ground temperature (MAGT), mean annual temperature, the permafrost table (MAPT), and active layer thickness (ALT) in selected sites of East Antarctica. The data were extracted from studies by [1]Kotzé and Meiklejohn, 2017; [2]Hrbáček et al., 2021b; [3]REAEDER database.

Vegetation cover in ice-free areas is sparse and consists of lichens, mosses, and algae.

Permafrost and active layer monitoring have mostly been undertaken in the vicinity of Russian research stations Molodezhnaya in Thalla Hills (Enderby Land); Progress II station in Larseman Hills (Princess Elizabeth Land), and Mirny station in Bunger Hills (Wilkes Land). The first Soviet Antarctic expedition (1956–57) brought permafrost scientists near Mirny station, whoinstalled boreholes for ground temperature measurements and studied ALT in a variety of landscape settings. Shallow (1 m) boreholes for ground temperature and sites for ALT measurements were later (1993–94) organised at Syowa (Sawagaki, 1995), and from 2007 at Molodezhnaya (Abramov et al., 2011).

MAGT is around −9 °C and ALT ranges from 60 to 80 cm (more than 100 cm for bedrock) near Molodezhnaya station. At Progress Station, ALT varies from 60 to 85 cm (Hrbáček et al., 2021b). Modelling of the topmost part of the permafrost revealed the highest temperatures between −6 to −8 °C in the coastal areas, decreasing to −20 °C in the Prince Charles Mountains and Mawson Escarpment in MacRobertson Land (Obu et al., 2020; Table 6).

3.5. Victoria Land

3.5.1. Ross Sea region and Transantarctic Mountains

The Ross Sea region (RSR) lies directly south of New Zealand and stretches from latitude 70°S to 90°S, and from longitude 150°E through 180° to 150°W. Ice-free areas with soil development cover an estimated area of 18,480 km^2 (e.g. ACBR10, Terauds and Lee, 2016), and soils occur in small pockets along the coastal margins, in the McMurdo Dry Valleys (MDVs) as well as in isolated areas in the Transantarctic Mountains (TAM) further south (Balks and O'Neill, 2016). The MDVs are the largest ice-free expanse in Antarctica, and depending on the portion of ice-free area considered, size estimates range from 2000 to 15,000 km^2 (Levy, 2013).

Basement rocks of the MDVs are mainly Precambrian to Ordovician schists, gneiss, marble, and granites (Isaac et al., 1996) overlain by a range of rock types dominated in many areas by Devonian to Triassic quartz sandstones (Isaac et al., 1996). Ross Island comprises mainly basaltic materials with shallow soils formed on regolith such as glacial till or colluvium that strongly reflect the parent rocks due to the relatively limited weathering that occurs (Campbell and Claridge, 1987).

During the last glacial maximum (LGM), the West Antarctic Ice Sheet (WAIS) expanded into the Ross Sea Embayment and terminated close to the continental shelf edge (Shipp et al., 1999; Denton and Hughes, 2000). Recent modelling by Lowry et al. (2019) show the earliest retreat of the WAIS in the Ross Sea Embayment during the Early Holocene, which was characterized by rapid terrestrial ice sheet thinning.

The timing of various glacial advances and retreats strongly influences soil development. Salt horizons, soil color, the amount of clay present, and the extent of staining, exfoliation, cavernous weathering, and ventifaction of surficial materials are distinctive indicators of age difference in many RSR soil sequences (Bockheim, 1997). The youngest soils are generally found on deposits closest to glaciers and on young features such as beaches, sand dunes, or stream deposits. The oldest, most strongly weathered, soils are often found on high, upland surfaces (Campbell and Claridge, 1987; Bockheim and McLeod, 2008; Bockheim, 2010), which have escaped the erosive effects of subsequent glacial fluctuations.

The MDV landscape has generally been considered stable over periods extending for millennia (Denton et al., 1993; Marchant and Head, 2007), particularly at higher elevations where soil temperatures remain below 0 °C, thus slowing weathering and geomorphic processes. However, recent observations in the coastal thaw zone by Fountain et al. (2014), Balks and O'Neill (2016) and Levy et al. (2018) describe short-lived erosion and depositional events, occurrence of stream erosion and incision, and melting of massive ice during summers that experienced above average incoming solar radiation. Future changes to soil-permafrost environments in the RSR are most likely to occur in areas of low elevation and in warm coastal zones and may be a result of warmer than average summers, higher than average snowfall, or human disturbances. In areas of ice-cemented (as opposed to dry-) permafrost such changes may lead to melting of ground ice and thermokarst erosion or subsidence (Fountain et al., 2014; Balks and O'Neill, 2016; Levy et al., 2018).

Mean annual air temperatures across latitudinal and altitudinal gradients from Cape Hallett (72°S) to Darwin Glacier (79.5°S), and from sea level to the edge of the Polar Plateau, over the period 2000 to 2018, ranged from −15 °C at Cape Hallett (2 m a.s.l.) to −25 °C at Mt. Fleming at the head of the Wright Valley (1700 m a.s.l.) (Seybold et al., 2009). In the inland MDVs snowfall occurs with no strong seasonal pattern (Fountain et al., 2010). Precipitation is higher in coastal areas with snow accumulating on the ground surface over winter, and following summer snowfall events. On the mid-valley floors precipitation is lowest with a mean annual precipitation of 45 mm recorded at Vanda Station over two years (Campbell and Claridge, 1987) and Fountain et al. (2010) report annual precipitation ranging from 3 to 50 mm in the MDVs. Snowfall is higher at the coastal ends of the valleys and at higher altitudes. In summer snowfall often sublimates within an hour of falling on the valley floors, and within a day or two at higher altitudes (Balks and O'Neill, 2016). Climate data in Antarctica is limited, however continuously monitored soil climate data, since 1999 shows some between-season variability but no significant trends of warming or cooling (Carshalton et al., 2022) (Table 7) .

In the MDVs there are no vascular plants, but where conditions are favourable (soil pH and salinity, available water, and shelter from the wind), algal crusts, mosses, lichen, and endolithic communities have been reported (Friedmann, 1982; Gilichinsky et al., 2007; Goordial et al., 2016).

Environmental parameters (pH, water activity) drive abundance, community structure and diversity of variable biological communities (Adams et al., 2006; Aislabie et al., 2006, 2008, 2011; Barrett et al., 2006; Chong et al., 2012; Hopkins et al., 2006; O'Neill et al., 2013; Yergeau et al., 2007). Lee et al. (2012) showed that soils from four geographically disparate dry valleys comprised structurally and phylogenetically distinct communities. In coastal areas (e.g. Capes Royds, Bird, and Hallett) penguin colonies provide high inputs of nutrients forming ornithogenic soils and distinct biological communities (Speir and Cowling, 1984).

The MDVs are one of the most studied permafrost regions in Antarctica (Bockheim et al., 2007; Adlam et al., 2010; Seybold et al., 2010; Levy, 2013; Obu et al., 2020). A soil-permafrost climate network has been maintained since 1999 (Carshalton et al., 2022). The network, comprising nine automated soil climate stations and two borehole sites, provides both a latitudinal and altitudinal gradient across the RSR. The coastal group includes Minna Bluff (78°30′41.6" S) (colder, windier, and some distance from the open sea), Scott Base, Marble Point, and Granite Harbour (77°00′23.7" S). The Granite Harbour site is not typical of the wider area, but was selected to capture a unique warm wet environment that has unusually lush biological growth. To complement the coastal latitudinal group, the network includes an altitudinal group ranging from Marble Point (60 m a.s.l.) through Wright Valley floor (160 m a.s.l.) and Victoria Valley (410 m a.s.l.) to Mt. Fleming (1697 m a.s.l.) which includes the dry valley floor environment through to the edge of the polar plateau. To capture the valley walls, and intermediate altitude, particularly to support climate modelling efforts, soil climate stations were installed on a terrace above Don Juan Pond (728 m a.s.l.) and on the high Wright Valley wall east of the entrance to Bull Pass (known as Bull Pass East, 832 m a.s.l.). Two 30 m deep boreholes are located in bedrock, one at Marble Point to capture the coastal environment and one on the floor of the Wright Valley (Guglielmin et al., 2011) to capture the more extreme dry climate. Overall, the network captures the range of soil, active layer, and permafrost environments in the McMurdo Dry Valleys region.

Each soil climate station includes an MRC temperature probe, 3-in-1 soil moisture probes which also measure temperature, and Campbell 107 temperature probes, giving at least 15 temperature measurements in the top 1.2 m. Atmospheric conditions (measured 1.5 m above the ground surface) include incoming solar radiation with a pyranometer, wind speed and direction, relative humidity, and air temperature, and sensors are connected to Campbell Scientific data loggers (ranging from CR10X to CR1000X). Measurements of atmospheric variables are made at 10-s intervals, and soil measurements at 20-min intervals, averaged hourly. The data are included in Adlam et al. (2010), Seybold et al. (2010), Vieira et al. (2010), Guglielmin et al. (2011), Balks and O'Neill (2016), Hrbáček et al. (2021b), and Obu et al. (2020).

Another soil climate monitoring network (LTER, Long Term Ecological Research Project) has also operated, since 1994, in the McMurdo Dry Valleys. Systematic soil measurement in the LTER network started in 1999 in the southern part of the RSR (Taylor Valley, Beacon Valley, University Valley). The longest published record (1999–2010) was provided from Beacon Valley by Lacelle et al. (2016); (Fig. 5). Data from the LTER network are not further discussed here, however are summarized in Table 7.

The air, ground and permafrost temperatures all decrease with increasing elevation and latitude (Adlam et al., 2010). Within the data set (gathered between 2006 and 2019) MAAT ranged from −14.8 °C at Granite Harbour (5 m a.s.l) to −25.1 °C at Mt. Fleming (1697 m a.s.l). The MAGT ranged from −13.1 °C at Granite Harbour to −24.6 °C at Mt. Fleming. The mean annual temperature in the uppermost part of the permafrost ranged from −12.9 °C at Granite Harbour to −24.2 °C at Mt. Fleming (Fig. 5, Table 7) All sites show interannual variability in MAAT and MAGT (both near surface and at the top of the permafrost). The inter-annual variability was lower at higher altitude sites such as Mt. Fleming than at the lower altitude coastal sites such as Marble Point (50 m a.s.l) (Fig. 5).

ALT ranged from 3.4 cm at Mt. Fleming to greater than 90 cm at Granite Harbour (Fig. 5, Table 7), and generally decreased with increasing altitude and latitude. At Granite Harbour, where a large amount of meltwater flows through the soil profile, conducting heat to depth, the maximum thaw depth exceeds the depth of the temperature sensors. At all other sites, the deepest sensors are within the permafrost, at depths of greater than about 50 cm. The ALT at the soil climate station sites showed large variability both in space and in time, reflecting differences in soil characteristics, permafrost types, annual variability in snow cover, and responding sensitively to climate variability (Balks and O'Neill, 2016; Hrbáček et al., 2021b; Seybold et al., 2010); however, no significant trends of increase or decrease in ALT, MAGT (near-surface or at the top of the permafrost) were observed between 2006 and 2019.

The three Wright Valley sites (Bull Pass, Bull Pass East and Don Juan Pond) have dry permafrost (Anhyorthels) while the remaining six sites have ice-cemented permafrost (Haplorthels or Haploturbels) (Carshalton et al., 2022). The coastal sites (Scott Base, Marble Point, Minna Bluff, and Granite Harbour) receive higher snowfall, resulting in some liquid moisture for short periods during snowmelt. The Victoria Valley site is relatively close to Lake Victoria and has moisture mainly derived from groundwater, whereas the predominant source of water at Mt. Fleming is windblown snow carried from the nearby margin of the Polar Plateau. Seybold et al. (2010) described the moisture regime of seven of the sites. There were no clear differences between ALT at ice-cemented sites compared to those with dry permafrost. Substantive vegetation is lacking at all sites and, therefore, would have no influence on the ground thermal regime and ALT.

Numerous studies into the thermal properties of MDV soils, the role

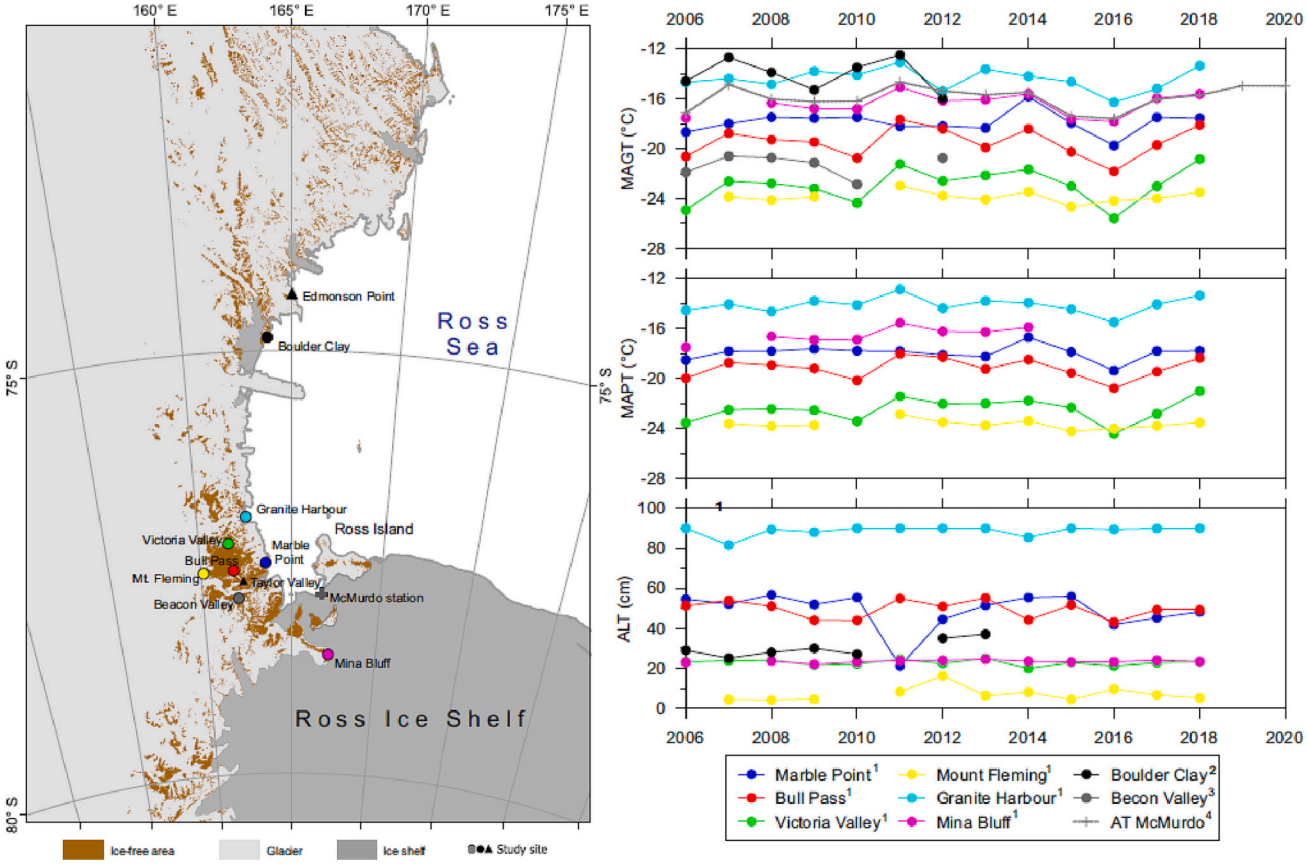

Fig. 5. The variability of mean annual near-surface ground temperature (MAGT), mean annual temperature on the permafrost table (MAPT) and active layer thickness (ALT) in the selected sites of Victoria Land. The data were extracted from studies [1]Carshalton et al., 2022; [2]Cannone et al., 2021; [3]Lacelle et al., 2016; [4]READER database. Black triangle indicate the position of other study sites in the region.

of soil moisture on ALT, short-term ground temperature monitoring, modelling of the subsurface thermal regime, and research into the impacts of climate change on soil thermal regimes and associated soil ecosystems have been undertaken in the RSR (e.g. Andriuzzi et al., 2018; Fisher et al., 2016; Fountain et al., 2016; Lacelle et al., 2016; Lapalme et al., 2017; Liu et al., 2018; Wlostowski et al., 2018). In a study conducted over a two-year period along moisture gradients associated with fluvial features in the Taylor Valley, MDVs, Wlostowski et al. (2018) showed that the rate and sensitivity of soil freeze/thaw processes was related to soil moisture content in the active layer; with wetter soils freezing less frequently and more gradually than dry soils. Wlostowski et al. (2018) concluded that if predicted increases in moisture and temperature occur in the MDVs, soil ecosystems (especially nematode diversity and abundances) will be impacted (Chapman and Walsh, 2007; Walsh, 2009). Similarly long-term observations by the MDV Long Term Ecological Research (LTER) project showed shifts in the dominant nematode species in the Taylor Valley resulting from fluctuations in ice-melt associated with warmer summers and more frequent discrete warming events since the 2000s (Andriuzzi et al., 2018).

3.5.2. *Northern Victoria Land*

Northern Victoria Land is part of the Ross Sea Sector, and was glaciated probably until 12,000 yrs. BP (Forte et al., 2016). It consists of an undulating upland rising to elevations exceeding 1000 m a.s.l., and in one case (Tarn Flat) descending below sea level. The bedrock is composed of Harbour Castle granite, Wilson Terrane meta-granite and high-grade metamorphics, and small areas of meta-sedimentary rocks, all Ordovician in age or older (Pour et al., 2018). Several large glaciers cut through the Trans-Antarctic Mountains (i.e. Reeves, Priestley and Campbell), and there are many smaller ones together with numerous cirque glaciers and snowbanks. The coasts of North Victoria Land consist of a sequence of cliffed headlands and beaches, several of which are raised beaches (i.e. Ponti and Guglielmin, 2021a).

The climate of the area surrounding the Italian Antarctic Research Station 'Mario Zucchelli' is characterized by a mean annual air temperature of −14.1 °C (Ponti et al., 2021), and is persistently dominated by strong Katabatic winds. The annual net precipitation, usually in the form of snow, ranges between 50 and 250 mm yr^{-1} (Bromwich et al., 2011). The climatic trend is towards a slight increase of MAAT (Cannone et al., 2021) and permafrost is continuous everywhere with a trend of increasing ALT (Guglielmin et al., 2014a; Cannone et al., 2021).

The geomorphological processes of northern Victoria Land are mostly related to wind or salt weathering (Ponti and Guglielmin, 2021 and thermal-contraction cracking polygons (French and Guglielmin, 1999) that may develop ice wedges (Raffi and Stenni, 2011). It is common to find perennially frozen lakes with frost mounds (Ponti et al., 2021) and also active rock glaciers (Guglielmin et al., 2018). Freeze-thaw and mass-wasting (solifluction) processes are limited because of the lack of moisture and the shallow active layer (French and Guglielmin, 1999). The vegetation of Victoria Land is composed exclusively of cryptogams and includes four main vegetation types, dominated by (a) mosses, (b) mosses encrusted by epiphytic lichens, (c) macrolichens, and (d) scattered epilithic lichens and mosses (Cannone and Seppelt, 2008).

3.5.2.1. Boulder Clay. Boulder Clay (74.74°S, 164.03°E, 205 m a.s.l.) is an ice-free area located at the Northern Foothills about 6 km south of the Italian station on a gentle slope (5°) with south-eastern exposure. The area consists of glacial ablation-sublimation till overlaying a body of a "dead" glacier ice. The till matrix is generally silty sand with confined zones of clayey silt (Guglielmin et al., 1997). The climate is characterized by a MAAT of −14.1 °C (Ponti et al., 2021).

Despite the low precipitation, areas of snow accumulation are formed by strong wind drift (Guglielmin et al., 2014a). Permafrost is continuous and estimated to be 420–900 m thick (Guglielmin, 2006). The ALT ranges between 23 and 92 cm with a thickening trend of +0.3 cm to 1.1 cm per year at different sites during the period 2000–2013 (Guglielmin et al., 2014b; Cannone et al., 2021). The Boulder Clay site is the first CALM-S grid in Antarctica with temperature data from a 3.6 m deep borehole since 1996 (Guglielmin, 2006).

The MAAT ranged between −12.5 and − 16.0 °C, while the MAGT was between −14.6 and − 16.7 °C. Surface annual TDD varied considerably, ranging from 90 to 195 °C·day. Consequently, the ALT recorded at the borehole site ranged between 25 and 37 cm (Guglielmin and Cannone, 2012; Cannone et al., 2021) (Table 7). Incoming radiation, rather than air temperature, is considered the principal driver of AL thickening (Guglielmin and Cannone, 2012).

3.5.2.2. Edmonson Point. Edmonson Point (74.33°S, 165.13°E, 50 m a.s.l.) is a small ice-free oasis, located in Wood Bay on the west coast of the Ross Sea, of about 1.8 km^2. Here, the volcanic activity of Mt. Melbourne produced a dark substrate composed of basaltic lavas, scoria, pumice, and tuff (Smykla et al., 2015). Periglacial processes include frost cracking of finer deposits (French and Guglielmin, 1999) and the influence of oceanic flooding on permafrost has been demonstrated (Ponti and Guglielmin, 2021).

The MAAT in the Edmonson Point is around −16.5 °C. The innermost area is sheltered from local katabatic winds and in summer easterly winds. Permafrost is continuous everywhere (Obu et al., 2020), and the active layer thickness ranges between 23 and 55 cm at vegetation covered and bare ground sites, respectively (Cannone and Guglielmin, 2009; Hrbáček et al., 2020a, 2020b). MAGT varied between −11.4 and − 14.7 °C. Surface TDD varied from 534 to 804 °C·day $year^{-1}$, producing an n-factor for thawing of between 40.4 and 101. Surface FDD range between −4982 and − 5940 °C·day $year^{-1}$, producing an n-factor for freezing of between 0.9 and 0.99 (Table 7).

3.6. *Sub-Antarctic Islands*

The sub-Antarctic islands encompass several islands that generally include the Antipodes, Auckland, Bounty, Bouvet, Campbell, Crozet, Heard and McDonald, Kerguelen, Macquarie, Prince Edward, South Georgia, South Sandwich, and Snares Islands, located between 40 and 60°S, near the Antarctic Polar Frontal Zone. These islands are further classified according to oceanographic, climate, and floristic data (van de Vijver and Beyens, 1999). They are largely of volcanic origin of varying ages, with some still active (e.g., Hodgson et al., 2014), ranging from volcanic cones, vents, and basal shelf volcanoes (Hodgson et al., 2014), to granite remnants (McGlone, 2002), and uplifted basaltic oceanic crust (Quilty, 2007). Most of the islands are characterized by maritime climates that are moist, cool, mostly cloudy, with strong prevailing westerly winds, brought about by eastward moving cyclonic depressions (e.g.; Hall, 2002; McGlone, 2002; Hodgson et al., 2014; Graham et al., 2017). Annual precipitation varies, ranging from 700 mm for Crozet to 2400 mm for the Prince Edward Islands (e.g.; le Roux and McGeoch, 2008), with those located above the Antarctic Convergence receiving less snowfall (Hall, 2002). Modelled MAAT ranges from −9 to −2 °C for South Georgia, to +2 to +8 °C for the Antipodes and + 11 °C for Snares Island; the MAAT for most islands is near 0 °C (Leihy et al., 2018)

3.6.1. *South Orkneys*

Unlike the other sub-Antarctic Islands, continuous research activities are carried out on the South Orkneys, in Signy Island (60°43′S, 45°38′W). Deglaciation of the area started around 6.6 ka cal BP (Jones et al., 2000) and continues nowadays, as thinning rates of 1 m per year have been measured over the last 20 years (Favero-Longo et al., 2012). The ice-free area of the island covers about 10 km^2 and is composed quartz-mica-schist bedrock, moraine sediments, scree slopes, beaches and alluvial deposits (Matthews and Maling, 1967). A cold oceanic climate dominates with MAAT of around −3.5 °C, an annual precipitation of around 400 mm, primarily in the form of summer rain

(Guglielmin et al., 2012). The warming trend of MAAT is +0.13 °C/decade during the period 1960–2009 (Oliva et al., 2017b). Precipitation shows also a slight increase in recent decades (Cannone et al., 2016). Vegetation on Signy Island is composed of both the Antarctic herb tundra formation, as well as the more common Antarctic nonvascular cryptogam tundra formation (Gimingham and Smith, 1970). Present-day geomorphological processes in Signy Island are characterized mainly by periglacial dynamics, including the development of low-centred sorted circles, sorted stripes, and stone-banked lobes, and widespread solifluction processes. One active rock glacier has been described in the island (Guglielmin et al., 2008).

MAGT ranges between −1.9 and − 2.9 °C on bare ground and between −2.0 and − 3.0 °C for vegetation (Fig. 6). The annual TDD varies between 230 and 540 °C·day in bare ground, and between 100 and 300 °C·day under vegetation carpets (Guglielmin et al., 2012; Hrbáček et al., 2020a). The presence of vegetation strongly affects ALT, which can range from 40 cm to >3 m (Guglielmin et al., 2008; Guglielmin and Cannone, 2012). The shallowest ALT sites are on vegetated surfaces that retain more water (wet mosses), while sites with thicker ALT were found under bare ground where water is more easily drained (Guglielmin and Cannone, 2012; Hrbáček et al., 2020a) (Table 8).

3.6.2. *Other areas*

The remaining Sub-Antarctic islands have distinct periglacial environments and periglacial landforms, such as sorted and non-sorted patterned ground, protalus ramparts, and stone-banked lobes are common (e.g., Hedding, 2008; Hansen, 2018). However, ground temperature monitoring is largely absent and MAGT on the top of the permafrost table was modelled by the Cryogrid 1 model (Obu et al., 2020), for the South Sandwich Islands, ice free areas of Heard Island, higher elevations of Kerguelen Islands, and South Georgia. Permafrost is absent on the Crozet Islands (Obu et al., 2020), the Prince Edward Islands (Nel et al., 2021), and Macquarie Island (Hodgson et al., 2014).

Investigations by Nel et al. (2021) indicate that Marion Island, of the Prince Edward Islands, may be used as a proxy in evaluating regional climatic trends within the Southern Ocean. Marion Island is characterized by ubiquitous, high-frequency low-intensity, diurnal frost cycles throughout the year (Hansen, 2018), like the Auckland, Campbell, and

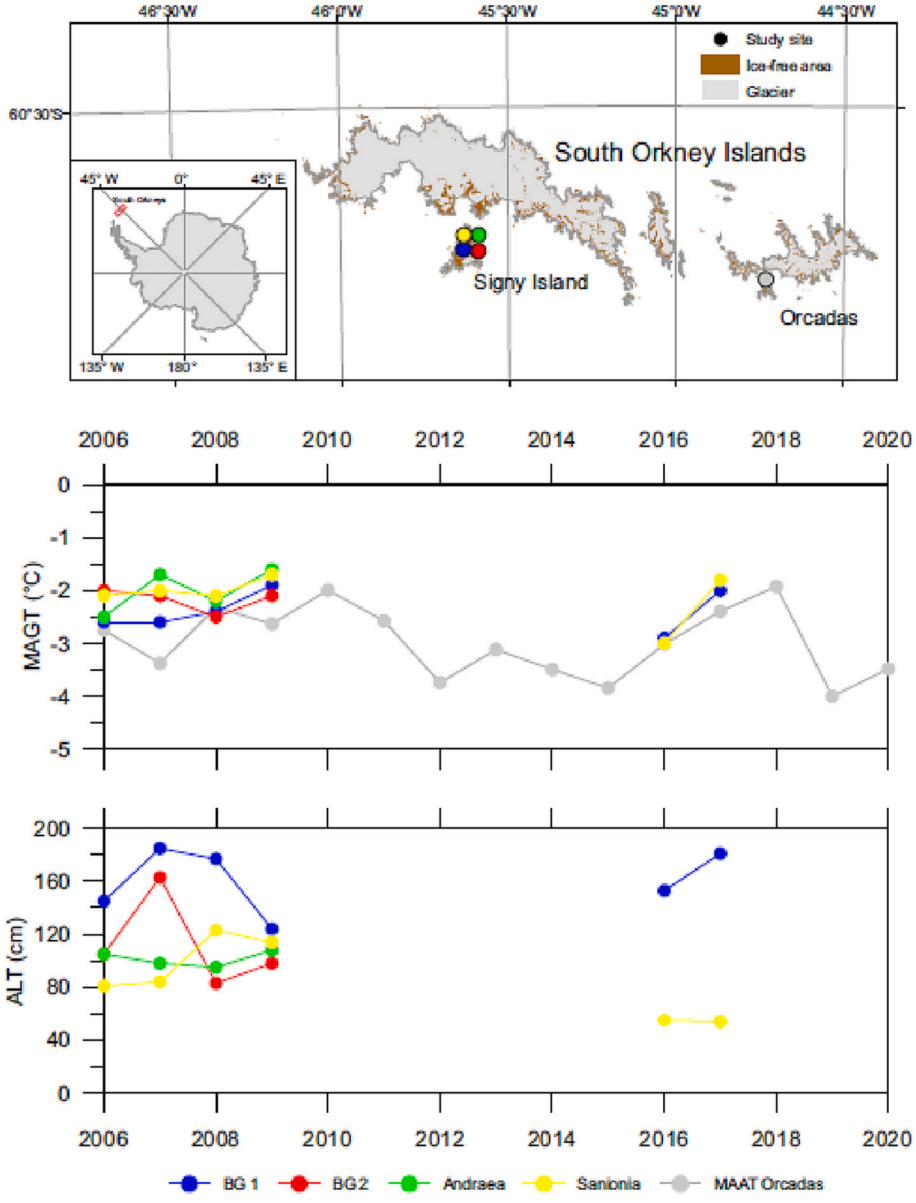

Fig. 6. The variability of mean annual near-surface ground temperature (MAGT) and active layer thickness (ALT) in selected sites of the Sub-Antarctic Islands. The data were extracted from studies by [1]Guglielmin et al., 2012; [2]Hrbáček et al., 2020a; [3]READER database.

Macquarie Islands (McGlone, 2002), with no evidence of permafrost, nor of seasonal freezing at lower elevations (Nel et al., 2021). Ground frost yields the lateral and vertical movement of particles within the soil column (Nel et al., 2021), and subsequent sorting of the ground (Hansen, 2018). MAGT ranges from 1 to 5 °C (Nel et al., 2021), MAAT from 1 to 6 °C (Hansen, 2018) at elevations ranging from 800 to 100 m a.s.l. Annual TDD are 392 °C·day at higher elevation, and 499 °C·day at lower elevation (Table 8). The annual FDD are −195 °C·day at higher, and −95 °C·day at lower elevations (Hansen, 2018). While the majority of the sub-Antarctic islands do not exhibit permafrost, all are undergoing rapid change leading to glacial retreat, reduction of ground ice and snow, changes in frost processes, as well as far-reaching effects on local fauna and flora.

4. Discussion

Permafrost in Antarctica is widespread in ice-free regions and is only absent near sea level in some areas across the South Shetland Islands and Western Antarctic Peninsula (Bockheim et al., 2013, Correia et al., 2017; Ferreira et al., 2017), as well as sub-Antarctic islands north of 60°S, where patchy permafrost occurs only in elevated areas (Obu et al., 2020). Permafrost thickness naturally ranges from a few meters on the warmest Antarctic part in the West Antarctic Peninsula (Bockheim et al., 2013), up to almost 1000 m estimated in the cold conditions of the McMurdo Dry Valleys (Decker and Bucher, 1977). The regional variability of permafrost thickness is mainly affected by geothermal heat-flow (Borzotta and Trombotto, 2004) in areas under active tectonic and volcanic processes (e.g., Burton-Johnson et al., 2020).

4.1. Active layer and permafrost thermal regime

The vast surface of the Antarctic continent, as well as the range of climatic, topographical, and lithological settings, makes it challenging to infer regional characteristics of spatial patterns of the active layer in terms of thermal regime, thickness, or spatio-temporal dynamics. The MAGT is strongly driven by latitude ($R^2 = 0.9$), showing a cooling trend of– ca. 0.9 °C/deg. (Fig. 7). The Antarctic Peninsula is the only area where strong temperature asymmetry can be found at the same latitude, with up to 5 °C difference between the western and eastern sides (Cook and Vaughan, 2010). The most of the study sites are elevated lower than 300 m a.s.l. The only area with clearly defined altitude trend is McMurdo Dry Valleys (MDV) where the elevations cover range from sea level up to 1700 m a.s.l. resulting into the lapse rate of MAGT of ca 0.6 °C/100 m (Adlam et al., 2010; Carshalton et al., 2022).

Data reveals (non-significant) warming trends in mean annual near-surface temperatures (Fig. 8) in the South Shetlands (SSI; 0.028 °C/year), Eastern Antarctic Peninsula (AP; 0.11 °C/year) and Victoria Land (VL; 0.027 °C/year), and a cooling (non-significant) trend was only detected in East Antarctica (EA; −0.062 °C/year). However, the trend analysis of MAAT revealed that all of the Antarctic regions experienced (non-significant) warming during the period 2006–2020 (Fig. 8). The results from AP region show that the initial cooling observed at the beginning of the 21st century (e.g. Turner et al., 2016; Oliva et al., 2017b) has already shifted to a regional warming pattern, following the warming occurred in this region since 1950s (e.g. Turner et al., 2020). This trend change was discussed by Kaplan Pastíriková et al. (2023), who detected the temperature trend change from cooling to warming around 2012–2014 on James Ross Island. Results from VL are in accordance with Cannone et al. (2021) observing slight warming in several sites in the period 2003–2013. The recent ground temperature trends in Antarctica reaching similar values between 0.3 and 1.0 °C/decade as was observed since 1990s in the Arctic regions (Smith et al., 2022) or.

Data for permafrost temperatures are restricted to several sites located in Western AP, EA and VL (Biskaborn et al., 2019) where there are boreholes that are deep enough to reach the depth of zero annual amplitude. Its depth varies from around 10 to 20 m in Antarctica (Vieira et al., 2010). Biskaborn et al., 2019 reported a non-significant warming trend of 0.37 + − 0.1 °C in the period 2008–2016 for six of the sites (three in Western AP, one in EA, two in VL) involved to the study. The permafrost temperature varied from −1.5 °C in the SSI up to ca. -19 °C in VL (Fig. 9) The variability of annual ground temperatures in the depths above the depth of zero annual amplitude is significantly greater in the colder regions of EA and VL then SSI (Fig. 9). Nevertheless, the mean annual ground temperature exhibits only small offset between surface and the deep part of profile suggesting high thermal stability of the first tens meter of permafrost. Notably, data from some of some boreholes deeper than 5 m suggest that permafrost is absent, which is the case of lower elevated parts on Hurd Peninsula on Livingston Island (Ferreira et al., 2017) and Palmer station in Western AP (Wilhelm et al., 2015).

4.2. Spatio-temporal distribution of active layer thickness

The ALT in Antarctica has higher regional variability than MAGT (Fig. 7). When considering the low-elevation (< 100 m a.s.l.) non-bedrock sites, the active layer follows the latitudinal gradient by thinning of 3.7 cm/deg. ($R^2 = 0.64$; $p < 0.05$). Similarly, to the latitudinal pattern, we found a strong and significant relationship ($R^2 = 0.6$; $p < 0.01$) between the MAGT and ALT at the continental scale (Fig. 7c). The highest variability of ALT is in the warmest sites of SSI and South

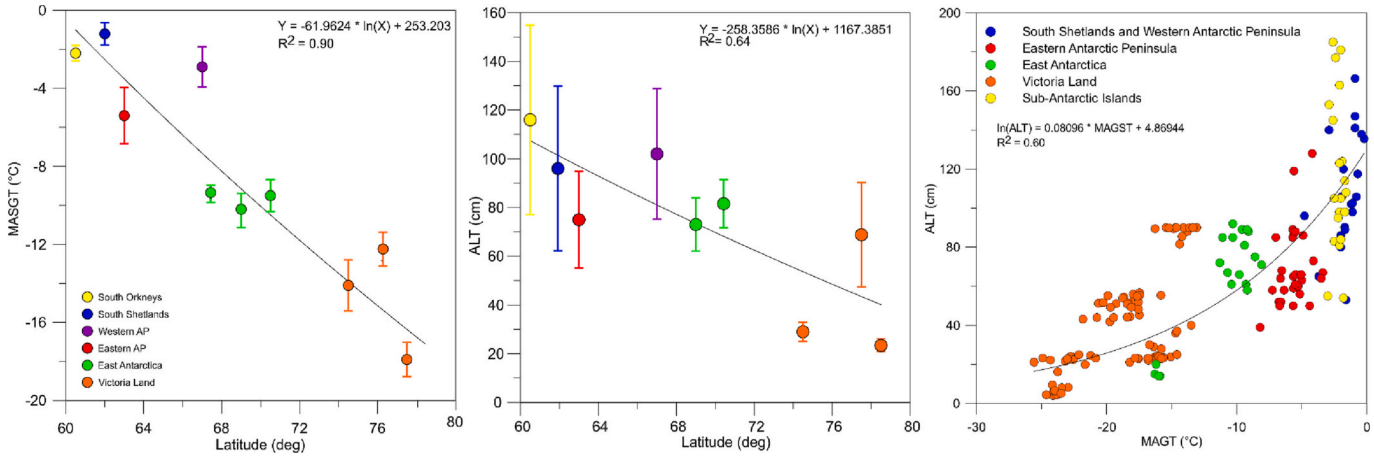

Fig. 7. The relationships between latitude and mean annual near-surface ground temperature and active layer thickness. The bars express standard deviance for each of the study region. The data in right figure represents individual years and was extracted from the studies presented in Tables 2-7.

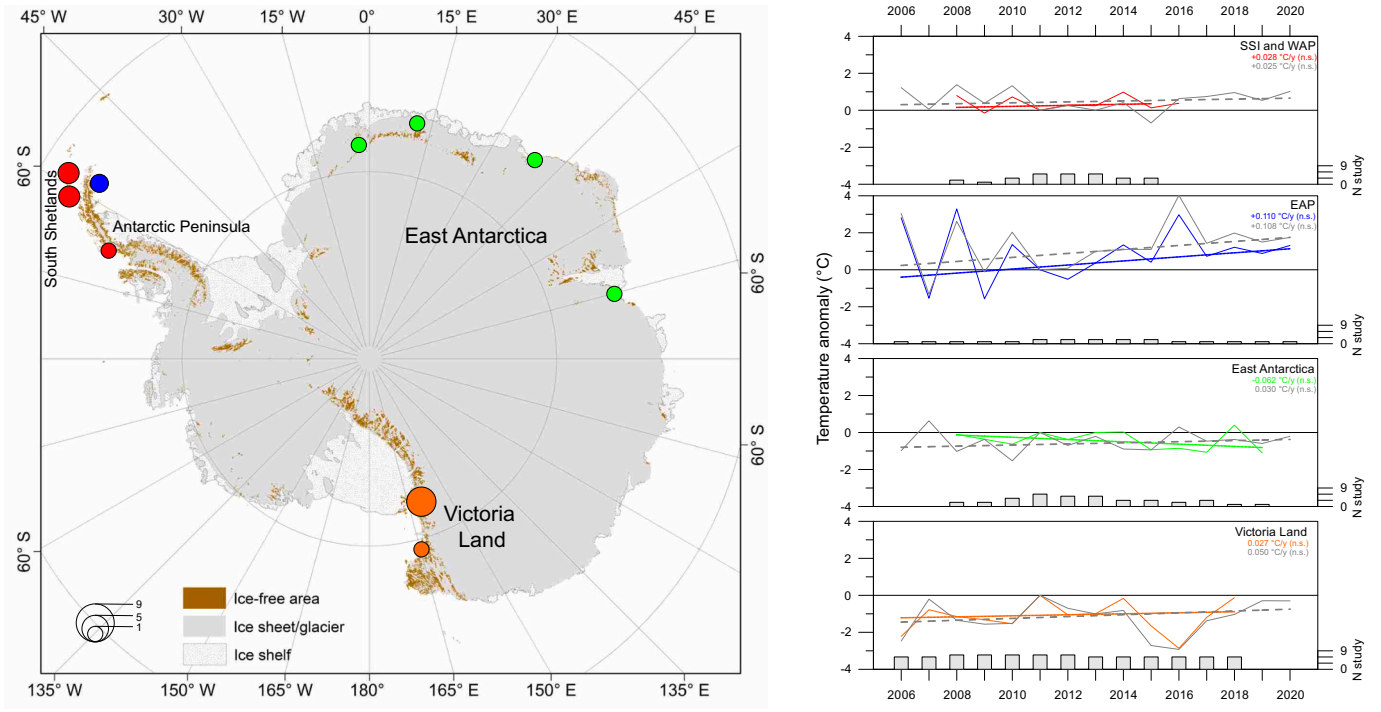

Fig. 8. Variability of annual temperature anomalies of near-surface ground temperature (color lines) and air temperature (grey lines) calculated for the regions of Antarctica. The dashed lines indicate the trends; the color labels distinguish between trends for near-surface and air temperatures (grey), n.s. express that the trend is not statistically significant, box plots indicate the number of studies used for anomaly calculation for individual years, the locations of the datasets are indicated on the map.

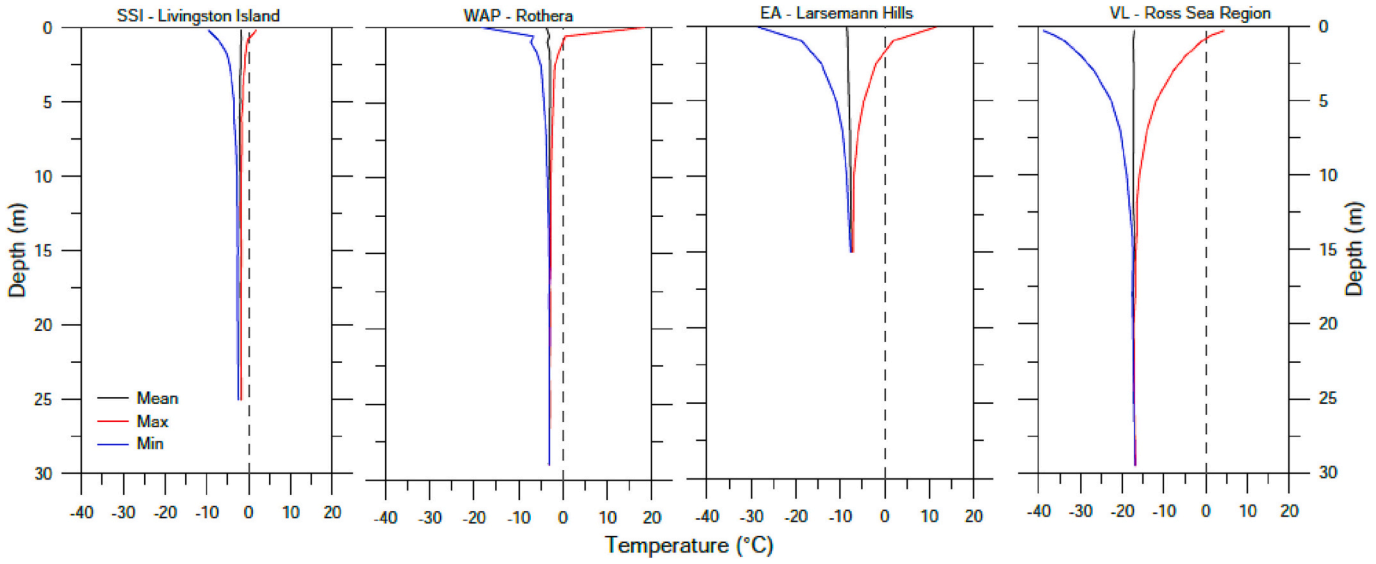

Fig. 9. Differences in the temperature profile on selected deep boreholes between South Shetlands (SSI; mean data from the period 2008 – 2016; Ramos, unpublished data) Western Antarctic Peninsula (WAP; mean data from the period 2009–2011; Guglielmin et al., 2014b), East Antarctica (EA, mean data from the period 2013 – 2019; Abramov, unpublished data) and Victoria Land (VL, data from year 2009; Guglielmin et al., 2011).

Orkneys where the local conditions clearly have a stronger effect than the temperature. The overall span of ALT observed in Antarctica is from 3 cm in the coldest parts of VL (Adlam et al., 2010; Carshalton et al., 2022) up to more than 500 cm in the bedrock sites in SSI and Western AP (Bockheim et al., 2013; Ferreira et al., 2017).

In general, high intersite variability of ALT in order of tens of centimetres is typical for each of the Antarctic regions (Fig. 7). Such a variability is mostly associated with specific in-situ factors such as local climate patterns and snow, lithology, topography, biota, and the hydric regime. The particular role of these factors is discussed in detail section 4.3. As in the case of near-surface ground temperature, the altitudinal gradient of ALT was identified in MDV region to be ca. 2.5 cm/100 m for the altitudes between 50 and 1700 m a.s.l. (Adlam et al., 2010; Carshalton et al., 2022).

Overall, the ALT on selected sites providing at least 7 years of data from different regions of Antarctica (Table 9) reaches comparable values of variation index as observed in sites across Arctic (e.g;Christiansen, 2004; Shur et al., 2005; Smith et al., 2009) over similarly long

Table 9
The temporal variability of active layer thickness (ALT) on the selected sites.

Site description	Monitoring period	Mean ALT	Variation index*	Trend
Eastern Antarctic Peninsula; James Ross Island, Johann Gregor Mendel [1]	10 years	60 cm	11%	+1.2 cm/yr (2011–2020)
South Shetlands, Deception Island, CALM-S Crater Lake[2]	9 years	37.5 cm[+]	17%	−1 cm/yr (2006–2014)
South Shetlands, Livingston Island, Limnopolar Lake [3]	12 years	41 cm[+]	29%	+0.4 cm/yr (2009–2020)
South Shetlands, King George Island, CALM-S Bellingshausen[4]	10 years	62.5 cm[+]	37%	0 cm/yr (2008–2019)
East Antarctica, Schirmacher Oasis[4]	9 years	82 cm[+]	12%	+2.7 cm/yr (2009–2018)
Victoria Land, Ross Sea region, Marble Point[5]	13 years	49 cm	16%	−0.5 cm/yr (2006–2018)
Victoria Land, Ross Sea region, Victoria Valley[5]	13 years	23 cm	9%	−0.05 cm/yr (2006–2018)
Victoria Land, Ross Sea Region, Bull Pass[5]	13 years	49 cm	11%	−0.17 cm/yr (2006–2018)
Victoria Land, Ross Sea Region, Mina Bluff[5]	12 years	23 cm	5%	+0.04 cm/yr (2006–2018)
Victoria Land, Northern Victoria Boulder Clay[6]	7 years	30 cm	22%	+1.75 cm/yr (2006–2013)

* Calculated using equation in Hinkel and Nelson (2003) (mean ALT – max ALT) / mean ALT.

+ Active layer measured by mechanical probing [1] Kaplan Pastíriková et al., 2023; [2] Ramos et al. (2017); [3] de Pablo et al. (2018) and CALM site (2022); [4]Hrbáček et al. (2021a, 2021b) and CALM site (2022); [4] Carshalton et al. (2022); [5] Cannone et al. (2021).

monitoring periods. However, unlike the sites in the northern hemisphere, there is not a clear thickening or thinning trend of ALT in Antarctica. The active layer thinning was observed on several sites in AP and SSI in the period 2006 to 2015 (de Pablo et al., 2017, 2020; Ramos et al., 2017; Hrbáček and Uxa, 2020) and was associated to regional temperature cooling in the beginning of 21st century (Turner et al., 2016; Oliva et al., 2017b). The most recent results, however, indicated that the cooling and thinning was turned to warming and thickening around 2013–2015 (Kaplan Pastíriková et al., 2023). The results from the network in Ross Sea Region indicates overall stable conditions during the period 2000–2018 (Carshalton et al., 2022), whereas Cannone et al. (2021) found slight active layer thickening in the sites of Northern VL. When comparing to region in the northern hemisphere where the rapid active layer thickening is observed over last few decades (e.g. Xu and Wu, 2021; Strand et al., 2021, Blunden and Boyer, 2022; Smith et al., 2022) the ALT in Antarctica appear to be relatively stable in the last two decades. Our results show that the trends on the selected study sites were both thinning and thickening, but mostly statistically non-significant (Table 9).

The thaw depth variability is well documented by CALM-S sites or similar experiments using probing for the active layer measurement. The thaw depth measurement in the SSI region exhibited much lower values than ALT and range from 12 to 53 cm and 23 to 36 cm on Livingston Island (de Pablo et al., 2014, 2017) and Deception Island (Ramos et al., 2017), respectively. Here, the observed lower thaw depth values are influenced by logistic constraints (Guglielmin, 2006) and do not report the maximum values but the values typical for the certain period of the year. Thawing depths ranging from ca. 50 to 120 cm were observed on CALM-S on James Ross Island in Eastern AP (Hrbáček et al., 2017a, 2017b, 2021a). Relatively high thaw depth variability (ca. 75 to 105 cm) was also reported by Mergelov (2014) from the transect in Larsemann Oasis in EA. In these sites the difference between probing depth and thermally derived ALT is small as the measurement timing was close to the natural seasonal ALT maximum (Hrbáček et al., 2017a). Even though the CALM-S grids provide important data on spatiotemporal dynamics of ALT, probe-based data has to be considered with the caution because in Antarctica stony soil materials may limit probe penetration and logistic constraints often prevent measurements at the time of maximum thaw when the active layer is the deepest (Guglielmin, 2006). Therefore, it is necessary to support thaw depths from probing with continuous temperature logging to accurately define the ALT.

4.3. Factors affecting active layer thermal regime and thickness in Antarctica

4.3.1. Climate

Air temperature is generally the most important parameter driving variability of the ground thermal regime worldwide (e.g.Lembrechts et al., 2022). Usually, near-surface ground temperature exhibits a high correlation with air temperature ($r > 0.7$) at daily, seasonal and annual time scales, which has been reported in all Antarctic regions (e.g. Michel et al., 2012; Lacelle et al., 2016; Kotzé and Meiklejohn, 2017; Hrbáček et al., 2020a). The only moderate correlations were reported for winter seasons when the surface was covered by thick snowpack (e.g. Guglielmin et al., 2012; Hrbáček et al., 2020a) or the site was densely vegetated (Cannone and Guglielmin, 2009).

With regards to ALT, the most important controlling factor on James Ross Island corresponds to air temperatures during the summer, whereas only medium and non-significant correlation was found against winter temperatures (Hrbáček and Uxa, 2020). Adlam et al. (2010) found, that 73% of ALT variability in the MDV can be explained by mean summer air temperature, mean winter air temperature, total summer solar radiation and mean and summer wind speed whereas the summer air temperature itself explained only 15%.

The most pronounced effect of solar radiation on the active layer thermal regime was reported in the MDV and VL sites (Guglielmin and Cannone, 2012). The near-surface temperature in these regions exhibits higher correlations (> 0.9) than in other locations AP, EA and sub-Antarctic regions, where it shows weak to moderate correlation (0.3 to 0.6; Lacelle et al., 2016; Kotzé and Meiklejohn, 2017; Hrbáček et al., 2020a). The intensive incoming radiation can effectively warm the surface to temperatures >30 °C, especially in areas of dark coloured volcanic soils. As a result, unusually high seasonal rates of near-surface TDD exceeding even 800 °C·days and thawing n-factor value >40 were observed (Cannone and Guglielmin, 2009; Hrbáček et al., 2020a). Even though such TDD represent the highest values reported in Antarctica, the ALT was only reported between 40 and 60 cm. Many of the MDV soils have extremely low moisture contents, thus relatively low thermal conductivity.

Snow cover seasonal duration and thickness is also an important factor affecting active layer dynamics in Antarctica. Areas with a relatively thick (> 40 cm) and long-lasting snow cover during winter months had higher ground temperatures and deeper active layers during summer compared to snow-free sites (de Pablo et al., 2014, 2017; Oliva et al., 2017a). Therefore, snow is a potential factor triggering permafrost degradation, especially in the warmest regions with MAAT close to 0 °C (Hrbáček et al., 2020b). As well as the insulating effect of snow, other scenarios were reported. A thick winter snowpack exceeding 1 m was recognized to cause permafrost cooling (Guglielmin et al., 2014b). The presence of snow during the summer months may reduce (Hrbáček et al., 2021a), or prevent, active layer thawing (Guglielmin et al., 2014a). The persistent presence of snow cover, exceeding 1 m, for a few years may promote permafrost aggradation and temporal disappearance of the active layer, as was observed in the SSI (Ramos et al., 2020). Long-lying snow patches also favour the presence or absence of the vegetation cover in ice-free areas as snow-melt supplies water and nutrients, enhancing

soil formation and vegetation growth, and, may therefore, modify ALT distribution and thickness at a very local scale (Guglielmin et al., 2014b).

4.3.2. Lithology and geomorphology

Besides climate, the specific local factors related to lithology or geomorphology, including soil texture, also play a role in active layer dynamics as they may affect soil thermal properties and/or moisture content. The effect of lithology has been studied in detail on James Ross Island, where ALT differences reached up to 40 cm across a short transect across two lithological units with large differences in soil thermal conductivity (Hrbáček et al., 2017a, 2017b, 2021a, 2021b). Certain lithological types, such as coarse-grained volcanic sediments, and varying albedo may explain ALTs that vary from regional averages. For example, the variable lithology on Deception Island is associated with ALTs in a range from between 30 and 40 cm (Ramos et al., 2017) up to 100 cm (Goyanes et al., 2014), whereas ALTs exceed 100 cm in neighbouring sites of the SSI (de Pablo et al., 2017; Ferreira et al., 2017; Oliva et al., 2017b).

The most pronounced effect of lithology is related to observations in bedrock drilled boreholes, where the active layer is typically tens to hundreds of centimetres thicker than in loose material in the same areas. Such differences can be related to the higher thermal conductivity of bedrock. Reported thermal conductivity observed in bedrock sites across Antarctica varied between 2.6 and 4.3 Wm^{-1} K^{-1} (Guglielmin et al., 2011; Correia et al., 2012; Wilhelm et al., 2015). In contrast, the thermal conductivity of soil or sediments was mainly lower than 1.0 W m^{-1} K^{-1} (Hrbáček et al., 2017b; Kaplan Pastíriková et al., 2023) and even lower values, to 0.3 W m^{-1} K^{-1} were detected in very dry and porous soils (Liu et al., 2018). Higher thermal conductivities in bedrock potentially create favourable conditions for rapid thawing and deepening of the active layer.

The geomorphological context may also explain local differences in active layer and permafrost characteristics (temperatures, thickness, distribution). The topographical setting and specific geomorphological features can, for example, significantly affect the redistribution of snow cover. Snow can accumulate in topographical depressions and around natural obstacles (Oliva et al., 2017b; Kňažková et al., 2020), and is also blown away from wind-exposed surfaces (Oliva et al., 2017b; Kavan et al., 2020). Landscape features, such as ice-cored moraines, can favour the development of a permafrost layer, even down to sea level in the SSI, where permafrost is generally absent at low altitudes (Oliva and Ruiz-Fernández, 2020, Correia et al., 2017; Ferreira et al., 2017).

4.3.3. Biota

In contrast to the Arctic or Alpine regions, vegetation is scarce or absent in most areas in Antarctica. Ice-free terrain corresponds mostly to bare ground. However, areas of dense vegetation cover have lower ground temperatures and thinner active layers than areas where vegetation is absent (Cannone and Guglielmin, 2009; Michel et al., 2012; Hrbáček et al., 2020a). The most apparent effect of moss carpets has been reported from Signy Island in sub-Antarctica, where the moss communities generally form thicker carpets, working as effective insulators. The active layer under such conditions can be >100 cm thicker in bare ground conditions than under mosses (Hrbáček et al., 2020a). We may anticipate that the predicted "greening" of the warmest part of the AP will lead to the expansion of new vegetation communities (e.g. Siegert et al., 2019), which will potentially insulate the ground, and thus slow the impact of warming air temperatures on the soil thermal regime.

4.3.4. Hydric regime

Soil moisture is one of the most crucial parameters affecting the Antarctic environment in terms of biological (e.g. Convey and Peck, 2019), geomorphological (Levy et al., 2011) or soil (e.g. Kennedy, 1993; Ugolini and Bockheim, 2008) evolution. Soil moisture contents also impact greatly on soil thermal conductivity and heat capacity, and thus ALT thickness. However, data on the temporal or spatial variability of soil moisture are almost missing from most of the continent. In the MDV there has been research focusing mostly on defining dry vs. ice-cemented permafrost starting in the 1970s/80s (e.g., Campbell et al., 1994, 1997; Campbell and Claridge, 2006; Seybold et al., 2010). The phenomenon called "water tracks" have been shown to have a role in soil moisture spatial variability, and subsurface flow which impact on the soil's physical and biogeochemical properties and thermal regime (Levy et al., 2011, Wlostowski et al., 2018). Information on soil moisture from other regions is scarce and often only descriptive, providing data on differences in water content between sites with varying lithologies and soil texture (Hrbáček et al., 2017a, 2017b), or a contrast between vegetated and bare ground conditions (Cannone and Guglielmin, 2009; Almeida et al., 2014; Hrbáček et al., 2020a). Antarctic soil gravimetric soil moisture contents can vary within a wide range from very dry conditions <5% (Mergelov et al., 2020) up to fully saturated soils with moisture content around 45–50% and to even greater than 100% where there are ice lenses.

4.4. Surface and thermal offset

The studied sites in Antarctica exhibited low thermal offsets mostly ranging from 0 to 3 °C (Table 10). Such values are lower than reported offsets summarized for Arctic tundra biomes, where they generally exceed 5 °C (Lembrechts et al., 2022). In the AP, we can clearly distinguish the offset differences between sites where prevails the effect of: 1) bare ground sites where the surface offset was generally positive 2) snow, that usually leads to increasing of the thermal offset with the only exception of Rothera where thick snow layer cooled the surface resulting in a negative thermal offset (Guglielmin et al., 2014b); 3) vegetation, where surfaces were cooler than adjacent bare-ground sites (e.g. Hrbáček et al., 2021a, 2021b) resulting in lower values thermal offset; (Table 10)

In EA and the MDV, where the majority of study sites are bare ground, the major factor causing offset differences is presumably soil water content. The higher offset (+1 to+3 °C) is typical at sites with higher contents (e.g. Lacelle et al., 2016) whereas even negative offset can occur on the sites with negligible moisture (Seybold et al., 2010). Similarly, a negative thermal offset was reported by Kotzé and Meiklejohn (2017) from the cold-dry area in EA.

The variation of thermal offsets is generally very low with the mean values between −0.2 °C and + 0.2 °C. Some year-to-year variability of thermal offset was observed for example on James Ross Island and MDV region where the it usually ranges from −1.0 to +0.5 °C (e.g.; Lacelle et al., 2016; Kaplan Pastíriková et al., 2023). The offset between the temperature on the top of the permafrost and the depth of zero annual amplitude was the highest on Larsemann Hills in EA (0.9 °C) whereas it was close to 0 °C in the remaining sites (Fig. 9).

5. Research opportunities

5.1. Monitoring site density and data availability

Sites for monitoring the active layer and the topmost permafrost remain scarce in Antarctica. Vieira et al. (2010) estimated the total number of boreholes to 73 mostly located in the AP and MDV. In this overview, we identified more than 80 profiles deeper than 50 cm or reaching the permafrost table (Tables 2-6) providing temperature data for the active layer and the topmost permafrost. Yet, we expect the number of all boreholes installed in Antarctica is much higher, but unevenly concentrated within a few areas of interest. Similarly, the CALM-S sites are unevenly distributed across the continent. Even though there are 28 sites registered in Antarctica, data from only 9 sites has been shared from 2017 to 2022 in CALM-S database. Overall, increasing data availability and regional coverage is crucial for more comprehensive and reliable results of long-term active layer and permafrost changes.

Table 10
The mean values of the surface and thermal offset for the Antarctic region. The threshold of 10% moisture (Seybold et al., 2010) was used for the definition of dry vs. wet sites for the Victoria Land region. N/A reports the non-available information.

Area	Surface offset			Thermal offset		
	Bare ground	Snow	Vegetation	Bare ground	Snow	Vegetation
SSI and WAP	1.29 ± 0.36	2.0 ± 0.33	0.81 ± 0.4	+0.02 ± 0.16	+0.25 ± 0.17	+0.16 ± 0.26
EAP	1.08 ± 0.6	N/A	0.2 ± 0.42	−0.10 ± 0.42	N/A	N/A
EA	−0.3 ± 0.1	N/A	N/A	N/A	N/A	N/A
VL (dry sites)	0.23 ± 1.13	N/A	N/A	−0.15 ± 0.34	N/A	N/A
VL (wet sites)	1.67 ± 0.65	N/A	1.3 ± 1.0	−0.22 ± 0.45	N/A	N/A
sub-Antar	1.41 ± 0.56	N/A	1.63 ± 0.68	N/A	N/A	N/A

Another challenge for active layer research relies on establishing a denser network for continuous monitoring of soil moisture. Despite the well-known importance of soil moisture, systematic measurements or observations have been carried out only in the MDV to date with only few case studies in Antarctic Peninsula region (e.g. Michel et al., 2012; Thomazini et al., 2020).

Finally, probably the biggest challenges related to monitoring site density relies on installing new deep boreholes, reaching at least the depth of zero annual temperature amplitude (likely to be 10–20 m deep) which is crucial for determining long-term changes in the permafrost (Biskaborn et al., 2019). Only a few boreholes are active in the SSI, Western AP regions and MDV and VL, which is insufficient to provide representative results for Antarctica.

5.2. Modelling approaches

According to recent predictions by Lee et al. (2017), the ice-free surfaces in Antarctica might increase by ca. 25% (17,000 km^2) by 2100. The vast majority of the potentially newly exposed area is likely to be located in the AP, where the ice-free surfaces may double their extent. The newly deglaciated areas will, therefore, provide a research challenge in terms of their geo-ecological development including active layer and permafrost related topics. The connection between different land-systems should be further addressed in future studies. The cold/warm-based (or polythermal) character of glaciers in some of the warmest regions in Antarctica (i.e.; SSI, Western AP, South Orkneys) may explain the presence or absence of permafrost once glaciers retreat. However, permafrost may form in some proglacial environments following deglaciation, as MAAT in glacier margins may range between −2 to −4 °C.

A more complex evaluation of the driving factors' that influence active layer temperature and thickness, and their mutual complementarity has not yet been sufficiently investigated. Notably, published studies often have spatial (one or two sites) and temporal limitations (less than five years long datasets). Some recent reports evaluating longer-term observations have, so far, shown opposing trends of the active layer and uppermost permafrost cooling in the AP (Ramos et al., 2017; Hrbáček and Uxa, 2020) compared to a general warming trend of the permafrost at a depth of zero annual amplitude (Biskaborn et al., 2019) observed over the similar study period (2006–2015). The mismatch may be because decadal datasets are insufficient to provide statistically significant trends (Hrbáček and Uxa, 2020), and there is also, generally, large diversity between the ice-free surfaces of Antarctica.

One possible solution for dataset spatial and temporal extension could be the implementation of high-resolution permafrost models. Several studies have only used the TTOP (Temperature at the Top of Permafrost) or derived Cryogrid-1 models for modelling the permafrost temperature (Ferreira et al., 2017; Hrbáček et al., 2020b; Obu et al., 2020; Kaplan Pastíriková et al., 2023). The models of Gold and Lachenbruch; Stefan; and Kudryavtsev have been used to estimate the active layer thickness (Guglielmin and Cannone, 2012; Wilhelm et al., 2015; Uxa, 2016; Hrbáček and Uxa, 2020; Hrbáček et al., 2020a; Kaplan Pastíriková et al., 2023) or ground thermal regime (Liu et al., 2018; Wlostowski et al., 2018). The models reproduce active layer and permafrost conditions at various temporal (e.g. Liu et al., 2018; Hrbáček and Uxa, 2020) and spatial scales (Obu et al., 2020). A possible reason for limited modelling within permafrost research might be a prevailing lack of knowledge of soil physical properties, particularly, soil moisture and thermal properties (thermal conductivity and heat capacity) represent the key input parameters for all of the above modelling approaches, and their precise assessment is crucial for accurate results (Hrbáček and Uxa, 2020).

5.3. Geophysical surveying

Geophysical surveying might be a key tool for identifying the permafrost presence, spatial distribution, or thickness, especially in areas with transition conditions between continuous – discontinuous or sporadic permafrost zones. Until now, only a few studies using different techniques have been undertaken. An electrical resistivity tomography survey revealed patches of thin sporadic permafrost on Livingston Island (Correia et al., 2017) and Deception Island (Goyanes et al., 2014). Further, detailed, automatic electrical resistivity tomography surveying of the active layer in Deception Island is planned to explore the spatial-temporal evolution over one year (Farzamian et al., 2020). Similarly, scarce is surveying with ground-penetrating radar, which was used for the detection of ALT spatial variability on James Ross Island (Hrbáček et al., 2021a), permafrost occurrence on SSI (Hauck et al., 2007), and the subsurface structures, including active layer and ground ice in MDV (Campbell et al., 2018.

6. Conclusions

In spite of some flaws, there has been obvious progress in permafrost and active layer research in Antarctica since the International Polar Year in 2007/08. This overview evaluated the current state of the research and discussed challenges for future research. On-going research is important to determine medium term (decadal) changes and to help better predict what changes may occur in the longer-term. In regions such as the South Shetland or sub-Antarctic Islands, where the mean annual temperature is close to 0 °C, small changes in climate may lead to marked changes in soil processes as the balance between liquid water and ice within the soil changes. However, in regions where MAATs are markedly below 0 °C, and where presence of liquid water is scarce, such as the McMurdo Dry Valleys, changes are likely to be less marked.

The mean annual, near-surface, ground temperature ranges from around −1 to −3 °C in the South Shetlands up to temperatures between -14 °C and − 24 °C in Victoria Land. The latitudinal gradient for the sites near to sea level is 0.9 °C/deg. In the McMurdo Dry Valleys area, we also observed an altitudinal gradient of near-surface ground temperature of 0.6 °C/100 m. Even though we identified many parameters which have a clear impact on the active layer thermal regime, the differences in surface and thermal offsets for the sites under the influence of variable factors was relatively low. Similarly, to near-surface, the permafrost temperature ranges from ca. -1.5 °C in the South Shetlands to ca - 19 °C

in the McMurdo Dry Valleys. Notably, the thermal offset between the top of the permafrost table and the depth of zero annual amplitude was not for any of the studied sites.

The active layer thickness was spatially variable and sensitive to local driving factors like air temperature, global radiation, snow occurrence, topography, lithology, soil moisture or vegetation. The highest spatial variability of active layer thickness was in the South Shetlands and Antarctic Peninsula regions (ca. 45 to >500 cm) and the lowest is in Victoria Land (ca. 5 to 90 cm). The index of active layer thickness variation was between 9 and 37% on the sites with long term monitoring. When considering the low elevation sites, we identified a mean latitudinal gradient of 3.7 cm/deg. In the McMurdo Dry Valleys, the altitudinal gradient was reported as reaching 2.5 cm/100 m.

Our study also reveals some challenges for future research. There is a lack of results allowing more detailed evaluation of long-term variability of the ground thermal regime. Such results are limited only to a few regions, which currently prevents reliable analysis for the entire continent from being undertaken. Further, very little is known about soil moisture, which should be, especially in harsh conditions of Antarctica, one of the most important parameters influencing the soil thermal regime, active layer thickness, ground thermal parameters, and vegetation distribution. Due to general remoteness of the individual study areas in Antarctica, we should emphasize that international cooperation is necessary for further successful progress in active layer and permafrost research in Antarctica.

Declaration of Competing Interest

The authors declare that they have no known competing financial interests or personal relationships that could have appeared to influence the work reported in this paper.

Data availability

Data will be made available on request.

Acknowledgements

FH and LKP acknowledge Czech Scientific Foundation project (GM22-28659M), Masaryk University internal project (MUNI/A/1323/2022) and Czech Antarctic Research Programme funded by MEYS of Czech Republic. MO acknowledges support from the project NUNANTAR (Fundação para a Ciência e Tecnologia of Portugal; 02/SAICT/2017 - 32002) and the research groups ANTALP (Antarctic, Arctic, Alpine Environments; 2017-SGR-1102) funded by the Agència de Gestió d'Ajuts Universitaris i de Recerca of the Government of Catalonia. TO'N acknowledge ongoing technical and dataset support of Dr. Cathy Seybold of the USDA. Over the years many people have contributed to installation and maintenance of the McMurdo Dry Valley Soil Climate stations, but special thanks are due to Cathy Seybold, Ron Paetzold, Deb Harms and Don Huffman from the USDA; Jackie Aislabie and Fraser Morgan from Landcare Research, New Zealand; Chris Morcom, Dean Sandwell from the University of Waikato, New Zealand; and Pete Wilson from the University of Canterbury. Antarctica New Zealand provided logistic support for annual station access. MG and SP wish to thank PNRA (Programma Nazionale di Ricerca in Antartica) for the logistical and financial support in Continental Antarctica, Antarctic Peninsula and in Signy Island. They want also to thank British Antarctic Survey and in particular the Met Group in Rothera Island and the Station Leader in Signy for their logistical support and to download the data. Finally we want to thank Pete Convey, Nicoletta Cannone, Francesco Malfasi for their support in AP and Signy and Riccardo Bono at Mario Zucchelli Station.

References

Abramov, A.A., Sletten, R.S., Rivkina, E.M., Mironov, V.A., Gilichinsky, D.A., 2011. Geocryological conditions of Antarctica. Earth's 15 (3), 3–19.

Adams, B.J., Bardgett, R.D., Ayres, E., Wall, D.H., Aislabie, J., Bamforth, S., Bargagli, R., Cary, C., Cavacini, P., Connell, L., Convey, P., Fell, J.W., Frati, F., Hogg, I.D., Newsham, K.K., O'Donnell, A., Russell, N., Seppelt, R.D., Stevens, M.I., 2006. Diversity and distribution of Victoria Land biota. Soil Biol. Biochem. 38 (10), 3003–3018. https://doi.org/10.1016/j.soilbio.2006.04.030.

Adlam, L.S., Balks, M.R., Seybold, C.A., Campbell, D.I., 2010. Temporal and spatial variation in active layer depth in the McMurdo Sound Region, Antarctica. Antarct. Sci. 22 (1), 45–52. https://doi.org/10.1017/S0954102009990460.

Aislabie, J.M., Chhour, K.L., Saul, D.J., Miyauchi, S., Ayton, J., Paetzold, R.F., Balks, M. R., 2006. Dominant bacteria in soils of Marble point and Wright valley, Victoria land, Antarctica. Soil Biol. Biochem. 38 (10), 3041–3056.

Aislabie, J.M., Jordan, S., Barker, G.M., 2008. Relation between soil classification and bacterial diversity in soils of the Ross Sea region, Antarctica. Geoderma 144 (1–2), 9–20.

Aislabie, J., McLeod, M., Ryburn, J., McGill, A., Thornburrow, D., 2011. Soil type influences the leaching of microbial indicators under natural rainfall following application of dairy shed effluent. Soil Res. 49 (3), 270. https://doi.org/10.1071/SR10147.

Almeida, I., Schaefer, C.E.G.R., Fernandes, R.B.A., Pereira, T.T.C., Nieuwendam, A., Pereira, A.B., 2014. Active layer thermal regime at different vegetation covers at Lions Rump, King George Island, Maritime Antarctica. Geomorphology 225, 36–46.

Almeida, I.C.C., Schaefer, C.E.G.R., Michel, R.F.M., Fernandes, R.B.A., Pereira, T.T.C., Andrade, A.M., Francelino, M.R., Elpidio, I., Filho, F., Bockheim, J.G., 2017. Long term active layer monitoring at a warm-based glacier front from maritime Antarctica. Catena 149 (2), 572–581.

Altmaier, M., Herpers, U., Delisle, G., Merchel, S., Ott., U., 2011. Glaciation history of Queen Maud Land (Antarctica) reconstructed from in-situ produced cosmogenic 10Be, 26Al and 21Ne. Polar Sci. 4 (1), 42–61. https://doi.org/10.1016/j.polar.2010.01.001.

Andriuzzi, W.S., Adams, B.J., Barrett, J.E., Virginia, R.A., Wall, D.H., 2018. Observed trends of soil fauna in the Antarctic Dry Valleys: early signs of shifts predicted under climate change. Ecology 99 (2), 312–321.

Balks, M.R., O'Neill, T.A., 2016. Soil and permafrost in the Ross Sea region of Antarctica: stable or dynamic? Cuadernos Investig. Geogr. 42 (2), 415–434. https://doi.org/10.18172/cig.2923.

Bañon, M., Vasallo, F., 2015. Aemet en la Antártida. Climatología y meteorología sinóptica en las estaciones meteorológicas en las estaciones meteorológicas españolas en la Antártida. AEMET Min. Madrid, 150 pp.

Bañón, M., Justel, A., Velázquez, A., Quesada, A., 2013. Regional weather survey in Byers Peninsula, Livingston Island, South Shetland Islands, Antarctica. Antarct. Sci. 25, 146–156. https://doi.org/10.1017/S0954102012001046.

Barrett, P.J., 1971. Geologic Maps of Antarctica, by Campbell Craddock. ARCTIC 24.

Barrett, J.E., Virginia, R.A., Hopkins, D.W., Aislabie, J., Bargagli, R., Bockheim, J.G., Wallenstein, M.D., 2006. Terrestrial ecosystem processes of Victoria land, Antarctica. Soil Biol. Biochem. 38 (10), 3019–3034.

Benayas, J., Pertierra, L., Tejedo, P., Lara, F., Bermudez, O., Hughes, K.A., Quesada, A., 2013. A review of scientific research trends within ASPA no. 126 Byers Peninsula, South Shetland Islands, Antarctica. Antarct. Sci. 25 (2), 128–145. https://doi.org/10.1017/S0954102012001058.

Biskaborn, B.K., Smith, S.L., Noetzli, J., Matthes, H., Vieira, G., Streletskiy, D.A., Schoeneich, P., Romanovsky, V.E., Lewkowicz, A.G., Abramov, A., Allard, M., Boike, J., Cable, W.L., Christiansen, H.H., Delaloye, R., Diekmann, B., Drozdov, D., Etzelmüller, B., Grosse, G., Guglielmin, M., Ingeman-Nielsen, T., Isaksen, K., Ishikawa, M., Johansson, M., Johannsson, H., Joo, A., Kaverin, D., Kholodov, A., Konstantinov, P., Kröger, T., Lambiel, C., Lanckman, J.P., Luo, D., Malkova, G., Meiklejohn, I., Moskalenko, N., Oliva, M., Phillips, M., Ramos, M., Sannel, A.B.K., Sergeev, D., Seybold, C., Skryabin, P., Vasiliev, A., Wu, Q., Yoshikawa, K., Zheleznyak, M., Lantuit, H., 2019. Permafrost is warming at a global scale. Nat. Commun. 10, 1–11. https://doi.org/10.1038/s41467-018-08240-4.

Björck, S., Olsson, S., Ellis-Evans, C., Håkansson, H., Humlum, O., de Lirio, J.M., 1996. Late Holocene palaeoclimatic records from lake sediments on James Ross Island, Antarctica. Palaeogeogr. Palaeoclimatol. Palaeoecol. 121 (3–4), 195–220. https://doi.org/10.1016/0031-0182(95)00086-0.

Blunden, J., Boyer, T. (Eds.), 2022. State of The Climate 2021. Bulletin of American Meteorological Society, pp. S1–S465. https://journals.ametsoc.org/view/journals/bams/103/8/2022BAMSStateoftheClimate.1.xml?tab_body=abstract-display.

Bockheim, J.G., 1997. Properties and classification of cold desert soils from Antarctica. Soil Sci. Soc. Am. J. 61 (1), 224–231.

Bockheim, J.G., 2010. Evolution of desert pavements and the vesicular layer in soils of the Transantarctic Mountains. Geomorphology 118 (3–4), 433–443. https://doi.org/10.1016/j.geomorph.2010.02.012.

Bockheim, J.G. (Ed.), 2015. The Soils of Antarctia. Springer. https://doi.org/10.1007/978-3-319-05497-1, 322 p.

Bockheim, J.G., McLeod, M., 2008. Soil distribution in the McMurdo Dry Valleys, Antarctica. Geoderma 144 (1–2), 43–49. https://doi.org/10.1016/j.geoderma.2007.10.015.

Bockheim, J.G., Campbell, I.B., McLeod, M., 2007. Permafrost distribution and active-layer depths in the McMurdo Dry Valleys, Antarctica. Permafr. Periglac. Process. 18 (3), 217–227. https://doi.org/10.1002/ppp.588.

Bockheim, J., Vieira, G., Ramos, M., López-Martínez, J., Serrano, E., Guglielmin, M., Wilhelm, K., Nieuwendam, A., 2013. Climate warming and permafrost dynamics in

the Antarctic Peninsula region. Glob. Planet. Chang. 100, 215–223. https://doi.org/10.1016/j.gloplacha.2012.10.018.
Borzotta, E., Trombotto, D., 2004. Correlation between frozen ground thickness measured in Antarctica and permafrost thickness estimated on the basis of the heat flow obtained from magnetotelluric soundings. Cold Reg. Sci. Technol. 40 (1–2), 81–96. https://doi.org/10.1016/j.coldregions.2004.06.002.
Boy, J., Godoy, R., Shibistova, O., Boy, D., McCulloch, R., Andrino de la Fuente, A., Morales, M.A., Mikutta, R., Guggenberger, G., 2016. Successional patterns along soil development gradients formed by glacier retreat in the Maritime Antarctic, King George Island. Rev. Chil. Hist. Nat. 89, 1–17. https://doi.org/10.1186/s40693-016-0056-8.
Bromwich, D.H., Guo, Z., Bai, L., Chen, Q., 2004. Modeled Antarctic Precipitation. Part I: Spatial and Temporal Variability. J. Clim. 17, 427–447. https://doi.org/10.1175/1520-0442(2004)017<0427:MAPIS>2.0.CO;2.
Bromwich, D.H., Steinhoff, D.F., Simmonds, I., Keay, K., Fogt, R.L., 2011. Climatological aspects of cyclogenesis near Adélie Land Antarctica. Tellus A 63 (5), 921. https://doi.org/10.1111/j.1600-0870.2011.00537.x.
Brooks, S.T., Jabour, J., van den Hoff, J., Bergstrom, D.M., 2019. Our footprint on Antarctica competes with nature for rare ice-free land. Nat. Sustain. 2 (3), 185–190. https://doi.org/10.1038/s41893-019-0237-y.
Brown, J., Hinkel, K.M., Nelson, F.E., 2000. The Circumpolar active layer monitoring (CALM) program: historical perspectives and initial results. Polar Geogr. 24 (3), 165–258.
Burton-Johnson, A., Dziadek, R., Martin, C., 2020. Review Article: Geothermal heat flow in Antarctica: current and future directions. The Cryosphere 14, 3843–3873. https://doi.org/10.5194/tc-14-3843-2020.
CALM site, 2022. Available online: https://www2.gwu.edu/~calm/.
Campbell, I.B., Claridge, G.G.C., 1987. Antarctica: Soils, Weathering Processes and Environment. Elsevier, 368 pp.
Campbell, I.B., Claridge, G.G.C., 2006. Permafrost properties, patterns and processes in the TransAntarctic Mountains Region. Permafr. Periglac. Process. 17, 215–232.
Campbell, I.B., Claridge, G.G.C., Balks, M.R., 1994. The effect of human activities on moisture content of soils and underlying permafrost from the McMurdo Sound region, Antarctica. Antarct. Sci. 6, 307–314.
Campbell, I.B., Claridge, G.G.C., Balks, M.R., Campbell, D.I., 1997. Moisture content in soils of the McMurdo Sound and Dry Valley region of Antarctica. In: Lyons, W.B., Howard-Williams, C., Hawes, I. (Eds.), Ecosystem Processes in Antarctic Ice-Free Landscapes. Balkema, Rotterdam, pp. 61–76.
Cannone, N., Guglielmin, M., 2009. Influence of vegetation on the ground thermal regime in continental Antarctica. Geoderma 151 (3–4), 215–223. https://doi.org/10.1016/j.geoderma.2009.04.007.
Cannone, N., Seppelt, R., 2008. A preliminary floristic classification of southern and northern Victoria Land vegetation, continental Antarctica. Antarct. Sci. 20 (6), 553–562. https://doi.org/10.1017/S0954102008001454.
Cannone, N., Augusti, A., Malfasi, F., Pallozzi, E., Calfapietra, C., Brugnoli, E., 2016. The interaction of biotic and abiotic factors at multiple spatial scales affects the variability of CO2 fluxes in polar environments. Polar Biol. 39 (9), 1581–1596. https://doi.org/10.1007/s00300-015-1883-9.
Cannone, N., Guglielmin, M., Malfasi, F., Hubberten, H.W., Wagner, D., 2021. Rapid soil and vegetation changes at regional scale in continental Antarctica. Geoderma 394, 115017. https://doi.org/10.1016/j.geoderma.2021.115017.
Carshalton, A.G., Balks, M.R., O'Neill, T.A., Bryan, K.R., Seybold, C.A., 2022. Climatic influences on active layer depth between 2000 and 2018 in the McMurdo Dry Valleys, Ross Sea Region, Antarctica. Geoderma Region. 29, e00497 https://doi.org/10.1016/j.geodrs.2022.e00497.
Chapman, W.L., Walsh, J.E., 2007. A Synthesis of Antarctic Temperatures. J. Clim. 20 (16), 4096–4117. https://doi.org/10.1175/JCLI4236.1.
Chaves, D.A., Lyra, G.B., Francelino, M.R., Silva, L.D.B., Thomazini, A., Schaefer, C.E.G. R., 2017. Active layer and permafrost thermal regime in a patterned ground soil in Maritime Antarctica, and relationship with climate variability models. Sci. Total Environ. 584-585, 572–585.
Chong, C.W., Pearce, D.A., Convey, P., Yew, W.C., Tan, I.K.P., 2012. Patterns in the distribution of soil bacterial 16S rRNA gene sequences from different regions of Antarctica. Geoderma 181, 45–55.
Christiansen, H.H., 2004. Meteorological control on interannual spatial and temporal variations in snow cover and ground thawing in two northeast Greenlandic Circumpolar-Active-Layer-Monitoring (CALM) sites. Permafrost Periglac. Process. 15, 155–169. https://doi.org/10.1002/ppp.489.
Colesie, C., Walshaw, C.V., Sancho, L.G., Davey, M.P., Gray, A., 2023. Antarctica's vegetation in a changing climate. WIREs Clim. Ch. 14 (1), e810. https://doi.org/10.1002/wcc.810.
Convey, P., Peck, L.S., 2019. Antarctic environmental change and biological responses. Science. Advances 5 (11), eaaz0888.
Cook, A.J., Vaughan, D.G., 2010. Overview of areal changes of the ice shelves on the Antarctic Peninsula over the past 50 years. Cryosphere 4 (1), 77–98. https://doi.org/10.5194/tc-4-77-2010.
Cuchi, J.J., Durán, J.A., Alfaro, D., Serrano, E., López-Martínez, J., 2004. Discriminación de diferentes tipos de agua en un área con permafrost, Antártida. Boletin Real Soc. Espanola Hist. Nat. (Sect. Geol.) 99 (1–4), 2004.
Davies, B.J., Glasser, N.F., Carrivick, J.L., Hambrey, M.J., Smellie, J.L., Nývlt, D., 2013. Landscape evolution and ice-sheet behaviour in a semi-arid polar environment: James Ross Island, NE Antarctic Peninsula. Geol. Soc. Lond., Spec. Publ. 381 (1), 353–395. https://doi.org/10.1144/SP381.1.
Dawson, E.J., Schroeder, D.M., Chu, W., Mantelli, E., Seroussi, H., 2022. Ice mass loss sensitivity to the Antarctic ice sheet basal thermal state. Nat. Commun. 13, 4957.
Decker, E.R., Bucher, G.J., 1977. Geothermal studies in Antarctica. Antarc. J. U.S. 12, 103–104.
Denton, G.H., Hughes, T.J., 2000. Reconstruction of the ross ice drainage system, Antarctica, at the last glacial maximum. Geogr. Ann. 82 (2–3), 143–166. https://doi.org/10.1111/j.0435-3676.2000.00120.x.
Denton, G.H., Sugden, D.E., Marchant, D.R., Hall, B.L., Wilch, T.I., 1993. East Antarctic Ice Sheet Sensitivity to Pliocene Climatic Change from a Dry Valleys Perspective. Geogr. Ann. 75 (4), 155–204. https://doi.org/10.1080/04353676.1993.11880393.
Dewar, G.J., 1970. The geology of Adelaide Island. Cambridge, British Antarctic Survey, 66pp. (British Antarctic Survey Scientific Reports, 57).
Dharwadkar, A., Shukla, S.P., Verma, A., Gajbhiye, D., 2018. Geomorphic evolution of Schirmacher Oasis, central Dronning Maud Land, East Antarctica. Polar Sci. 18.
Emslie, S.D., 2001. Radiocarbon dates from abandoned penguin colonies in the Antarctic Peninsula region. Antarct. Sci. 13 (3), 289–295. https://doi.org/10.1017/S0954102001000414.
Farzamian, M., Vieira, G., Monteiro Santos, F.A., Yaghoobi Tabar, B., Hauck, C., Paz, M. C., Bernardo, I., Ramos, M., de Pablo, M.A., 2020. Detailed detection of active layer freeze–thaw dynamics using quasi-continuous electrical resistivity tomography (Deception Island, Antarctica). Cryosphere 14 (3), 1105–1120. https://doi.org/10.5194/tc-14-1105-2020.
Favero-Longo, S.E., Worland, M.R., Convey, P., Lewis Smith, R.I., Piervittori, R., Guglielmin, M., Cannone, N., 2012. Primary succession of lichen and bryophyte communities following glacial recession on Signy Island, South Orkney Islands, Maritime Antarctic. Antarct. Sci. 24 (4), 323–336. https://doi.org/10.1017/S0954102012000120.
Ferreira, A., Vieira, G., Ramos, M., Nieuwendam, A., 2017. CATENA 149, 560–571. https://doi.org/10.1016/j.catena.2016.08.027.
Fisher, D.A., Lacelle, D., Pollard, W., Davila, A., McKay, C.P., 2016. Ground surface temperature and humidity, ground temperature cycles and the ice table depths in University Valley, McMurdo Dry Valleys of Antarctica. J. Geophys. Res. Earth Surf. 121 (11), 2069–2084. https://doi.org/10.1002/2016JF004054.
Forte, E., Dalle Fratte, M., Azzaro, M., Guglielmin, M., 2016. Pressurized brines in continental Antarctica as a possible analogue of Mars. Sci. Rep. 6, 33158 (2016). https://doi.org/10.1038/srep33158.
Fountain, A.G., Nylen, T.H., Monaghan, A., Basagic, H.J., Bromwich, D., 2010. Snow in the McMurdo dry valleys, Antarctica. Int. J. Climatol. 30 (5), 633–642.
Fountain, A.G., Levy, J.S., Gooseff, M.N., Van Horn, D., 2014. The McMurdo Dry Valleys: a landscape on the threshold of change. Geomorphology 225, 25–35.
Fountain, A.G., Basagic, H.J., Niebuhr, S., 2016. Glaciers in equilibrium, McMurdo Dry Valleys, Antarctica. J. Glaciol. 62 (235), 976–989. https://doi.org/10.1017/jog.2016.86.
Francelino, M.R., Schaefer, C.E.G.R., Simas, F.N.B., Filho, E.I.F., de Souza, J.J.L.L., da Costa, L.M., 2011. Geomorphology and soils distribution under paraglacial conditions in an ice-free area of Admiralty Bay, King George Island, Antarctica. Catena 85 (3), 194–204. https://doi.org/10.1016/j.catena.2010.12.007.
French, H.M., Guglielmin, M., 1999. Observations on the ice-marginal, periglacial geomorphology of Terra Nova Bay, Northern Victoria Land, Antarctica. Permafr. Periglac. Process. 10 (4), 331–347. https://doi.org/10.1002/(SICI)1099-1530(199910/12)10:4<331::AID-PPP328>3.0.CO;2-A.
Friedmann, E.I., 1982. Endolithic microorganisms in the Antarctic cold desert. Science 215 (4536), 1045–1053.
Fukuda, M., Shimokawa, K., Takahashi, N., Sone, T., 1992. Permafrost in Seymour Island and James Ross Island, Antarctic Peninsula region. Geogr. Rev. Jpn. Ser. A 65 (2), 124–131.
Gerrish, L., Frettwel, P., Cooper, P., 2020. High Resolution Vector Polygons of Antarctic Rock Outcrop (7.3) [dataset]. UK Polar Data Centre, Natural Environment Research Council, UK Research and Innovation.
Gilichinsky, D.A., Nolte, E., Basilyan, A.E., Beer, J., Blinov, A.V., Lazarev, V.E., Kholodov, A.L., Meyer, H., Nikolskiy, P.A., Schirrmeister, L., Tumskoy, V.E., 2007. Dating of syngenetic ice wedges in permafrost with 36Cl. Quat. Sci. Rev. 26 (11−12), 1547–1556. https://doi.org/10.1016/j.quascirev.2007.04.004.
Gimingham, C.H., Smith, R.I.L., 1970. Bryophyte and lichen communities in 603 the Maritime Antarctic. In: Holdgate, M.W. (Ed.), Antarctic Ecology, vol. 1. Academic Press, London, pp. 752–785.
Gjorup, D.F., Schaefer, C.E.G.R., Simas, F.N.B., Francelino, M.R., Michel, R.F.M., Bockheim, J.G., 2020. Sulfurization, acid-sulfate soils and active layer monitoring at the semiarid Seymour Island, Antarctica. Geoderma Region. 22, e00305 https://doi.org/10.1016/j.geodrs.2020.e00305.
Goordial, J., Raymond-Bouchard, I., Riley, R., Ronholm, J., Shapiro, N., Woyke, T., LaButti, K.M., Tice, H., Amirebrahimi, M., Grigoriev, I.V., Greer, C., Bakermans, C., Whyte, L., 2016. Improved high-quality draft genome sequence of the Eurypsychrophile Rhodotorula sp. JG1b, isolated from permafrost in the hyperarid Upper-Elevation McMurdo Dry Valleys, Antarctica. Genome Announc. 4 (2) https://doi.org/10.1128/genomeA.00069-16.
Gore, D.B., Rhodes, E.J., Augustinus, P.C., Leishman, M.R., Colhoun, E.A., Rees-Jones, J., 2001. Bunger Hills, East Antarctica: ice free at the last Glacial Maximum. Geology 29 (12), 1103. https://doi.org/10.1130/0091-7613(2001)029<1103:BHEAIF>2.0.CO;2.
Goyanes, G., Vieira, G., Caselli, A., Cardoso, M., Marmy, A., Santos, F., Bernardo, I., Hauck, C., 2014. Local influences of geothermal anomalies on permafrost distribution in an active volcanic island (Deception Island, Antarctica). Geomorphology 225, 57–68. https://doi.org/10.1016/j.geomorph.2014.04.010.
Graham, A., Kuhn, G., Meisel, O., et al., 2017. Major advance of South Georgia glaciers during the Antarctic Cold Reversal following extensive sub-Antarctic glaciation. Nat. Commun. 8, 14798. https://doi.org/10.1038/ncomms14798.

Guglielmin, M., 2006. Ground surface temperature (GST), active layer, and permafrost monitoring in continental Antarctica. Permafr. Periglac. Process. 17, 133–143. https://doi.org/10.1002/ppp.553.
Guglielmin, M., Cannone, N., 2012. A permafrost warming in a cooling Antarctica? Clim. Chang. 111 (2), 177–195. https://doi.org/10.1007/s10584-011-0137-2.
Guglielmin, M., Biasini, A., Smiraglia, C., 1997. The Contribution of Geoelectrical Investigations in the Analysis of Periglacial and Glacial Landforms in Ice Free areas of the Northern Foothills (Northern Victoria Land, Antarctica). Geogr. Ann. Ser. A Phys. Geogr. 79A (1–2), 17–24. https://doi.org/10.1111/1468-0459.00003.
Guglielmin, M., Ellis Evans, C.J., Cannone, N., 2008. Active layer thermal regime under different vegetation conditions in permafrost areas. A case study at Signy Island (Maritime Antarctica). Geoderma 144 (1–2), 73–85. https://doi.org/10.1016/j.geoderma.2007.10.010.
Guglielmin, M., Balks, M.R., Adlam, L.S., Baio, F., 2011. Permafrost thermal Regime from two 30-m Deep Boreholes in Southern Victoria Land, Antarctica. Permafr. Periglac. Process. 22, 129–139. https://doi.org/10.1002/ppp.715.
Guglielmin, M., Worland, M.R., Convey, P., Cannone, N., 2012. Schmidt Hammer studies in the maritime Antarctic: Application to dating Holocene deglaciation and estimating the effects of macrolichens on rock weathering. Geomorphology 155–156, 33–34. https://doi.org/10.1016/j.geomorph.2011.12.015.
Guglielmin, M., Dalle Fratte, M., Cannone, N., 2014a. Permafrost warming and vegetation changes in continental Antarctica. Environ. Res. Lett. 9 (4), 045001.
Guglielmin, M., Worland, M.R., Baio, F., Convey, P., 2014b. Permafrost and snow monitoring at Rothera Point (Adelaide Island, Maritime Antarctica): Implications for rock weathering in cryotic conditions. Geomorphology 225, 47–56.
Guglielmin, M., Ponti, S., Forte, E., 2018. The origins of Antarctic rock glaciers: periglacial or glacial features? Earth Surf. Process. Landf. 43 (7), 1390–1402. https://doi.org/10.1002/esp.4320.
Hall, K., 2002. Review of present and Quaternary periglacial processes and landforms of the maritime and sub-Antarctic region. S. Afr. J. Sci. 98, 71–81.
Hansen, C.D., 2018. On High-Altitude and –Latitude Diurnal Frost Environments. Rhodes University.
Hansen, C.D., Meiklejohn, K.I., Nel, W., Loubser, M.J., Van Der Merwe, B.J., 2013. Aspect-controlled Weathering Observed on a Blockfield in Dronning Maud Land, Antarctica. Geogr. Ann.: Series A, Phys. Geogr. 95, 305–313. https://doi.org/10.1111/geoa.12025.
Harris, S.A., French, H.M., Heginbottom, J.A., Johnston, G.H., Ladanyi, B., Sego, D.C., van Everdingen, R.O., 1988. Glossary of Permafrost and Related Ground-Ice Terms. National Research Council of Canada. Associate Committee on Geotechnical Research. https://doi.org/10.4224/20386561. Permafrost Subcommittee, 159 p.
Hathway, B., Lomas, S.A., 1998. The Jurassic–Lower Cretaceous Byers Group, South Shetland Islands, Antarctica: revised stratigraphy and regional correlations. Cretac. Res. 19 (1), 43–67. https://doi.org/10.1006/cres.1997.0095.
Hauck, C., Vieira, G., Gruber, S., Blanco, J., Ramos, M., 2007. Geophysical identification of permafrost in Livingston Island, maritime Antarctica. J. Geophys. Res. 112 (F2), F02S19. https://doi.org/10.1029/2006JF000544.
Hedding, D.W., 2008. Spatial inventory of landforms in the recently exposes Central Highland of Sub-Antarctic Marion Island. S. Afr. Geogr. J. 90 (1), 11–21. https://doi.org/10.1080/03736245.2008.9725307.
Hodgson, D.A., Graham, A.G.C., Roberts, S.J., Bentley, M.J., Cofaigh, C.Ó., Verleyen, E., Vyverman, W., Jomelli, V., Favier, V., Brunstein, D., Verfaillie, D., Colhoun, E.A., Saunders, K.M., Selkirk, P.M., Mackintosh, A., Hedding, D.W., Nel, W., Hall, K., McGlone, M.S., Smith, J.A., 2014. Terrestrial and submarine evidence for the extent and timing of the last Glacial Maximum and the onset of deglaciation on the maritime-Antarctic and sub-Antarctic islands. Quat. Sci. Rev. 100, 137–158. https://doi.org/10.1016/j.quascirev.2013.12.001.
Hopkins, D.W., Sparrow, A.D., Novis, P.M., Gregorich, E.G., Elberling, B., Greenfield, L. G., 2006. Controls on the distribution of productivity and organic resources in Antarctic Dry Valley soils. Proc. R. Soc. B Biol. Sci. 273 (1602), 2687–2695. https://doi.org/10.1098/rspb.2006.3595.
Hrbáček, F., Uxa, T., 2020. The evolution of a near-surface ground thermal regime and modeled active-layer thickness on James Ross Island, Eastern Antarctic Peninsula, in 2006–2016. Permafr. Periglac. Process. 31 (1), 141–155. https://doi.org/10.1002/ppp.2018.
Hrbáček, F., Oliva, M., Laska, K., Ruiz-Fernández, J., de Pablo, M.A., Vieira, G., Ramos, M., Nývlt, D., 2016a. Active layer thermal regime in two climatically contrasted sites of the Antarctic Peninsula region. Cuadernos Investig. Geogr. 42 (2), 457–474. https://doi.org/10.18172/cig.2915.
Hrbáček, F., Láska, K., Engel, Z., 2016b. Effect of snow cover on the active-layer thermal regime - a case study from James Ross Island, Antarctic Peninsula. Permafr. Periglac. Process. 27 (3), 307–315. https://doi.org/10.1002/ppp.1871.
Hrbáček, F., Kňažková, M., Nývlt, D., Láska, K., Mueller, C.W., Ondruch, J., 2017a. Active layer monitoring at CALM-S site near J.G. Mendel station, James Ross Island, eastern Antarctic Peninsula. Sci. Total Environ. 601–602, 987–997. https://doi.org/10.1016/j.scitotenv.2017.05.266.
Hrbáček, F., Nývlt, D., Láska, K., 2017b. Active layer thermal dynamics at two lithologically different sites on James Ross Island, Eastern Antarctic Peninsula. Catena 149 (2), 592–602.
Hrbáček, F., Nývlt, D., Láska, K., Kňažková, M., Kampová, B., Engel, Z., Oliva, M., Mueller, C.W., 2019. Permafrost and active layer research on James Ross Island: an overview. Czech Polar Rep. 9 (1), 20–36. https://doi.org/10.5817/CPR2019-1-3.
Hrbáček, F., Cannone, N., Kňažková, M., Malfasi, F., Convey, P., Guglielmin, M., 2020a. Effect of climate and moss vegetation on ground surface temperature and the active layer among different biogeographical regions in Antarctica. Catena 190, 104562. https://doi.org/10.1016/j.catena. 2020. 104562.
Hrbáček, F., Oliva, M., Fernández, J.-R., Kňažková, M., de Pablo, M.A., 2020b. Modelling ground thermal regime in bordering (dis)continuous permafrost environments. Environ. Res. 181, 108901 https://doi.org/10.1016/j.envres.2019.108901.
Hrbáček, F., Engel, Z., Kňažková, M., Smolíková, J., 2021a. Effect of summer snow cover on the active layer thermal regime and thickness on CALM-S JGM site, James Ross Island, eastern Antarctic Peninsula. Catena 207, 105608. https://doi.org/10.1016/j.catena.2021.105608.
Hrbáček, F., Vieira, G., Oliva, M., Balks, M., Guglielmin, M., de Pablo, M.A., Molina, A., Ramos, M., Goyanes, G., Meiklejohn, I., Abramov, A., Demidov, N., Fedorov-Davydov, D., Lupachev, A., Rivkina, E., Láska, K., Kňažková, M., Nývlt, D., Raffi, R., Strelin, J., Sone, T., Fukui, K., Dolgikh, A., Zazovskaya, E., Mergelov, N., Osokin, N., Miamin, V., 2021b. Polar Geogr. 44 (3), 217–231. https://doi.org/10.1080/1088937X.2017.1420105.
Isaac, M.J., Chinn, T.J., Edbrooke, S.W., Forsyth, P.J., 1996. Geology of the Olympus Range Area, Southern Victoria Land, Antarctica. Institute of Geological and Nuclear Science 1:50 000 geological map 20. Lower Hutt, Institute of Geological & Nuclear Sciences, 1 sheet + 60 p.
Jones, V.J., Hodgson, D.A., Chepstow-Lusty, A., 2000. Palaeolimnological evidence for marked Holocene environmental changes on Signy Island, Antarctica. The Holocene 10 (1), 43–60. https://doi.org/10.1191/095968300673046662.
Kaplan Pastíriková, L., Hrbáček, F., Uxa, T., Láska, K., 2023. Permafrost table temperature and active layer thickness variability on James Ross Island, Antarctic Peninsula, in 2004–2021. Sci. Total Environ. 869, 161690 https://doi.org/10.1016/j.scitotenv.2023.161690.
Kavan, J., Nývlt, D., Láska, K., Engel, Z., Kňažková, M., 2020. High-latitude dust deposition in snow on the glaciers of James Ross Island, Antarctica. Earth Surf. Process. Landf. 45, 1569–1578. https://doi.org/10.1002/esp.4831.
Kennedy, A.D., 1993. Water as a Limiting Factor in the Antarctic Terrestrial Environment: A Biogeographical Synthesis. Arct. Alp. Res. 25 (4), 308–315.
Kňažková, M., Hrbáček, F., Kavan, J., Nývlt, D., 2020. Effect of hyaloclastite breccia boulders on meso-scale periglacial-aeolian landsystem in semi-arid Antarctic environment, James Ross Island, Antarctic Peninsula. Cuadernos Investig. Geogr. 46 (1), 7–31. https://doi.org/10.18172/cig.3800.
Kotzé, C., Meiklejohn, I., 2017. Temporal variability of ground thermal regimes on the northern buttress of the Vesleskarvet nunatak, western Dronning Maud Land, Antarctica. Antarct. Sci. 29 (1), 73–81. https://doi.org/10.1017/S095410201600047X.
Lacelle, D., Lapalme, C., Davila, A.F., Pollard, W., Marinova, M., Heldmann, J., McKay, C. P., 2016. Solar Radiation and Air and Ground Temperature Relations in the Cold and Hyper-Arid Quartermain Mountains, McMurdo Dry Valleys of Antarctica. Permafr. Periglac. Process. 27 (2), 163–176. https://doi.org/10.1002/ppp.1859.
Lapalme, C.M., Lacelle, D., Pollard, W., Fortier, D., Davila, A., McKay, C.P., 2017. Cryostratigraphy and the Sublimation Unconformity in Permafrost from an Ultraxerous Environment, University Valley, McMurdo Dry Valleys of Antarctica. Permafr. Periglac. Process. 28 (4), 649–662. https://doi.org/10.1002/ppp.1948.
Lee, C.K., Barbier, B.A., Bottos, E.M., McDonald, I.R., Cary, S.C., 2012. The Inter-Valley Soil Comparative Survey: the ecology of Dry Valley edaphic microbial communities. ISME J. 6 (5), 1046–1057. https://doi.org/10.1038/ismej.2011.170.
Lee, J.Y., Lim, H.S., Yoon, H.I., 2016. Thermal characteristics of soil and water during summer at King Sejong Station, King George Island, Antarctica. Geosci. J. 20 (4), 503–516. https://doi.org/10.1007/s12303-016-0026-9.
Lee, J.R., Raymond, B., Bracegirdle, T.J., Chadés, I., Fuller, R.A., Shawn, J.D., Terauds, A., 2017. Climate change drives expansion of Antarctic ice-free habitat. Nature 547, 49–54. https://doi.org/10.1038/nature22996.
Leihy, R.I., Duffy, G.A., Nortje, E., Chown, S.L., 2018. Data descriptor: High resolution temperature data for ecological research and management on the Southern Ocean Islands. Sci. Data 5, 1–13.
Lembrechts, J.J., van den Hoogen, J., Aalto, J., Ashcroft, M.B., De Frenne, P., Kemppinen, J., Kopecký, M., Luoto, M., Maclean, I.M.D., Crowther, T.W., Bailey, J. J., Haesen, S., Klinges, D.H., Niittynen, P., Scheffers, B.R., Van Meerbeek, K., Aartsma, P., Abdalaze, O., Abedi, M., Lenoir, J., 2022. Global maps of soil temperature. Glob. Change Biol. 28, 3110–3144. https://doi.org/10.1111/gcb.16060.
Levy, J., 2013. How big are the McMurdo Dry Valleys? Estimating ice-free area using Landsat image data. Antarct. Sci. 25 (1), 119–120. https://doi.org/10.1017/S0954102012000727.
Levy, J.S., Fountain, A.G., Obryk, M.K., Telling, J., Glennie, C., Pettersson, R., Gooseff, M., van Horn, D.J., 2018. Decadal topographic change in the McMurdo Dry Valleys of Antarctica: Thermokarst subsidence, glacier thinning, and transfer of water storage from the cryosphere to the hydrosphere. Geomorphology 323, 80–97. https://doi.org/10.1016/j.geomorph.2018.09.012.
Liu, L., Sletten, R.S., Hallet, B., Waddington, E.D., 2018. Thermal Regime and Properties of Soils and Ice-Rich Permafrost in Beacon Valley, Antarctica. J. Geophys. Res. Earth Surf. 123 (8), 1797–1810. https://doi.org/10.1029/2017JF004535.
López-Martínez, J., Serrano, E., 2002. Geomorphology of Deception Island. In: López-Martínez, J., Smellie, J.L., Thomson, J.W., Thomson, M.R.A. (Eds.), Geology and Geomorphology of Deception Island: 31–39. BAS Geomap Series, Sheets 6-A and 6-B. British Antarctic Survey, Cambridge.
López-Martínez, J., Serrano, E., Schmid, T., Mink, S., Linés, C., 2012. Periglacial processes and landforms in the South Shetland Islands (northern Antarctic Peninsula region). Geomorphology 155–156, 62–79. https://doi.org/10.1016/j.geomorph.2011.12.018.
López-Martínez, J., Schmid, T., Serrano, E., Mink, S., Nieto, A., Guilasso, S., 2016. Geomorphology and landforms distribution in selected ice-free areas in the South Shetland Islands, Antarctic Northern Peninsula region. Cuadernos Investig. Geogr. 42 (2), 435–455. https://doi.org/10.18172/cig.2965.

Lowry, D.P., Golledge, N.R., Bertler, N.A.N., Jones, R.S., McKay, R., 2019. Deglacial grounding-line retreat in the Ross Embayment, Antarctica, controlled by ocean and atmosphere forcing. Sci. Adv. 5 (8) https://doi.org/10.1126/sciadv.aav8754.

Mackintosh, A.N., Verleyen, E., O'Brien, P.E., White, D.A., Jones, R.S., McKay, R., Dunbar, R., Gore, D.B., Fink, D., Post, A.L., Miura, H., Leventer, A., Goodwin, I., Hodgson, D.A., Lilly, K., Crosta, X., Golledge, N.R., Wagner, B., Berg, S., Masse, G., 2014. Retreat history of the East Antarctic Ice Sheet since the last Glacial Maximum. Quat. Sci. Rev. 100, 10–30. https://doi.org/10.1016/j.quascirev.2013.07.024.

Marchant, D.R., Head, J.W., 2007. Antarctic dry valleys: Microclimate zonation, variable geomorphic processes, and implications for assessing climate change on Mars. Icarus 192 (1), 187–222. https://doi.org/10.1016/j.icarus.2007.06.018.

Matthews, D.H., Maling, D.H., 1967. The geology of the South Orkney Islands: I Signy Island, Falkland Islands. Depend. Surv. Sci. Rep. 25, 32 pp.

McGlone, M.S., 2002. The late Quaternary peat, vegetation and climate history of the Southern Oceanic Islands of New Zealand. Quat. Sci. Rev. 21 (4–6), 683–707. https://doi.org/10.1016/S0277-3791(01)00044-0.

McKay, C., Balaban, E., Abrahams, S., Lewis, N., 2019. Dry permafrost over ice-cemented ground at Elephant Head, Ellsworth Land, Antarctica. Antarct. Sci. 31 (5), 263–270. https://doi.org/10.1017/S0954102019000269.

Mergelov, N.S., 2014. Soils of wet valleys in the Larsemann Hills and Vestfold Hills oases (Princess Elizabeth Land, East Antarctica). Eurasian Soil Sc 47, 845–862. https://doi.org/10.1134/S1064229314090099.

Mergelov, N., Dolgikh, A., Shorkunov, I., et al., 2020. Hypolithic communities shape soils and organic matter reservoirs in the ice-free landscapes of East Antarctica. Sci. Rep. 10, 10277. https://doi.org/10.1038/s41598-020-67248-3.

Michel, R.F.M., Schaefer, C.E.G.R., Poelking, E.L., Simas, F.N.B., Filho, E.I.F., Bockheim, J.G., 2012. Active layer temperature in two Cryosols from King George Island, Maritime Antarctica. Geomorphology 155-156, 12–19. https://doi.org/10.1016/j.geomorph.2011.12.013.

Michel, R.F.M., Schaefer, C.E.G.R., Simas, F.N.B., Francelino, M.R., Filho, E.I.F., Lyra, G. B., Bockheim, J.G., 2014. Active-layer thermal monitoring on the Fildes Peninsula, King George Island, maritime Antarctica. Solid Earth 5, 1361–1374. https://doi.org/10.5194/se-5-1361-2014.

Mori, J., Sone, T., Strelin, J.A., Torieli, C., Fukui, K., 2006. Characteristics of air and ground temperatures and the reconstruction of active layer thickness on the Rink Plateau, James Ross Island, Antarctic Peninsula. J. Jpn. Soc. Snow Ice 68, 287–298 (in Japanese with English abstract. 1–317).

Moura, P.A., Francelino, M.R., Schaefer, C.E.G.R., Simas, F.N.B., Mendonca, B.A.F., 2012. Distribution and characterization of soils and landform relationships in Byers Peninsula, Livingston Island, Maritime Antarctica. Geomorphology 155-156, 45–54. https://doi.org/10.1016/j.geomorph.2011.12.011.

Navarro, F.J., Jonsell, U.Y., Corcuera, M.I., Martín-Español, A., 2013. Decelerated mass loss of Hurd and Johnsons Glaciers, Livingston Island, Antarctic Peninsula. J. Glaciol. 59 (213), 115–128. https://doi.org/10.3189/2013JoG12J144.

Navas, A., López-Martínez, J., Casas, J., Machín, J., Durán, J.J., Serrano, E., Cuchi, J.-A., Mink, S., 2008. Soil characteristics on varying lithological substrates in the South Shetland Islands, maritime Antarctica. Geoderma 144 (1–2), 123–139. https://doi.org/10.1016/j.geoderma.2007.10.011.

Nel, W., Boelhouwers, J.C., Borg, C.-J., Cotrina, J.H., Hansen, C.D., Haussmann, N.S., Hedding, D.W., Meiklejohn, K.I., Nguna, A.A., Rudolph, E.M., Sinuka, S.S., Sumner, P.D., 2021. Earth science research on Marion Island (1996–2020): a synthesis and new findings. S. Afr. Geogr. J. 103 (1), 22–42. https://doi.org/10.1080/03736245.2020.1786445.

Nelson, P.H.H., 1975. The James Ross Island Volcanic Group of North-East Graham Land. Brit. Antarct. Surv. Sci. Rep. 54 (62 pp.).

Ó Cofaigh, C., Davies, B.J., Livingstone, S.J., Smith, J.A., Johnson, J.S., Hocking, E.P., Hodgson, D.A., Anderson, J.B., Bentley, M.J., Canals, M., Domack, E., Dowdeswell, J. A., Evans, J., Glasser, N.F., Hillenbrand, C.-D.D., Larter, R.D., Roberts, S.J., Simms, A.R., 2014. Reconstruction of ice-sheet changes in the Antarctic Peninsula since the last Glacial Maximum. Quat. Sci. Rev. 100, 87–110. https://doi.org/10.1016/j.quascirev.2014.06.023.

Obu, J., Westermann, S., Vieira, G., Abramov, A., Balks, M.R., Bartsch, A., Hrbáček, F., Kääb, A., Ramos, M., 2020. Pan-Antarctic map of near-surface permafrost temperatures at 1 km2 scale. Cryosphere 14, 497–519. https://doi.org/10.5194/tc-14-497-2020.

Oliva, M., Ruiz-Fernández, J. (Eds.), 2020. The Past Antarctica, 1st edition. Elsevier. 299 pp.

Oliva, M., Antoniades, D., Giralt, S., Granados, I., Pla-Rabes, S., Toro, M., Liu, E.J., Sanjurjo, J., Vieira, G., 2016. The Holocene deglaciation of the Byers Peninsula (Livingston Island, Antarctica) based on the dating of lake sedimentary records. Geomorphology 261, 89–102. https://doi.org/10.1016/j.geomorph.2016.02.029.

Oliva, M., Hrbacek, F., Ruiz-Fernández, J., de Pablo, M.Á., Vieira, G., Ramos, M., Antoniades, D., 2017a. Active layer dynamics in three topographically distinct lake catchments in Byers Peninsula (Livingston Island, Antarctica). CATENA 149, 548–559. https://doi.org/10.1016/j.catena.2016.07.011.

Oliva, M., Navarro, F., Hrbáček, F., Hernández, A., Nývlt, D., Perreira, P., Ruiz-Fernández, J., Trigo, R., 2017b. Recent regional climate cooling on the Antarctic Peninsula and associated impacts on the cryosphere. Sci. Total Environ. 580, 210–223. https://doi.org/10.1016/j.scitotenv.2016.12.030.

Oliva, M., Antoniades, D., Serrano, E., Giralt, S., Liu, E.J., Granados, I., Pla-Rabes, S., Toro, M., Hong, S.G., Vieira, G., 2019. The deglaciation of Barton Peninsula (King George Island, South Shetland Islands, Antarctica) based on geomorphological evidence and lacustrine records. Polar Rec. 55 (3), 177–188.

Oliva, M., Palacios, D., Fernández-Fernández, J.M., Fernandes, M., Schimmelpfennig, I., Vieira, G., Antoniades, D., Pérez-Alberti, A., García-Oteyza, J., ASTER Team, 2023. Holocene Deglaciation of the Northern Fildes Peninsula. Land Degradation & Development, King George Island, Antarctica. https://doi.org/10.1002/ldr.4730.

Olivero, E., Scasso, R.A., Rinaldi, C.A., 1986. Revision of the Marambio Group, James Ross Island, Antarctica. Instituto Antártico Argentino. Contribución 331 (28 pp.).

O'Neill, T., Balks, M., Stevenson, B., López-Martínez, J., Aislabie, J., Rhodes, P., 2013. The short-term effects of surface soil disturbance on soil bacterial community structure at an experimental site near Scott Base, Antarctica. Polar Biol. 36 (7), 985–996. https://doi.org/10.1007/s00300-013-1322-8.

Ortiz, R., García, A., Aparicio, A., Blanco, I., Felpeto, A., Rey, R., Villegas, M., Ibañez, M., Morales, J., Pezzo, E., Olmedillas, J., Astiz, M., Vila, J., Ramos, M., Viramonte, J., Risso, C., Caselli, A., 1997. Monitoring of the volcanic activity of Deception Island, South Shetland islands, Antarctica (1986-1995). In: Ricci, C.A. (Ed.), The Antarctic Region: Geological Evolution and Processes. Terra Antartica Publication, pp. 1071–1076 (ISBN: 88-900221-0-8).

Osokin, N.I., Sosnovkii, A.V., Mavlyudlov, B.R., 2020. Glaciation and Permafrost Dynamics on the Antarctic Peninsula in the 21st Century. Russ. Meteorol. Hydrol. 45, 124–131.

de Pablo, M.A., Blanco, J.J., Molina, A., Ramos, M., Quesada, A., Vieira, G., 2013. Interannual active layer variability at the Limnopolar Lake CALM site on Byers Peninsula, Livingston Island, Antarctica. Antarct. Sci. 25 (2), 167–180. https://doi.org/10.1017/S0954102012000818.

de Pablo, M.A., Ramos, M., Molina, A., 2014. Thermal characterization of the active layer at the Limnopolar Lake CALM-S site on Byers Peninsula (Livingston Island), Antarctica. Solid Earth 5 (2), 721–739. https://doi.org/10.5194/se-5-721-2014.

de Pablo, M.A., Ramos, M., Molina, A., Vieira, G., Hidalgo, M.A., Prieto, M., Jiménez, J. J., Fernández, S., Recondo, C., Calleja, J.F., Peón, J.J., Mora, C., 2016. Frozen ground and snow cover monitoring in the South Shetland Islands, Antarctica: Instrumentation, effects on ground thermal behaviour and future research. Cuadernos Investig. Geogr. 42 (2), 475–495. https://doi.org/10.18172/cig.2917.

de Pablo, M.A., Ramos, M., Molina, A., 2017. Snow cover evolution, on 2009-2014, at the Limnopolar Lake CALM-S site on Byers Peninsula, Livingston Island, Antarctica. CATENA 149, 538–547. https://doi.org/10.1016/j.catena.2016.06.002.

de Pablo, M.A., Ramos, M., Molina, A., Prieto, M., 2018. Thaw depth spatial and temporal variability at the Limnopolar Lake CALM-S site, Byers Peninsula, Livingston Island, Antarctica. Sci. Total Environ. 615, 814–827. https://doi.org/10.1016/j.scitotenv.2017.09.284.

de Pablo, M.A., Jiménez, J.J., Ramos, M., Prieto, M., Molina, A., Vieira, G., Hidalgo, M. A., Fernández, S., Recondo, C., Calleja, J.F., Peón, J.J., Corbea-Pérez, A., Maior, C.N., Morales, M., Mora, C., 2020. Frozen ground and snow cover monitoring in Livingston and Deception islands, Antarctica: preliminary results of the 2015-2019 PERMASNOW project. Cuadernos Investig. Geogr. 46 (1), 187–222. https://doi.org/10.18172/cig.4381.

Peat, H.J., Clarke, A., Convey, P., 2009. Diversity and biogeography of the Antarctic flora. J. Biogeogr. 34 (1), 132–146. https://doi.org/10.1111/j.1365-2699.2006.01565.x.

Pimpirev, C., Stoykova, K., Ivanov, M., Dimov, D., 2006. The sedimentary sequences of Hurd Peninsula, Livingston Island, South Shetland Islands: part of the late Jurassic — Cretaceous depositional history of the Antarctic Peninsula. In: Fütterer, D.K., Damaske, D., Kleinschmidt, G., Miller, H., Tessensohn, F. (Eds.), Antarctica. Springer, Berlin, Heidelberg. https://doi.org/10.1007/3-540-32934-X_30.

Ponti, S., Guglielmin, M., 2021. Shore evidences of a high Antarctic Ocean wave event: geomorphology, event reconstruction and coast dynamics through a remote sensing approach. Remote Sens. 13 (3), 518. https://doi.org/10.3390/rs13030518.

Ponti, S., Scipinotti, R., Pierattini, S., Guglielmin, M., 2021. The spatio-temporal variability of frost blisters in a perennial Frozen Lake along the Antarctic Coast as indicator of the groundwater supply. Remote Sens. 13 (3), 435. https://doi.org/10.3390/rs13030435.

Pour, A.B., Hashim, M., Park, Y., Hong, J.K., 2018. Mapping alteration mineral zones and lithological units in Antarctic regions using spectral bands of ASTER remote sensing data. Geocarto Int. 33 (12), 1281–1306. https://doi.org/10.1080/10106049.2017.1347207.

Prater, I., Hrbáček, F., Braun, C., Vidal, A., Meier, L.A., Nývlt, D., Mueller, & C.W., 2021. How vegetation patches drive soil development and organic matter formation on polar islands. Geoderma Region. 27, e00429.

Quesada, A., Camacho, A., Rochera, C., Velázquez, D., 2009. Byers Peninsula: A reference site for coastal, terrestrial and limnetic ecosystem studies in maritime Antarctica. Polar Sci. 3 (3), 181–187. https://doi.org/10.1016/j.polar.2009.05.003.

Quilty, P., 2007. Origin and evolution of the sub-Antarctic islands: the foundation. In: Papers and Proceedings of the Royal Society of Tasmania, pp. 35–58. https://doi.org/10.26749/rstpp.141.1.35.

Raffi, R., Stenni, B., 2011. Isotopic composition and thermal regime of ice wedges in northern Victoria Land, East Antarctica. Permafr. Periglac. Process. 22 (1), 65–83. https://doi.org/10.1002/ppp.701.

Ramos, M., Aguirre-Puente, J., 1994. Correlation between heat flux on the ground and permafrost thermal regime near the Spanish Antarctic Station. Ground Freez. 94, 395–397. Ed. balkema. ISBN: 90 5410 518 6. Libro. HOLANDA.

Ramos, M., Vieira, G., 2009. Evaluation of the ground surface Enthalpy balance from bedrock temperatures (Livingston Island, Maritime Antarctic). Cryosphere 3 (1), 133–145. https://doi.org/10.5194/tc-3-133-2009.

Ramos, M., Vieira, G., Gruber, S., Blanco, J.J., Hauck, C., Hidalgo, M.A., Tome, D., Neves, M., Trindade, A., 2007. Permafrost and active layer monitoring in the Maritime Antarctic: Preliminary results from CALM sites on Livingston and Deception Islands. In: USGS OF-2007-1047, Short Research Paper 070. U.S. Geological Survey and the National Academies. https://doi.org/10.3133/of 2007-1047. srp070.

Ramos, M., Vieira, G., Guilichinski, D., de Pablo, M.A., 2010. Nuevas estaciones de medida del régimen térmico del permafrost en el área de "Crater Lake". Isla Decepción (Antártida). Resultados preliminares. In: Blanco, J.J., Ramos, M., de Pablo, M.A. (Eds.), Proceedings of II Iberian Conference of the International Permafrost Association Periglacial, Environments, Permafrost and Climate Variability. UAH, pp. 93–109. ISBN: 978-84-9138-885-5. Libro. ESPAÑA.

Ramos, M., Vieira, G., de Pablo, M.A., Molina, A., Abramov, A., Goyanes, G., 2017. Recent shallowing of the thaw depth at Crater Lake, Deception Island, Antarctica (2006–2014). Catena 149 (2), 519–528. https://doi.org/10.1016/j.catena.2016.07.019.

Ramos, M., Vieira, G., de Pablo, M.A., Molina, A., Jimenez, J.J., 2020. Transition from a Subaerial to a Subnival Permafrost Temperature Regime following increased Snow Cover (Livingston Island, Maritime Antarctic). Atmosphere 11, 1332. https://doi.org/10.3390/atmos11121332.

Recondo, C., Corbea-Pérez, A., Peón, J., Pendás, E., Ramos, M., Calleja, J.F., de Pablo, M.Á., Fernández, S., Corrales, J.A., 2022. Empirical Models for estimating Air Temperature using MODIS Land Surface Temperature (and Spatiotemporal Variables) in the Hurd Peninsula of Livingston Island, Antarctica, between 2000 and 2016. Remote Sens. 14 (13), 3206. https://doi.org/10.3390/rs14133206.

le Roux, P.C., McGeoch, M.A., 2008. Changes in climate extremes, variability and signature on sub-Antarctic Marion Island. Clim. Chang. 86 (3–4), 309–329. https://doi.org/10.1007/s10584-007-9259-y.

Ruiz-Fernández, J., Oliva, M., García-Hernández, C., 2017. Topographic and geomorphologic controls on the distribution of vegetation formations in Elephant Point (Livingston Island, Maritime Antarctica). Sci. Total Environ. 587, 340–349. https://doi.org/10.1016/j.scitotenv.2017.02.158.

Ruiz-Fernández, J., Oliva, M., Nývlt, D., Cannone, N., García-Hernández, C., Guglielmin, M., Hrbáček, F., Roman, M., Fernández, S., López-Martínez, J., Antoniades, D., 2019. Patterns of spatio-temporal paraglacial response in the Antarctic Peninsula region and associated ecological implications. Earth-Sci. Rev. 192, 379–402. https://doi.org/10.1016/j.earscirev.2019.03.014.

Salmi, T., Määttä, A., Anttila, P., Ruoho-Airola, T., Amnell, T., 2002. Detecting Trends of Annual Values of Atmospheric Pollutants by the Mann-Kendall Test and Sen's Slope Estimates. Finnish Meteorological Institute, Helsinki.

Sawagaki, T., 1995. Ground temperature regimes and frost heave activity in the vicinity of Syowa Station, East Antarctica. In: Proceedings of the NIPR Symposium on Antarctic Geosciences, 8, pp. 239–249.

Schaefer, C.E.G.R., Pereira, T.T.C., Almeida, I.C.C., Michel, R.F.M., Corrêa, G.R., Figueiredo, L.P.S., Ker, J.C., 2017a. Penguin activity modify the thermal regime of active layer in Antarctica: A case study from Hope Bay. CATENA 149, 582–591. https://doi.org/10.1016/j.catena.2016.07.021.

Schaefer, C.E.G.R., Michel, R.F.M., Delpupo, C., Senra, E.O., Bremer, U.F., Bockheim, J., 2017b. Active layer thermal monitoring of a Dry Valley of the Ellsworth Mountains, Continental Antarctica. Catena 149, 603–615.

Serrano, E., 2003. Natural landscape and geoecological belts on ice free areas of the maritime Antarctica (South Shetland Islands). AGE Bull. 35, 5–32.

Serrano, E., Martínez de Pisón, E., López-Martínez, J., 1996. Periglacial and nival landforms and deposits. In: López-Martínez, J., Thomson, M.R.A., Thomson, J.W. (Eds.), Geomorphological Map of Byers Peninsula, Livingston Island, BAS GEOMAP Series. British Antarctic Survey, Cambridge, pp. 28–34. Sheet 5-A, Scale 1:25 000.

Seybold, C.A., Harms, D.S., Balks, M., Aislabie, J., Paetzold, R.F., Kimble, J., Sletten, R., 2009. Soil climate monitoring project in the Ross Island region of Antarctica. Soil Surv. Horiz. 50 (2), 52–57.

Seybold, C.A., Balks, M.R., Harms, D.S., 2010. Characterization of active layer water contents in the McMurdo Sound region, Antarctica. Antarct. Sci. 22 (6), 633–645. https://doi.org/10.1017/S0954102010000696.

Shipp, S.S., Anderson, J.B., Domack, E.W., 1999. Late Pleistocene–Holocene retreat of the West Antarctic Ice-Sheet system in the Ross Sea:Part 1 – Geophysical results. Geol. Soc. Am. Bull. 111, 1486–1516.

Shur, Y., Hinkel, K.M., Nelson, F.E., 2005. The transient layer: implications for geocryology and climate-change science. Permafrost Periglac. Process. 16, 5–17. https://doi.org/10.1002/ppp.518.

Siegert, M., Atkinson, A., Banwell, A., Brandon, M., Convey, P., Davies, B., Downie, R., Edwards, T., Hubbard, B., Marshall, G., Rogelj, J., Rumble, J., Stroeve, J., Vaughan, D., 2019. The Antarctic Peninsula under a 1.5°C Global Warming Scenario. Front. Environ. Sci. 7 (102) https://doi.org/10.3389/fenvs.2019.00102.

Simas, F.N.B., Schaefer, C.E.G.R., Albuquerke Filho, M.R., Francelino, M.R., Costa, L.M., 2008. Genesis, properties and classification of Cryosols from Admiralty Bay, Maritime Antarctica. Geoderma 144 (1–2), 116–122. https://doi.org/10.1016/j.geoderma.2007.10.019.

Simms, A.R., Milliken, K.T., Anderson, J.B., Wellnerc, J.S., 2011. The marine record of deglaciation of the South Shetland Islands, Antarctica since the last Glacial Maximum. Quat. Sci. Rev. 30 (13–14), 1583–1601. https://doi.org/10.1016/j.quascirev.2011.03.018.

Smellie, J.L., Davies, R.E.S., Thomson, M.R.A., 1980. Geology of a Mesozoic intra-arc sequence on Byers Peninsula, Livingston Island, South Shetland Islands. Brit. Antarct. Surv. Bull. 50, 55–76.

Smellie, J.L., Pankhurst, R.J., Thomson, M.R.A., Davies, R.E.S., 1984. The geology of the South Shetland Islands. VI: stratigraphy, geochemistry and evolution. Brit. Antarct. Surv. Sci. Rep. 87, 1–85.

Smith, S.L., O'Neill, H.B., Isaksen, K., Noetzli, J., Romanovsky, V.E., 2022. The changing thermal state of permafrost. Nat. Rev. Earth Environ. 3, 10–23. https://doi.org/10.1038/s43017-021-00240-1.

Smith, S.L., Wolfe, S.A., Riseborough, D.W., Nixon, F.M., 2009. Active-layer characteristics and summer climatic indices, Mackenzie Valley, Northwest Territories, Canada. Permafrost Periglac. Process. 20, 201–220. https://doi.org/10.1002/ppp.651.

Smykla, J., Drewnik, M., Szarek-Gwiazda, E., Hii, Y.S., Knap, W., Emslie, S.D., 2015. Variation in the characteristics and development of soils at Edmonson Point due to abiotic and biotic factors, northern Victoria Land, Antarctica. CATENA 132, 56–67. https://doi.org/10.1016/j.catena.2015.04.011.

Speir, T.W., Cowling, J.C., 1984. Ornithogenic soils of the Cape Bird adelie penguin rookeries, Antarctica. Polar Biol. 2 (4), 199–205.

Strand, S.M., Christiansen, H.H., Johansson, M., Åkerman, J., Humlum, O., 2021. Active layer thickening and controls on interannual variability in the Nordic Arctic compared to the circum-Arctic. Permafr. Periglac. Process. 32, 47–58. https://doi.org/10.1002/ppp.2088.

Terauds, A., Lee, J., 2016. Antarctic biogeography revisited: updating the Antarctic Conservation Biogeographic Regions. Divers. Distrib. 22 (8), 836–840. https://doi.org/10.1111/ddi.12453.

Thomazini, A., Francelino, M.R., Pereira, A.B., Schünemann, A.L., Mendonca, E.S., Michel, R.F.M., Schaefer, C.E.G.R., 2020. The current response of soil thermal regime and carbon exchange of a paraglacial coastal land system in maritime Antarctica. Land Degrad. Dev. 31, 655–666. https://doi.org/10.1002/ldr.3479.

Thomson, M.R.A., López-Martínez, J., 1996. Introduction to the Geology and Geomorphology of Byers Peninsula. In: López-Martínez, J., Thomson, M.R.A., Thomson, J.W. (Eds.), Geomorphological Map of Byers Peninsula, Livingston Island BAS Geomap Series 5-A. British Ant Surv, Cambridge, pp. 1–4.

Tucker, N.M., Hand, M., Clark, C., 2020. The Bunger Hills: 60 years of geological and geophysical research. Antarct. Sci. 32 (2), 85–106. https://doi.org/10.1017/S0954102019000403.

Turner, J., Lu, H., White, I., King, J.C., Phillips, T., Scott Hosking, J., Bracegirdle, T.J., Marshall, G.J., Mulvaney, R., Deb, P., 2016. Absence of 21st century warming on Antarctic Peninsula consistent with natural variability. Nature 535. https://doi.org/10.1038/nature18645.

Turner, J., Marshall, G., Clem, K., Colwell, S., Phillips, T., Lu, H., 2020. Antarctic temperature variability and change from station data. Int. J. Climatol. 40 (6), 2986–3007. https://doi.org/10.1002/joc.6378.

Ugolini, F.C., Bockheim, J.G., 2008. Antarctic soils and soil formation in a changing environment: A review. Geoderma 144 (1–2), 1–8. https://doi.org/10.1016/j.geoderma.2007.10.005.

Uxa, T., 2016. Discussion on, 'active layer thickness prediction on the Western Antarctic peninsula' by Wilhelm et al. 2015. Permafr. Periglac. Process. 28, 493–498.

Vera, E.I., 2011. Livingstonites Gabrielae gen. et sp. nov., Permineralized Moss (Bryophyta: Bryopsida) from the Aptian Cerro Negro Formation of Livingston Island (South Shetland Islands, Antarctica). Ameghiniana 48 (1), 122–128. https://doi.org/10.5710/AMGH.v48i1(477).

Vieira, G., Ramos, M., 2003. Geographic factors and geocryological activity in Livingston Island, Antarctic. Preliminary results. In: Phillips, M., Springman, S.M., Arenson, L.U. (Eds.), Permafrost. Proceedings of the eight International Conference on Permafrost, 21-25 July 2003, Zurich, Switzerland, Balkema – Swets & Zeitlinger, Lisse: 1183-1188.

Vieira, G., López, J., Serrano, E., Ramos, M., Gruber, S., Hauck, C., Blanco, J.J., 2008. Geomorphological observations of permafrost and Ground-Ice Degradation on Deception and Livingston Islands, Maritime Antarctica. In: Kane, Douglas L., Hinkel, Kenneth M. (Eds.), Proceedings of the Ninth International Conference on Permafrost University of Alaska Fairbanks June 29–July 3. 2008. Institute of Northern Engineering, pp. 1839–1843. NICOP-2008. ISBN: 978-0-980 017 9 -2-2.

Vieira, G., Bockheim, J., Guglielmin, M., Balks, M., Abramov, A.A., Boelhouwers, J., Cannone, N., Ganzert, L., Gilichinsky, D., Goryachkin, S., López-Martínez, J., Raffi, R., Ramos, M., Schaefer, C., Serrano, E., Simas, F., Sletten, R., Wagner, D., 2010. Thermal state of permafrost and active-layer monitoring in the Antarctic: advances during the international polar year 2007–2008. Permafr. Periglac. Process. 21, 182–197.

Vieira, G., Mora, C., Pina, P., Schaefer, C., 2014. A proxy for snow cover and winter ground surface cooling: mapping Usnea sp communities using high resolution remote sensing imagery (Maritime Antarctica). Geomorphology 225 (15), 69–75. https://doi.org/10.1016/j.geomorph.2014.03.049.

van de Vijver, B., Beyens, L., 1999. Biogeography and ecology of freshwater diatoms in Subantarctica: a review. J. Biogeogr. 26 (5), 993–1000. https://doi.org/10.1046/j.1365-2699.1999.00358.x.

Walsh, J.E., 2009. A comparison of Arctic and Antarctic climate change, present and future. Antarct. Sci. 21 (3), 179–188. https://doi.org/10.1017/S0954102009001874.

Webers, G.F., Craddock, C., Splettstoesser, J.F., 1992. Geological history of the Ellsworth Mountains, West Antarctica. In: Webers, G.F., Craddock, C., Splettstoesser, J.F. (Eds.), Geology and Paleontology of the Ellsworth Mountains.

van Wessem, J.M., Ligtenberg, S.R.M., Reijmer, C.H., van de Berg, W.J., van den Broeke, M.R., Barrand, N.E., Thomas, E.R., Turner, J., Wuite, J., Scambos, T.A., van Meijgaard, E., 2016. The modelled surface mass balance of the Antarctic Peninsula at 5.5 km horizontal resolution. Cryosphere 10, 271–285. https://doi.org/10.5194/tc-10-271-2016.

White, D.A., Fink, D., 2014. Late Quaternary glacial history constrains glacio-isostatic rebound in Enderby Land, East Antarctica. J. Geophys. Res. Earth Surf. 119 (3), 401–413. https://doi.org/10.1002/2013JF002870.

Wilhelm, K., Bockheim, J., 2016. Influence of soil properties on active layer thermal propagation along the western Antarctic Peninsula. Earth Surf. Process. Landf. 41 (11), 1550–1563. https://doi.org/10.1002/esp.3926.

Wilhelm, K., Bockheim, J., 2017. Climatic controls on active layer dynamics: Amsler Island, Antarctica. Antarct. Sci. 29 (2), 173–182.

Wilhelm, K.R., Bockheim, J.G., Kung, S., 2015. Active Layer Thickness Prediction on the Western Antarctic Peninsula. Permafr. Periglac. Process. 26 (2), 188–199. https://doi.org/10.1002/ppp.1845.

Wlostowski, A.N., Gooseff, M.N., McKnight, D.M., Lyons, W.B., 2018. Transit Times and Rapid Chemical Equilibrium Explain Chemostasis in Glacial Meltwater Streams in the McMurdo Dry Valleys, Antarctica. Geophys. Res. Lett. 45 (24) https://doi.org/10.1029/2018GL080369.

Xu, X., Wu, Q., 2021. Active layer thickness variation on the Qinghai-Tibetan Plateau: Historical and projected trends. J. Geophys. Res. Atmos. 126 e2021JD034841. https://doi.org/10.1029/2021JD034841.

Yergeau, E., Newsham, K.K., Pearce, D.A., Kowalchuk, G.A., 2007. Patterns of bacterial diversity across a range of Antarctic terrestrial habitats. Environ. Microbiol. 9 (11), 2670–2682.

Yoon, H.I., Han, M.W., Park, B.K., Oh, J.K., Chang, S.K., 1997. Glaciomarine sedimentation and paleo-glacial setting of Maxwell Bay and its tributary embayment, Marian Cove, South Shetland Island, West Antarctica. Mar. Geol. 140, 265–282.

Levy, J.S., Fountain, A.G., Gooseff, M.N., Welch, K.A., Lyons, W.B., 2011. Water tracks and permafrost in Taylor Valley, Antarctica: Extensive and shallow groundwater connectivity in a cold desert ecosystem. GSA Bulletin 123 (11–12), 2295–2311. https://doi.org/10.1130/B30436.1.

Hinkel, K.M., Nelson, F.E., 2003. Spatial and temporal patterns of active layer thickness at Circumpolar Active Layer Monitoring (CALM) sites in northern Alaska, 1995–2000. J. Geophys. Res. 108 https://doi.org/10.1029/2001JD000927, 81–68.

López-Martínez, J., Martínez de Pisón, E., Serrano, E., Arche, A., 1996. Geomorphological map of Byers Peninsula. Livingston Island. Geomap Series. British Antarctic Survey, Cambridge (UK) (Sheet 5-A).

Correia, A., Oliva, M., Ruiz-Fernández, J., 2017. Evaluation of frozen ground conditions along a coastal topographic gradient at Byers Peninsula (Livingston Island, Antarctica) by geophysical and geoecological methods. Catena 149 (2), 529–537. https://doi.org/10.1016/j.catena.2016.08.006.

Correia, A., Vieira, G., Ramos, M., 2012. Thermal conductivity and thermal diffusivity of cores from a 26 meter deep borehole drilled in Livingston Island, Maritime Antarctic. Geomorphology 155-156, 7–11. https://doi.org/10.1016/j.geomorph.2011.12.012.

Campbell, S., Affleck, R.T., Sinclair, S., 2018. Ground-penetrating radar studies of permafrost, periglacial, and nearsurface geology at McMurdo Station, Antarctica. Cold Reg. Sci. Technol. 148, 38–49. https://doi.org/10.1016/j.coldregions.2017.12.008.